WADC TECHNICAL REPORT 54-343



# PREFERRED ORIENTATION AND DEFORMATION IN TITANIUM AND TITANIUM ALLOYS

*CARL J. McHARGUE*
*CULLIE J. SPARKS, JR.*
*JOSEPH P. HAMMOND*

*UNIVERSITY OF KENTUCKY*

*DECEMBER 1954*

AERONAUTICAL RESEARCH LABORATORY
CONTRACT No. AF 33(038)-19574
PROJECT No. 7351



WRIGHT AIR DEVELOPMENT CENTER
AIR RESEARCH AND DEVELOPMENT COMMAND
UNITED STATES AIR FORCE
WRIGHT-PATTERSON AIR FORCE BASE, OHIO

Carpenter Litho & Prtg. Co., Springfield, O.
200 - 28 July 1955

# FOREWORD

This report was prepared by Cullie J. Sparks, Jr. with aid from previous progress reports of Carl J. McHargue, Samuel E. Adair, and James R. Holland and under the supervision of Joseph P. Hammond at the University of Kentucky, Lexington, Kentucky. This work was performed by the Kentucky Research Foundation in connection with Air Force Contract No. AF 33(038)-19574 under Task No. 70608 "The Effect of Composition and Internal Structure on the Properties of Alloys", and Project No. 7351 "Metallic Materials". The work was administered under the direction of the Aeronautical Research Laboratory, Directorate of Research, Wright Air Development Center with Mr. E. J. Hassell acting as Project Engineer.

The assistance of Lt. Arthur W. Mullendore and Lt. Lawrence R. Bidwell during partial tenure of this contract is gratefully acknowledged.

Acknowledgement is given to Charles S. Crouse for his congenial guidance, to Roy E. Swift for suggestions and to James A. Burka, C. Lyndon Langley, Carl C. Duncan, Douglas W. Cox, Thomas A. Kendall, and Fritz Mangelsen for their supporting activities on this contract. This report summarizes the work on this project beginning February 1951 through August 1954.

## ABSTRACT

Preferred orientations in titanium and titanium alloys containing aluminum, columbium, tantalum, molybdenum, and zirconium in solid solution were produced by cold rolling, annealing and hot rolling. The effect of cycling through the alpha-beta transformation on the texture of cold-rolled titanium was determined. Preferred orientations in titanium were varied by changing the amount of reduction in cross-sectional area. All resulting textures were determined by x-ray methods, evaluated and compared with previously determined textures of titanium and other metals and alloys. Texture layer effect as influenced by varying reduction was related to bendability. Alloying and low temperatures of hot rolling and annealing produced no major change from the cold-rolled texture of titanium. Higher temperatures of hot rolling and annealing (above 1300° F) produced textures differing from the cold-rolled textures by 30° rotations about the C-axis.

Large crystals of titanium were produced and then deformed in tension at 1500°F and others of 4% Al-Ti, 10% Ta-Ti and 15% Zr-Ti deformed at room temperature were examined for deformation mechanisms. Slip occurred generally on the $(10\bar{1}0)$, $(10\bar{1}1)$ and (0001) planes and twinning on the $(10\bar{1}2)$, $(11\bar{2}1)$ and $(11\bar{2}2)$.


## PUBLICATION REVIEW

This report has been reviewed and is approved.

FOR THE COMMANDER:

Leslie B. Williams

Leslie B. Williams
Colonel, USAF
Chief, Aeronautical Research Laboratory
Directorate of Research

# TABLE OF CONTENTS

# LIST OF ILLUSTRATIONS

Figure Page

Figure | Page

# LIST OF TABLES

# INTRODUCTION

This technical report presents the results and interpretations of work performed during the period February 1951 to August 1954. The objective of this work was to investigate as thoroughly as time permitted the textures of titanium and titanium alloys produced by cold rolling, hot rolling and annealing after cold rolling. Several related experiments were carried out in order to better understand the development of these textures and their significance in terms of properties.

Prior to the initiation of this research there had been little work done on the deformation mechanisms and textures of titanium and no work whatsoever on the influence of alloying thereon. As a hexagonal metal, titanium performed differently with respect to preferredness of texture and deformation mechanisms than those commonly associated metals Zn, Mg and Cd. Titanium ranks as a low c/a ratio metal and this is generally associated with its deformation behavior.

Alloys for study were selected with as wide a variance in c/a as possible in order to ascertain its significance. The room temperature deformation mechanisms were determined in tension for three alloys of titanium as well as the high temperature mechanisms of unalloyed titanium. These results are compared to the room temperature deformation mechanisms of unalloyed titanium determined by two separate investigations. In addition to sheet textures resulting from cold rolling, hot rolling and annealing, fiber textures were determined for the cold-rolled and annealed conditions. The effect of the alpha-beta-alpha transformation on texture was investigated with the view of developing greater randomness in texture. Layer studies were made of textures resulting from cold rolling, hot rolling and annealing of thicker sheet to determine how texture varied from the surface in. These latter results are correlated with those of bendability conducted for the same conditions. Thus, the effect of preferredness of texture on ductility due to the anisotropy of hexagonal metal crystals is compared.

The findings reported herein are fundamental to the principles upon which the texture formation and properties of mechanically and thermally treated titanium and titanium alloys are based.

# PREPARATION OF MATERIALS AND METHODS

## A. MATERIALS

With two exceptions, the titanium used in this work was iodide titanium produced by the New Jersey Zinc Company. The bend tests and layer studies were conducted on commercial Ti-75A. The analyses of the titanium and the alloying elements used are given below.

TABLE I

ANALYSES OF TITANIUM AND ALLOYING ELEMENTS

| Impurity | Iodide Ti | Ti-75A | Ta | Al | Cb | Zr | Mo |
|---|---|---|---|---|---|---|---|
| Ti | - | - | - | - | Tr | - | - |
| Mn | 0.004 | - | - | - | - | 0.001 | - |
| Fe | 0.0065 | 0.10 | 0.02 | - | Tr | 0.04 | - |
| Al | 0.0065 | - | - | 99.983 | - | 0.01 | - |
| Pb | 0.0025 | - | - | - | - | 0.001 | - |
| Cu | 0.01 | - | - | - | - | 0.01 | - |
| Sn | 0.002 | - | - | - | Tr | 0.001 | - |
| Mg | - | - | - | - | - | 0.003 | - |
| C | - | - | 0.01 | - | 0.05 | 0.001 | none |
| W | - | - | 0.04 | - | - | 0.001 | - |
| Cb | - | - | 0.05 | - | - | - | - |
| $N_2$ | 0.002 | 0.02 | - | - | - | 0.01 | - |
| Ni | - | - | - | - | - | - | Tr Max |
| $O_2$ | - | - | - | - | - | - | 0.05 Max |

## B. MELTING PROCEDURE

The crystallites of titanium were broken from the as deposited bar as far as practical, then the bar was rolled into sheet and cut into small pieces. The procedure for preparing these alloys of iodide titanium has been established as follows. The material is screened to a size range of 3 to 20 mesh and subsequently cleaned with acetone. The alloying addition is made and the 10- to 25-gm charge is thoroughly mixed before being pressed to a button of about 1.25 inches in diameter. The electric-arc furnace with a water-cooled copper hearth and 0.25-inch diameter tungsten electrode is charged with the pressed button. The system is then evacuated to a pressure of the order of $10^{-6}$ mm of Hg. After outgassing, the system is flushed 4 or 5 times by introducing 0.6 to 0.8 atmospheres of high-purity argon that has been passed through a cold trap. This is followed by evacuating to 6 to 8 x $10^{-4}$ mm of Hg. Prior to melting the charge, 0.2 atmospheres of argon are introduced

and the furnace proper shut off from the rest of the vacuum system. The arc is struck on a tungsten button in the side of the hearth and the melting started. A charge of 5 to 25 grams can be completely melted in about 30 seconds when the furnace is operated from 200 to 250 amperes and 20 to 22 volts. The buttons are allowed to cool to room temperature in the furnace. It has been found that operation under these conditions gives rise to negligible contamination from the tungsten electrode (1,2). For a 25-gram melt of 7.1% Zr-Ti alloy which had been thrice melted, spectrographic analysis revealed only 0.07% tungsten after three melts.

TABLE 2

COMPOSITION OF ALLOYS

| Button No. | Concentration of Addition |
|---|---|
| 52 | 0.27 % Al |
| 49 | 0.47 % Al |
| 15a | 1.1 % Al |
| 53 | 1.05 % Al |
| 50 | 1.43 % Al |
| 46 | 3.13 % Al |
| 15 | 3.8 % Al |
| 51 | 4.0 % Al |
| 14 | 7.1 % Al |
| 17 | 14.3 % Al |
| 16 | 15.0 % Al |
| 17a | 19.2 % Al |
| 18 | 25.0 % Al |
| 19 | 27.5 % Al |
| 27 | 0.99 % Cb |
| 26 | 1.63 % Cb |
| 30 | 3.59 % Cb |
| 34 | 5.12 % Cb |
| 13a | 0.59 % Ta |
| 11a | 1.73 % Ta |
| 10 | 3.58 % Ta |
| 13 | 5.82 % Ta |
| 11 | 8.03 % Ta |
| 54 | 9.96 % Ta |
| 18 | 11.98 % Ta |
| 47 | 12.95 % Ta |
| 12 | 15.44 % Ta |
| 22 | 0.48 % Zr |
| 24 | 3.02 % Zr |
| 21 | 6.3 % Zr |
| 25 | 7.1 % Zr |
| 28 | 10.2 % Zr |
| 29 | 12.0 % Zr |
| 45 | 14.63 % Zr |
| 23 | 14.75 % Zr |
| 48 | 14.97 % Zr |

## C. CHEMICAL ANALYSIS

The procedures for the chemical analyses were taken from several different sources. The aluminum content was determined by the chloroform separation procedure described in the Handbook on Titanium Metal published by the Titanium Metals Corporation. The molybdenum and columbium contents were determined by the colorimetric procedure described in the Summary of Final Report of Phase Diagrams of Ti-Mo, Ti-Cb and Ti-Si Alloy Systems, Armour Research Foundation. The method of determining the tantalum concentration was the same as that used for columbium. Chemical analyses for zirconium were run according to the procedure outlined by Scott's Standard Methods of Chemical Analysis, Fifth Edition, Vol. I. The results were then corrected colorimetrically for $TiO_2$ precipitated with the oxides of the alloying elements. The composition of alloys used in this investigation are listed in Table 2 with exception of three molybdenum alloys.

The weight of the compacted pellet was determined before charging into the furnace, and weighed upon removal. On the average the difference in weight due to losses in the furnace were less than 0.1% of the original charge. With accurate weighing, the analytical results should show a close comparison to the intended composition. This conclusion is based on the consideration that if the 0.1% loss were entirely of the alloying addition a still very small change in composition would result. This has been found to be the case. When preparing additional alloys of the same intended composition, slight additions of the alloying elements above that used previously were made when prior experience showed a loss of the alloy concentration during melting.

## D. TREATMENT OF INGOTS

All alloy ingots were homogenized at 1400°F. for 72 hours and radiographed for gross segregations.

The as-cast ingots of metal were cold-forged and ground into sizes and shapes suitable for the rolling schedule. The materials are then enclosed in tantalum foil and vacuum annealed in quartz tubes at 1300°F. for one hour.

In the case of the Ti-75A forging, the material was only ground to shape and vacuum annealed as above.

## E. SPECIMEN PREPARATION AND PROCEDURE FOR POLE FIGURE DETERMINATION

Since specimen preparation is important to good technique in texture studies, the procedure is given here.

Whether cold- or hot-rolled, the specimens were reduced 10% per pass using a two high Stanat rolling mill with 4-inch diameter rolls. The rolling direction was changed 180° after each pass. When hot rolling, the specimens were placed between mica sheets to minimize

heat loss. All cold-rolled material underwent a total reduction in thickness of 93 % or more. All hot-rolled material was given a reduction of 90 %. The final sheet thickness was approximately 0.012 in. For all fine grained material, the sheets were ground, polished and etched to rods of approximately 0.005 in. in diameter, one specimen taken parallel to the rolling direction and a second parallel to the cross direction. The etchant used was 1.5 % hydrofluoric acid, 12% nitric and the remainder water (volume percentages).

For specimens annealed at temperatures above 1300° F. for one hour, the specimens used were as sheet or posts mounted in a structure integrating camera (3).

Transmission photograms were taken using molybdenum radiation (45 kv., 18 ma.) and a 0.010-in. pinhole. Since titanium fluoresces under these conditions, it was necessary to use a zirconium filter between the specimen and film.

Exposures were made with the beam perpendicular to the rolling direction at 0, 11, 26, 41, 56, 71 and 79° to the cross direction, and with the beam perpendicular to the cross direction at 11, 26, 56, 71 and 79° to the rolling direction. Additional exposures were then made where necessary. The variations in intensity of the diffraction rings were estimated by eye with the aid of an exposure chart. Intensity readings of 0, 1, 2 and 3 were made on all specimens except those hot-rolled, for which intensities of 0, 1 and 2 were generally used.

Any different or additional procedures not outlined above will be mentioned subsequently in their appropriate places.

## SECTION II

## COLD-ROLLED AND COLD-ROLLED RECRYSTALLIZED FIBER TEXTURES

### A. EXPERIMENTAL METHOD

Rods, which had been treated as described in Section I of this report under treatment of ingots were reduced from 0.303 in. to 0.027 in. in 24 steps using a Stanat rolling mill for rolling rounds. In order for the orientation of the central region to be studied, portions of these rods were electrolytically reduced to a diameter of 0.005 in. using the procedure described by Sutcliffe and Reynolds (4).

X-ray data were obtained using a Laue type camera and molybdenum radiation. As in the case for sheet texture work, a zirconium filter was used between the specimen and film. Exposures for both the surface and center areas were made chiefly with the rolling direction perpendicular to the beam. Several were made with the rolling direction tilted toward the beam.

## B. RESULTS

The orientation of the cold-rolled wire can be described as having the $[10\bar{1}0]$ direction, or Type II digonal axis, parallel to the wire axis with all azimuthal positions possible. This is shown schematically in Figure 1a. Burgers, Fast and Jacobs report the same wire texture for zirconium (5), and Morell and Hanawalt report it for Dowmetal (6).

The texture at the surface and the center is essentially the same, varying only in the degree of scatter about the ideal. From a measurement of the spread of the diffraction spots (7), it was found that the $[10\bar{1}0]$ direction has a spread of $\pm 6°$ to the wire axis in the central region and a spread of $\pm 15°$ in the surface layers.

The maxima of the diffraction rings for the central region of specimens annealed 40 minutes at 1000° F were found to be split and joined by regions of lesser intensity. The average values of the maxima for the $(0002)$, $(10\bar{1}0)$, $(10\bar{1}1)$ and $(11\bar{2}0)$ planes reveal an average orientation having the $[11\bar{2}0]$ direction, or Type I digonal axis, parallel to the wire axis. However, this recrystallization orientation is accurately described in Figure 1b as having concentrations of the basal planes tilted $\pm 11°$ to the wire axis with some basal planes at all positions between these. The $[11\bar{2}0]$ direction is located so that it would be parallel to the wire axis if the basal plane were rotated until parallel to the wire axis. This orientation is such that the $(21\bar{3}0)$ plane is normal to the wire axis.

The cold-rolled fiber texture found for the 3.8 % aluminum alloy had the $[10\bar{1}0]$ direction parallel to the wire axis. Thus the aluminum addition did not basically effect the fiber axis of titanium.

Exposures on the surface layer of the annealed 3.8% aluminum alloys do not show the strong, split maxima, but indicate the average position of $[11\bar{2}0]$ to lie along the wire axis with a spread of $\pm 35°$.

The recrystallized wire texture of zirconium (5) has been found to be $[11\bar{2}0]$.

b. Recrystallized

a. Cold-rolled

Fig. 1 Fiber Axis in iodide Titanium.

SECTION III

# EFFECTS OF SOLID SOLUTION ALLOYING ON COLD-ROLLED TEXTURES OF TITANIUM

## A. INTRODUCTION

There have been relatively few studies of the effect of alloying on deformation textures. A second element may be present in the base metal in solid solution and/or as a second phase. The literature offers no satisfactory explanation for the effects of solid solution alloying on textures noted thus far. For example, there is no satisfactory explanation of the differences in the textures of copper and alpha brass.

The most complete study of the effects of solid solution alloying on deformation textures is that of Brick, Martin and Angier (8). These investigators reported that the copper texture was retained by alloys of copper with up to 30% Ni, less than 5% Zn, less than 2% Al or Co up to the limit of solubility. Copper containing more than 5% Zn, more than 2% Al, or the maximum soluble concentration of tin, silicon or manganese showed the deformation texture of alpha brass.

Bakarian (9) reported that additions of 0.20% Ca to 99.98% magnesium or 2.0 % Mn plus 0.15% Ca to magnesium resulted in entirely different textures than for the pure magnesium. The texture obtained for high-purity magnesium sheet showed the basal plane to be concentrated parallel to the rolling plane. The texture obtained for the alloy containing 0.20% Ca had the basal planes concentrated in elliptical areas whose centers were tilted 15° from the center of the pole figure toward the rolling direction. This split basal orientation was even more pronounced in the alloy containing 2.0% Mn and 0.15% Ca.

Fuller and Edmunds (10) studied the rolled sheet textures in a zinc alloy containing 1.0% Cu and 0.01% Mn. The basal pole figure of this alloy contained a region of strong concentration not found in the pole figure for pure zinc (11).

In the above cases, results were discussed in terms of possible changes in slip and/or twinning systems and critical shear stresses. However, there were no experimental data to relate these speculations with the observed textures.

It has been suggested that the deformation textures of titanium, zirconium and beryllium could be directly ascribed to their low c/a ratios. The complexity of the deformation mechanisms of titanium (12) also has been suggested to be characteristic of hexagonal close-packed metals with low c/a ratios. The purpose of this phase of the work was to study the cold-rolled sheet textures in binary titanium-base alpha alloys in which the c/a ratios were greater than, less than, and about the same as the c/a for iodide titanium.

## B. COMPOSITION-PARAMETER STUDIES

To facilitate filing to fine mesh, alloys were heated to 1300°F. and quenched in water. The filings were then stress relieved at 925°F. in titanium capsules which were sealed in evacuated quartz tubes to obtain sharp-line spectra.

Films for the alpha lattice parameter determinations were obtained with a 114.59 mm powder camera with the film mounted according to the method of Straumanis. Nickel-filtered copper radiation was used, and a 0.001-in. aluminum foil was placed inside the camera to reduce the high background encountered with titanium. The parameters were calculated by a least squares solution of the five strongest high-angle lines which provided an accuracy of $\pm 0.005$°A or better. The results of the parameter studies are presented in conjunction with the corresponding textures below.

## C. RESULTS OF TEXTURE STUDIES

### Unalloyed Titanium

The cold-rolled sheet texture for iodide titanium is presented in Figure 2. Figure 2a shows that two high intensity regions are developed for (0002) planes which correspond to a rotation of $\pm 27°$ in the transverse direction from the ideal orientation of (0002) $[10\bar{1}0]$ reported for other hexagonal metals. This was reported originally by Clark (13) and later by Williams and Eppelsheimer (14). Variations of this tilt were observed also in cold-rolled zirconium (15, 16, 17). Figure 2b shows that the $[10\bar{1}0]$ direction is aligned parallel to the rolling direction. These observations are confirmed by the $(10\bar{1}1)$ pole figure, Figure 2c. Most of the spread of the basal poles is in the cross direction and the minor intensity area extends completely to the cross direction. The c/a ratio for iodide titanium is 1.588.

### Titanium-Aluminum

The effect of alloying on the lattice parameters of the Ti-Al alloys is shown in Figure 45*. These results are similar to those published by Rostoker (18), differing mainly in rapidity of the rise of the c/a curve for low aluminum concentrations. It was desired to determine the texture for an alloy with the greatest possible c/a ratio, but alloys containing more than approximately 5 wt % Al could not be cold-reduced the desired amount (90% or better). The material selected for study contained 3.8% Al and had a c/a ratio of 1.600.

The cold-rolled sheet textures of this alloy are shown in Figure 3. These pole figures show an "ideal" texture differing from that of iodide titanium, Figure 2 . Figures 3a and b indicate that the basal

* An asterisk following a Figure denotes that those figures are located in the Appendix.

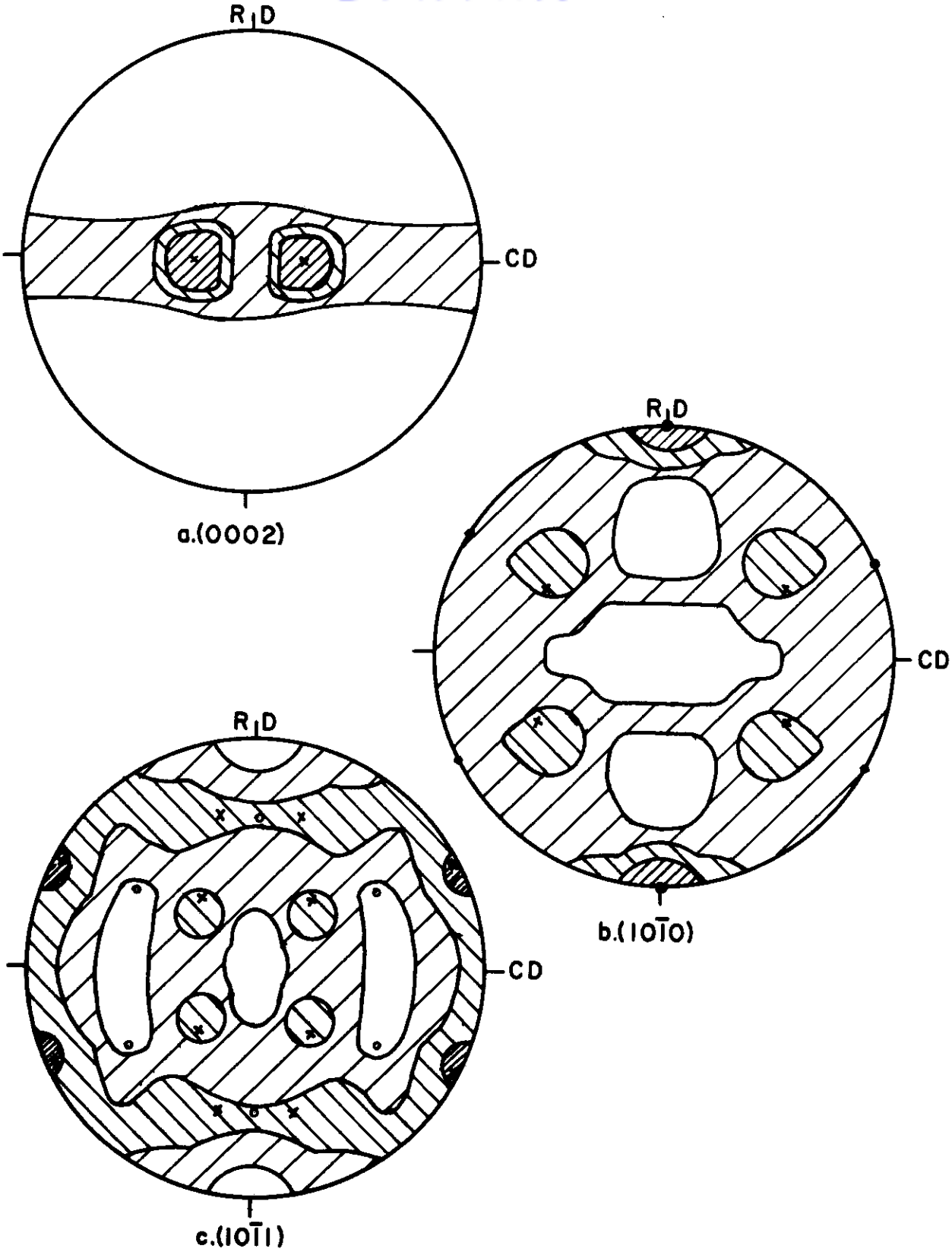


Fig. 2 Texture of Iodide Titanium cold-rolled 97%. o = (0002) [10$\bar{1}$0], x = (0002) rotated 27° about Rolling Direction, [10$\bar{1}$0] ∥ R. D.

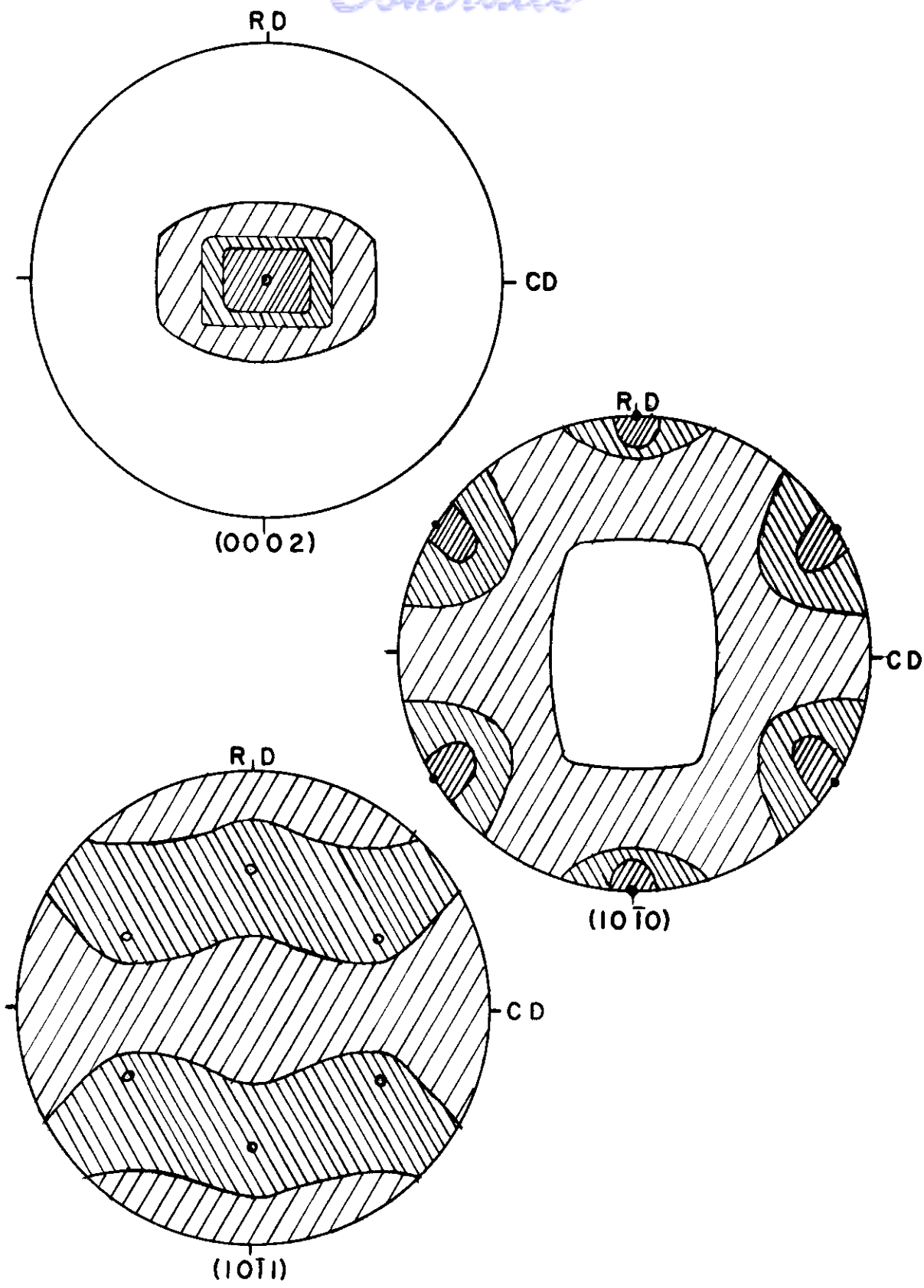


Fig. 3 Texture of 3.8% Al-Ti alloy cold-rolled 94%. o = (0002) [10$\bar{1}$0].

planes are concentrated parallel to the rolling plane and that the [10$\bar{1}$0] is parallel to the rolling direction, or that the "ideal" texture is (0002) [10$\bar{1}$0]. The major spread is in the cross direction.

Titanium-Columbium

It is seen from Figure 46* that there are only slight changes in the parameters of the Ti-Cb alloys. The c/a ratio for 3.6% Cb was 1.592 compared to 1.588 for unalloyed titanium.

The cold-rolled sheet pole figures for an alloy containing 3.6% Cb and having c/a = 1.592 are shown in Figure 4. These are similar in form to those of titanium; however, the maxima in the (0002) pole figure are positioned approximately 40° from the center of the pole figure in the cross directions instead of 27° as for titanium. There is a region of second high intensity in the (0002) pole figure approximately 15° to 20° from the center in the rolling direction which did not appear for unalloyed titanium. The lowest intensity region of the (0002) pole figure of the Ti-Cb alloy shows a break near the basic circle, whereas that lowest intensity region for the iodide titanium extended all the way across the figure. The figures for the (10$\bar{1}$0) and (10$\bar{1}$1) planes are consistent with the split basal [10$\bar{1}$0] texture and show much spread in the cross direction.

Titanium-Tantalum

It will be observed that the c/a ratio of the alpha solid solution decreased with increasing concentrations of tantalum, Figure 47*. Textures were determined for two alloys of titanium containing tantalum. One alloy contained 3.6% Ta and had a c/a ratio of 1.584, while the other contained 15.4% Ta and had a c/a ratio of 1.575.

The pole figures for the 3.6% Ta alloy illustrated in Figure 5, show the split basal [10$\bar{1}$0] texture. The only differences in the basal pole figure for this alloy and iodide titanium are the absence of (0002) poles near the basic circle and the presence of the region of second high intensity near the center of the figure in the rolling direction. In other respects the alloyed texture was essentially the same as the unalloyed.

The texture for the 15.4% Ta alloy showed no significant differences from the results on the 3.6% Ta alloy, Figure 5. The regions of maximum intensity in the (0002) pole figure were approximately 25° to 27° from the center in the transverse direction as for iodide titanium and the alloy of 3.6% Ta.

Titanium-Zirconium

Titanium and zirconium show complete solid solubility in both

* An asterisk following a Figure denotes that those figures are located in the Appendix.

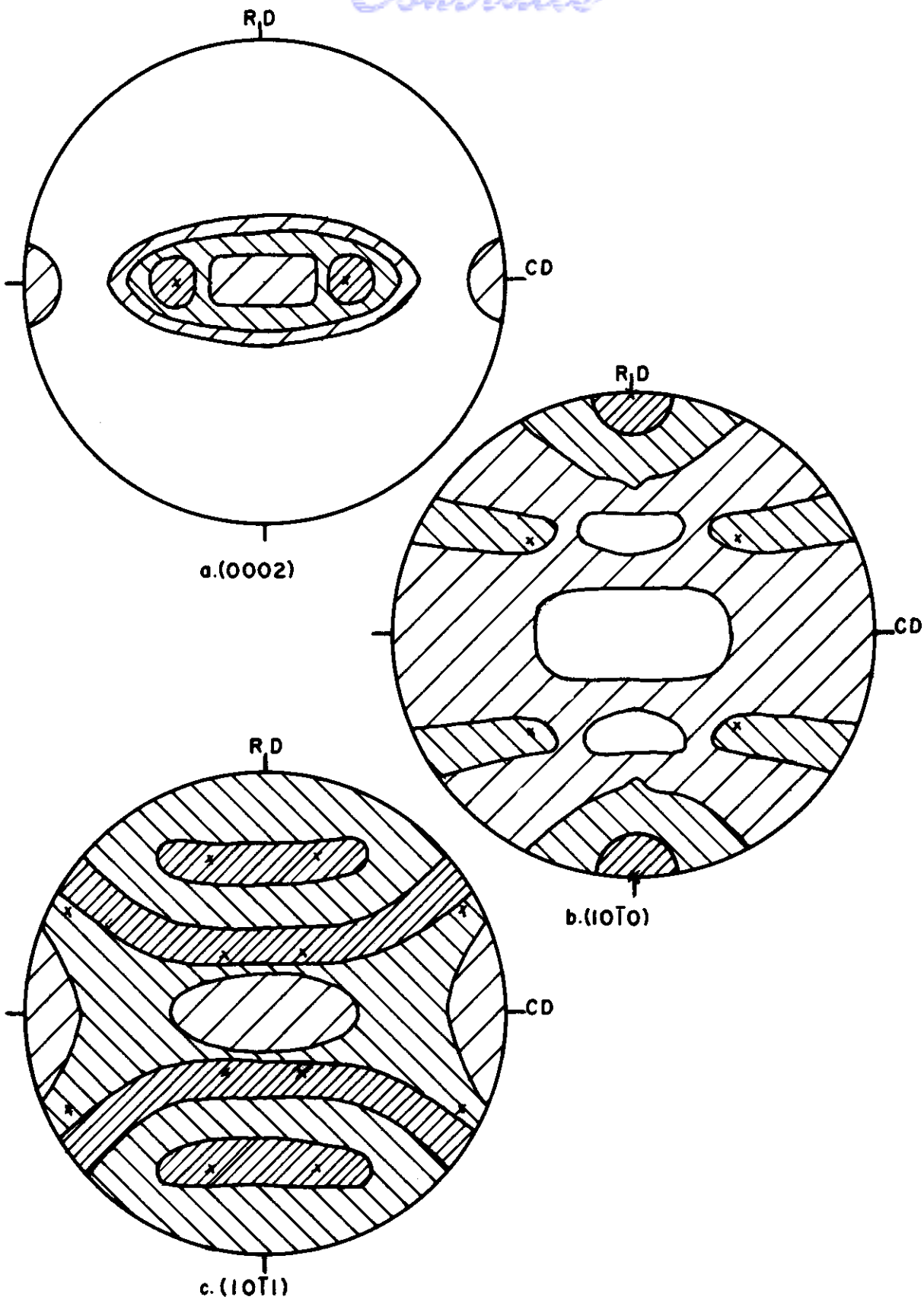


Fig. 4 Texture of 3.6% Cb-Ti alloy cold-rolled 94%. x = (0002) rotated 40° [10$\bar{1}$0] ll R.D.

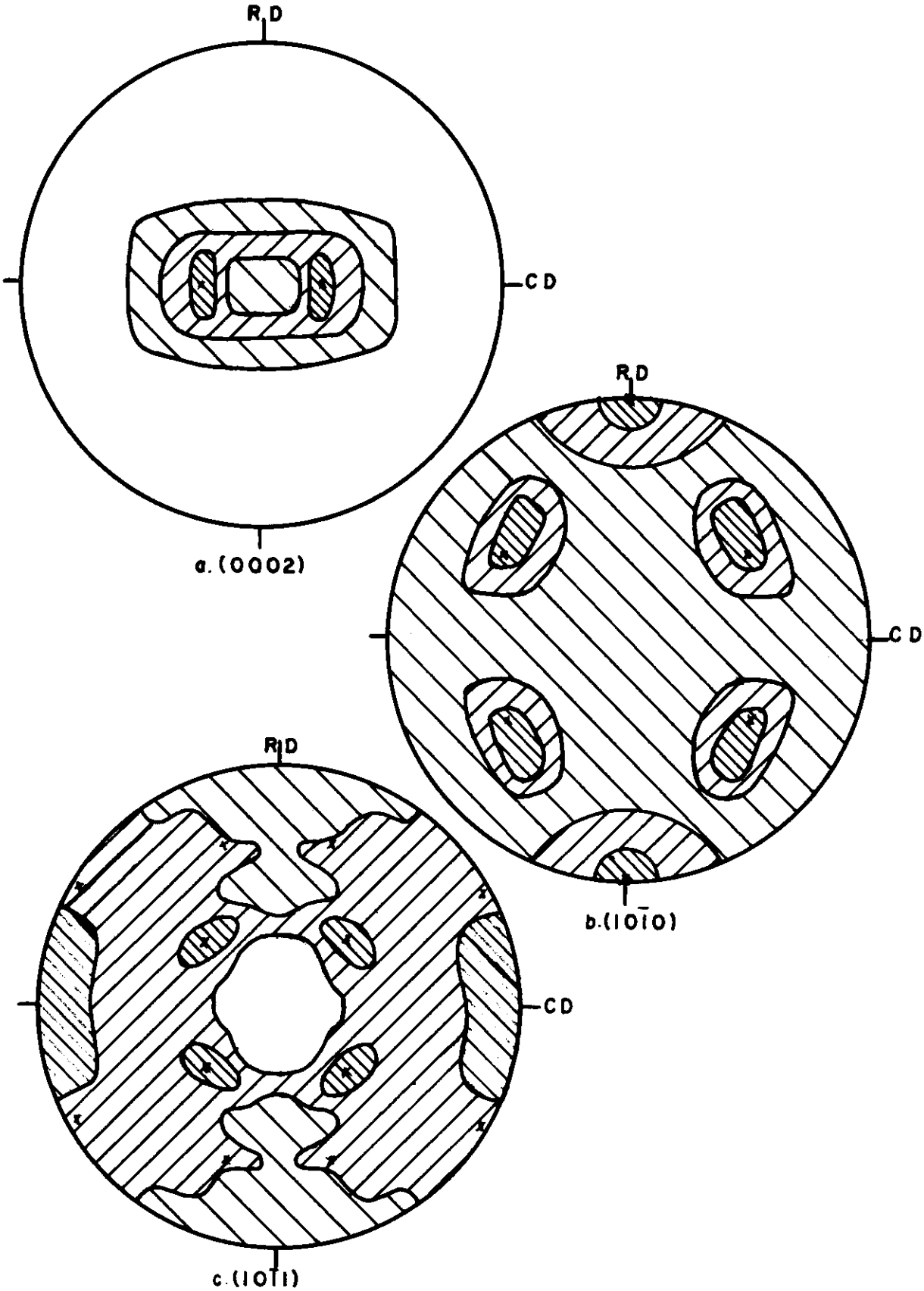


Fig. 5 Texture of 3.6% Ta - Ti alloy cold - rolled 94%. x = (0002) rotated 27°, [10$\bar{1}$0] II R. D.

crystal forms and the alpha lattice parameters have a negative deviation from Vegard's law (19). The composition-parameter results for these alloys are shown in Figure 48*.

Textures were studied for alloys containing 7.1% Zr (c/a = 1.590) and 14.75% Zr (c/a = 1.602). Figure 6 contains the pole figures for the 7.1% Zr alloy. The figures for both alloys were similar to each other and differ from those for iodide titanium only in the respects discussed for the Ti-Ta textures. These alloys showed the split basal $[10\bar{1}0]$ texture.

## D. DISCUSSION OF RESULTS

It has been suggested that the deformation mechanisms and deformation textures of hexagonal close-packed metals are peculiar to the deviation of their c/a ratios from the ideal packing. On this basis, it was suggested that the textures of metals or alloys having the same c/a ratio would be similar. However, as can be seen in Table 3, the results for the present alloys indicate that c/a ratio is not the sole governing factor.

TABLE 3

SUMMARY OF TEXTURES LISTING C/A RATIOS AND TYPE OF PHASE DIAGRAMS

| Material | C/A | Texture | Type of Phase Diagram |
|---|---|---|---|
| Ti | 1.588 | (0002) tilted 27°, $[10\bar{1}0]$ | |
| Zr | 1.589 | (0002) tilted 40°, $[10\bar{1}0]$ (16) | |
| Be | 1.57 | (0002) $[10\bar{1}0]$ (20) | |
| 3.8% Al-Ti | 1.600 | (0002) $[10\bar{1}0]$ | Wide alpha range, intermediate phases |
| 3.6% Cb-Ti | 1.592 | (0002) tilted 40°, $[10\bar{1}0]$ | Narrow alpha range, beta stabilized |
| 3.6% Ta-Ti | 1.584 | (0002) tilted 27°, $[10\bar{1}0]$ | Moderate alpha range, beta stabilized |
| 15.4% Ta-Ti | 1.575 | (0002) tilted 27°, $[10\bar{1}0]$ | Moderate alpha range, beta stabilized |
| 7.1% Zr-Ti | 1.590 | (0002) tilted 30°, $[10\bar{1}0]$ | Complete solid solubility |
| 14.75% Zr-Ti | 1.602 | (0002) tilted 30°, $[10\bar{1}0]$ | Complete solid solubility |

* An asterisk following a Figure denotes that those figures are located in the Appendix.

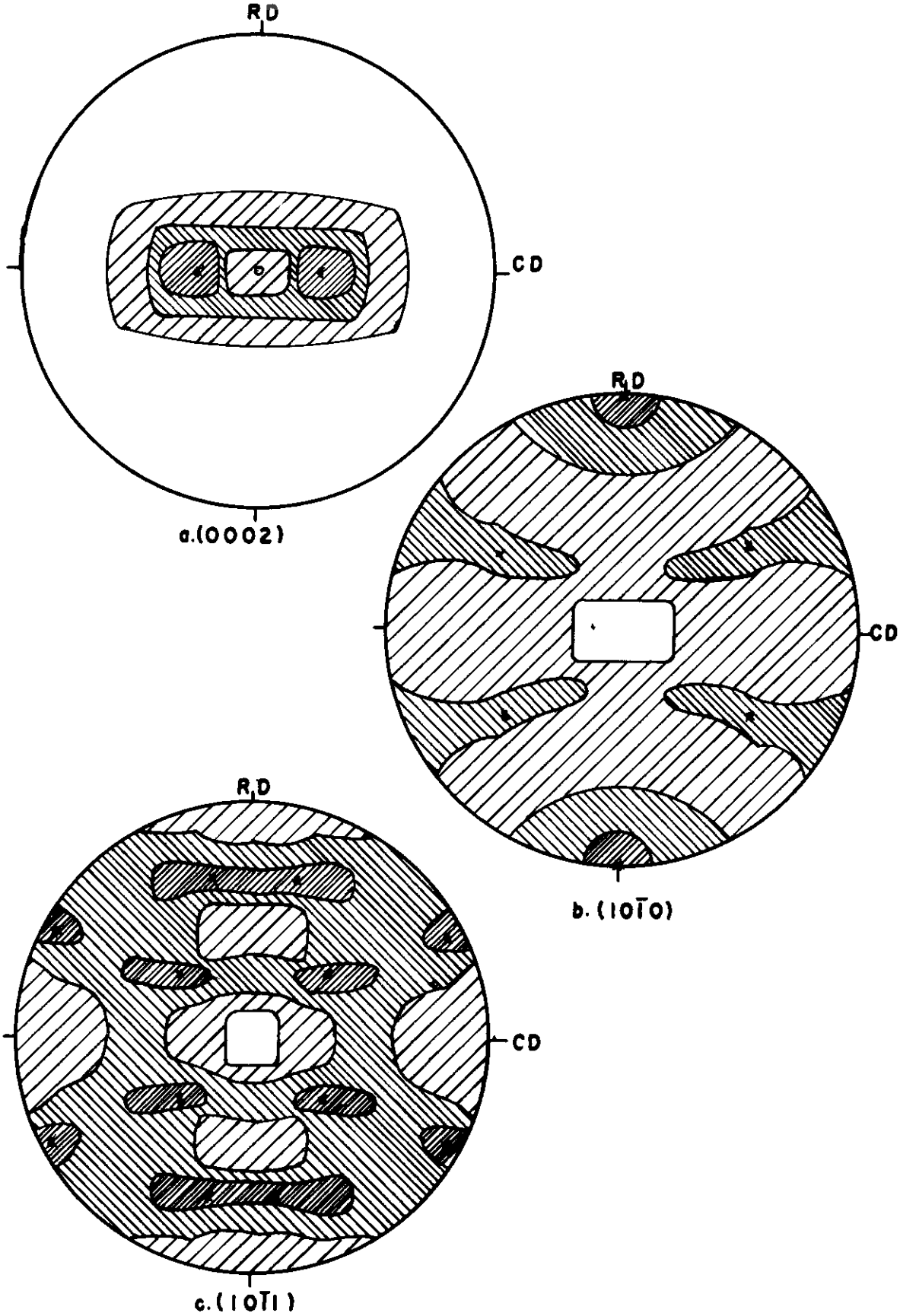


Fig. 6 Texture of 7.1% Zr-Ti alloy cold-rolled 94%. x = (0002) rotated 30° [10$\bar{1}$0] ll R. D.

In the cases of the titanium-base alloys containing 3.8% Al and 14.75% Zr, having c/a ratios of 1.600 and 1.602, respectively, there were entirely different textures. The Ti-Al alloy possessed a cold-rolled texture described as (0002) [ $10\bar{1}0$ ] and the Ti-Zr alloy possessed a tilted (0002) [ $10\bar{1}0$ ] texture similar to that of iodide titanium (c/a = 1.588).

It has been observed that the cold-rolled texture of beryllium (20), (0002), [ $10\bar{1}0$ ], resembles that of magnesium. However, the scatter from this mean orientation is toward the cross direction, whereas that for magnesium is toward the rolling direction. The texture of beryllium (c/a = 1.57) is inconsistent with any relationship between c/a and texture since the texture tends toward that associated with higher c/a ratios (near 1.63). Furthermore, a Ti-Ta alloy was investigated during this study which has a c/a ratio close to that of beryllium (1.575 and 1.57 respectively). This Ti-Ta alloy had the tilted (0002) [ $10\bar{1}0$ ] texture in contrast to the (0002) [ $10\bar{1}0$ ] texture of beryllium.

The textures of titanium alloyed with columbium (c/a = 1.592), tantalum (c/a = 1.584 and 1.575) and zirconium (c/a = 1.590 and 1.602) have the same basic textures and differ from the texture of iodide titanium only, by having areas of second high intensity 15° to 20° from the center of the (0002) pole figure in the rolling direction, by shifts in the positions of the basal maxima along the cross direction and, in general, by more scatter. In addition to these differences, the basal pole figures of the alloys containing zirconium, columbium and tantalum did not show the low intensity region extending completely across the figure.

An interesting observation may be made from consideration of the phase diagrams of the systems studied. As indicated in Table 3, the Ti-Al system shows a wide alpha solid solution range and two intermediate phases. The Ti-Cb and Ti-Ta systems show more restricted alpha regions, and the beta phase is stabilized to room temperature for higher concentrations of the solute. The Ti-Zr system shows complete solid solubility. At least in this investigation, the system showing intermediate phases has a deformation texture different from that of the pure solvent, whereas those systems with no intermediate phases retained the texture of the solvent. The possibility that the factors determining the nature of the phase diagram are related also to deformation textures is worthy of further study.

Most rationalizations of textures have been based on considerations of the crystal structure, deformation mechanisms and relative ease of deformation on the various systems. Before analysis of the effect of alloying on textures can be carried out along these lines, it will be necessary to determine the effect of alloying on the deformation mechanisms. This has been done for these alloys and will be discussed in later sections.

SECTION IV

# CHANGE IN SPLIT BASAL TEXTURE OF COLD-ROLLED TITANIUM WITH VARYING ALUMINUM CONCENTRATION

## A. RESULTS AND DISCUSSION

Cold-rolled titanium was found to have a texture best described by (0002) rotated 27° in the cross direction with $[10\bar{1}0]$ parallel to the rolling direction. A solid solution alloy of titanium with 3.8% aluminum cold-reduced 90% was found to have a texture best described by (0002) 11 R.P., $[10\bar{1}0]$ 11 R.D. with greatest basal scatter in the cross direction. These basal pole figures are reproduced in Figure 7 along with that for titanium containing approximately 1/4, 1/2, 1 and 1-1/2% aluminum after 90% cold reduction. Comparison of these basal pole figures shows the gradual forming of the non-split basal texture with increasing aluminum content.

It is noted that as little as 0.27% aluminum has an effect on the degree of scatter of the basal poles in the cross direction. As the aluminum content increases the basal poles are brought closer to the normal direction but tend to scatter in the rolling direction leaving a secondary intensity region immediate to the normal direction about which the most intense region of poles are located. At a higher concentration of aluminum (1.05%), the basal poles have been rotated to produce highest intensity immediate to the normal direction. Thus, it seems that there is some resistance to further basal pole movement to the normal direction when the poles are already near the normal direction. As is discussed in Section VIII, where application of the Calnan and Clews theory was made to the deformation textures, the presence of the basal poles in the rolling plane normal were attributed to compressive slip on the (0001) by Williams and Eppelsheimer (21) and to tension twinning on the $(11\bar{2}1)$ or $(11\bar{2}2)$ by the present investigator. Since the frequence of (0001) slip occurance was practically nil and aluminum additions tend to increase the frequency of occurance of twinning, the increase in (0001) poles in the rolling plane normal could be attributed to increased twinning on the $(11\bar{2}1)$ and $(11\bar{2}2)$ planes.

A more detailed discussion is given in Section VIII where many processes of texture formation are compared without any decisive conclusions.

Thus, it can be said that the formation of the non-split basal texture is gradual with increasing aluminum content and is definitely present at concentrations above 1.5% by weight aluminum in titanium.

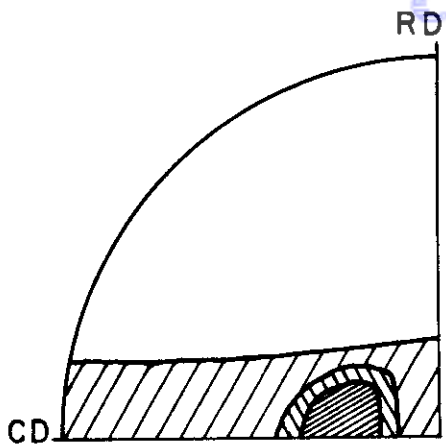


Iodide Titanium

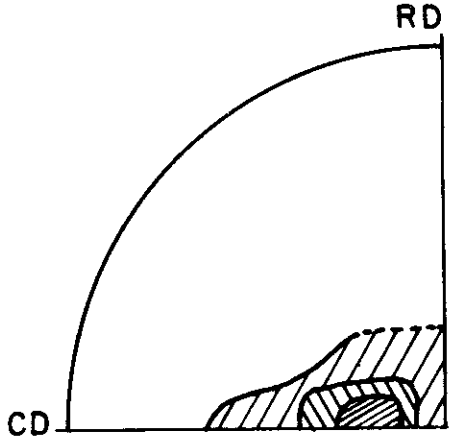


Ti - 0.27% Al

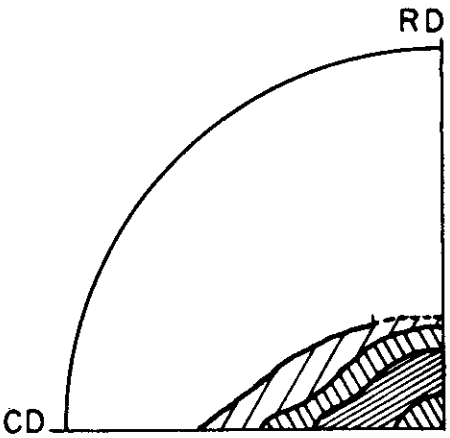


Ti - 0.47% Al

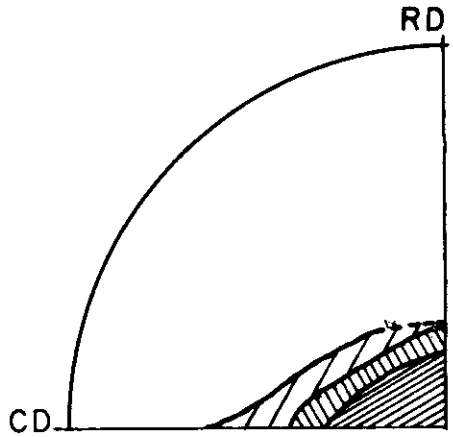


Ti - 1.05% Al

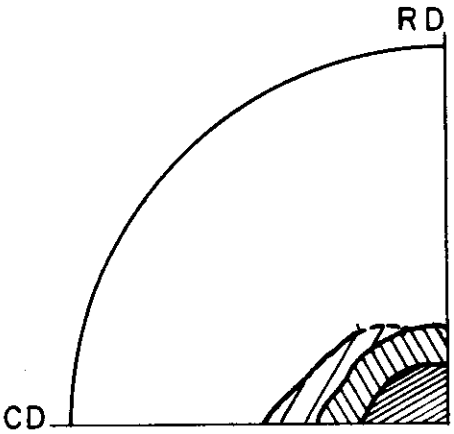


Ti - 1.43% Al

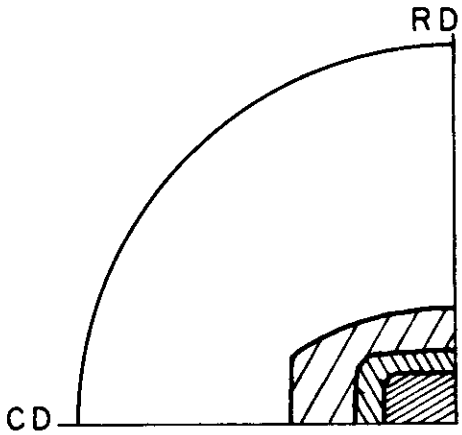


Ti - 3.8% Al

Fig. 7 Basil pole figure showing effect of Al on Ti in changing from split to non-split texture. (0002). Cold-rolled 90%.

SECTION V

# EFFECTS OF ANNEALING ON TEXTURES OF COLD-ROLLED TITANIUM AND TITANIUM SOLID SOLUTION ALLOYS

## A. INTRODUCTION

It was noted in Section III that the only major difference existing between the cold-rolled textures of titanium and its alloys was that the 3.8% Al-Ti alloy displayed the non-split basal while all the other alloys showed the split basal texture. By observing the effects of annealing on the cold-worked texture, it is possible to receive some insight into the mechanisms of recrystallization, such as 'oriented nucleation' or 'oriented growth', or a combination of both. The knowledge of the annealing textures together with information relative to the hot-deformation mechanisms will contribute much to a rationalization of the hot-rolled textures.

The cold-rolled textures of zinc (11), magnesium (11), and beryllium (20), are best described as (0001) [$10\bar{1}0$]. However, on recrystallizing the textures are basically the same as before annealing (11,20). For zirconium which has been cold-rolled and annealed at 1112° F for one hour, the reported texture has changed essentially from a tilted (0001) [$10\bar{1}0$] to a tilted (0001) [$11\bar{2}0$] (15,17). This annealed texture can be related to the cold-rolled texture by rotations of 20° or 40° about the C-axis of the rolled texture. The effects of annealing temperature on preferred orientation and grain size of titanium solid solution alloys are reported in this section.

The experimental procedure used in this work was described in Section I.

## B. RESULTS

The summary of results on textures and grain sizes for annealed titanium and titanium alloys are presented in Table 4.

### Unalloyed Titanium

The pole figures of cold-rolled titanium and of titanium annealed for one hour at 1000°, 1300°, and 1500° F and for three hours at 1000° F are shown in Figures 2,8,9,10 and 11. The cold-rolled texture has the basal planes inclined approximately 30° to the rolling plane toward the transverse direction and the [$10\bar{1}0$] directions aligned with the rolling direction, Figure 2. Annealing for one hour at 1000° F caused a slight sharpening of the deformation texture, Figure 8, whereas the three hour anneal at this temperature, Figure 11, and the one hour anneal at 1500°F, Figure 10,

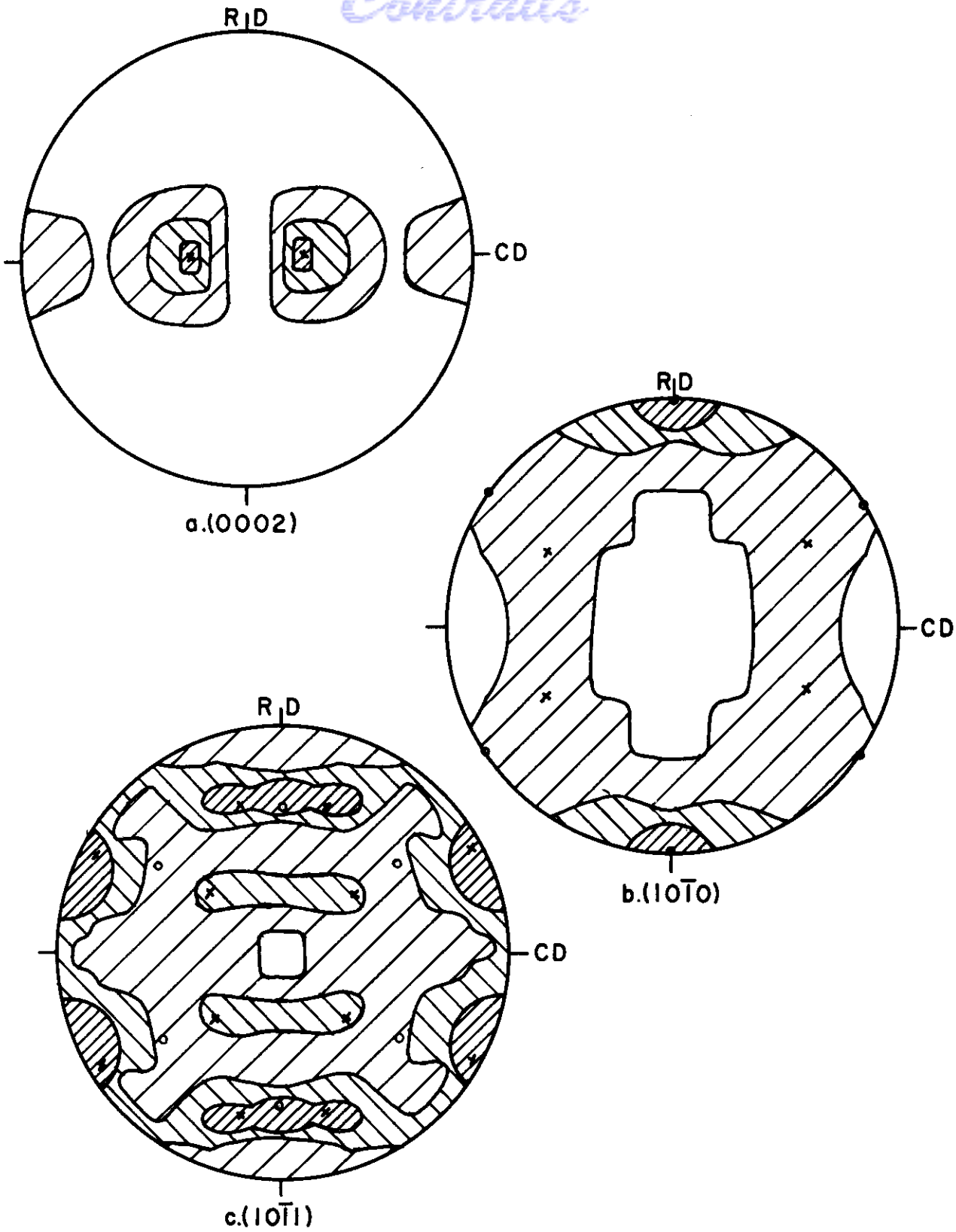


Fig. 8 Texture of Iodide Titanium cold-rolled 97% and annealed one hour at 1000°F. o = (0002) [10$\bar{1}$0], x = (0002) rotated 27° from R.P. [10$\bar{1}$0] ∥ R.D.

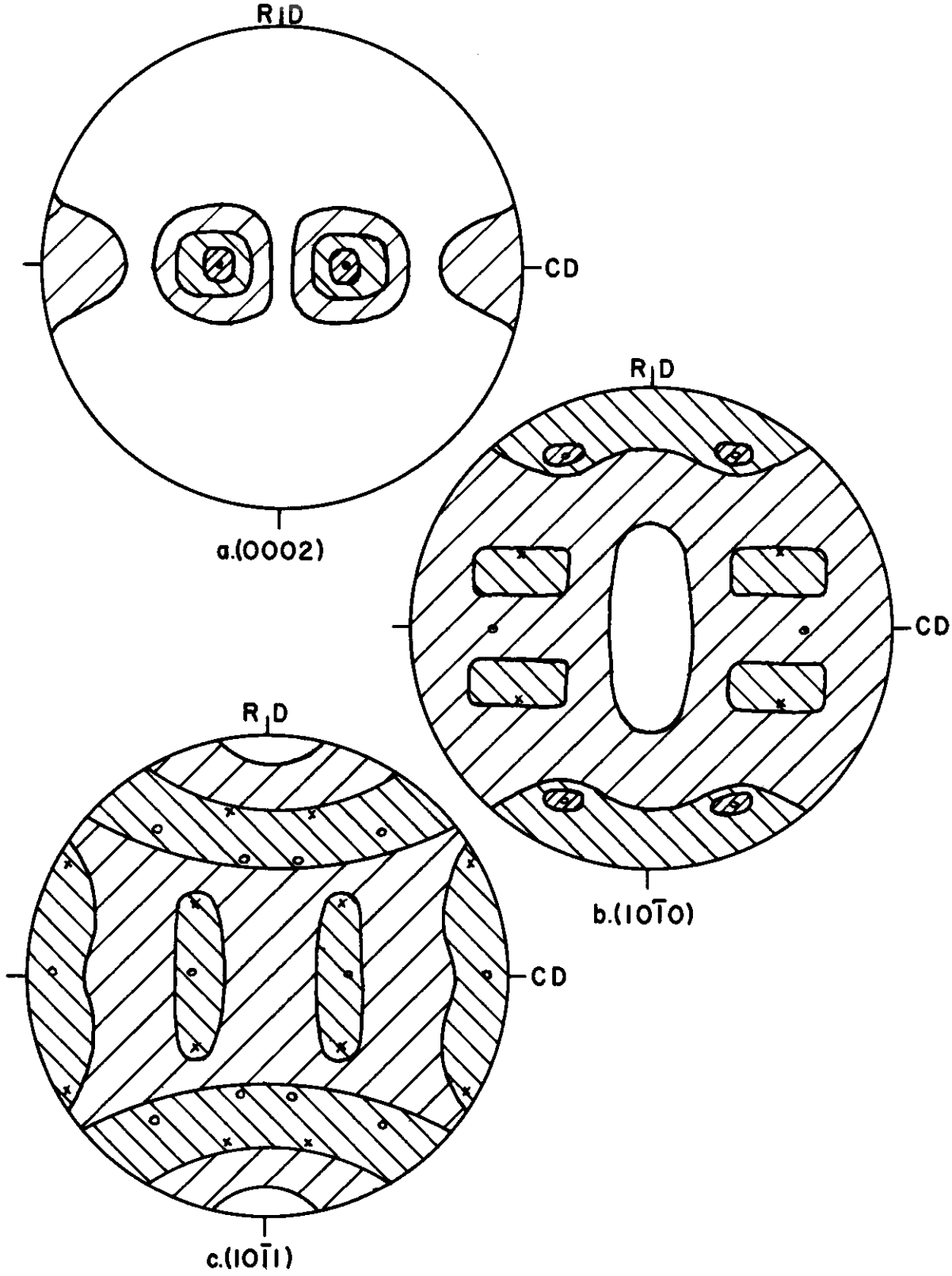


Fig. 9 Texture of Iodide Titanium cold-rolled 97% and annealed one hour at 1300°F.. o = (0002) rotated 27° from R.P. [11$\bar{2}$0] ∥ R.D. x = (0002) rotated 27° from R.P. [10$\bar{1}$0] ∥ R.D.

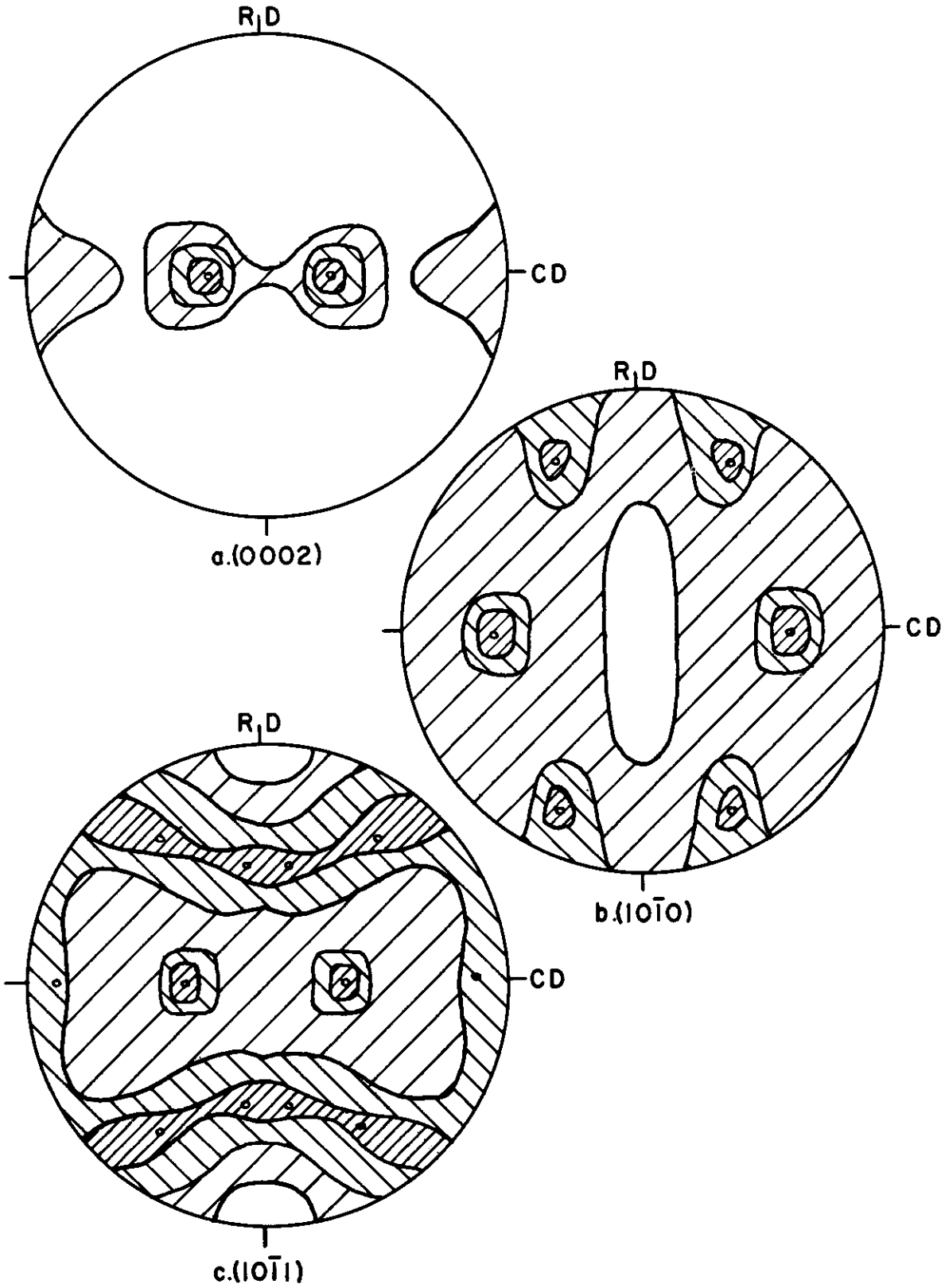


Fig.10 Texture of Iodide Titanium cold-rolled 97% and annealed one hour at 1500°F. o = (0002) rotated 27° from R. P. [11$\bar{2}$0] ∥ R. D.

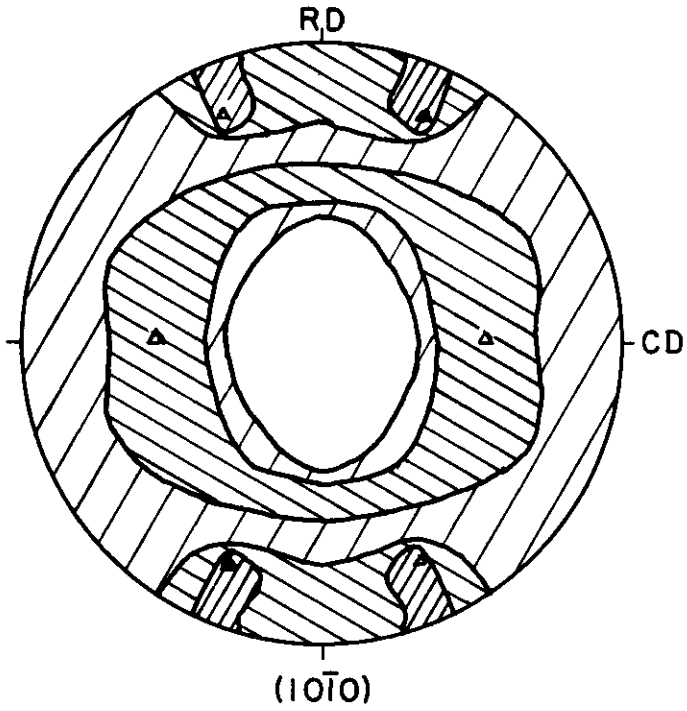


Fig.11 Texture of Iodide Titanium cold-rolled 97% and annealed three hours at 1000°F. Δ = (0002) rotated 27° from R.P. [11$\bar{2}$0]

resulted in textures with the tilted basal planes but with [ $11\bar{2}0$ ] directions approximately parallel to the rolling direction. The texture of the 1300°F specimen contained components of each of the above textures.

Grain size determinations on the specimen annealed for one hour at 1000°F, made by counting the number of grains in a representative area of a photomicrograph, revealed grains of uniform size averaging less than 2 microns in diameter, Table 4. The differences in orientation of adjacent areas appeared to be slight. The iodide titanium specimen annealed one hour at 1300°F contained some grains with diameters as large as 20 microns and others on the order of 2 microns. The microstructure of the specimen annealed one hour at 1500°F contained grains ranging up to 0.10 mm, with an average size of 0.051 mm. The grain size of the three-hour, 1000°F annealed specimen was 0.01 mm and uniform, Figure 12.

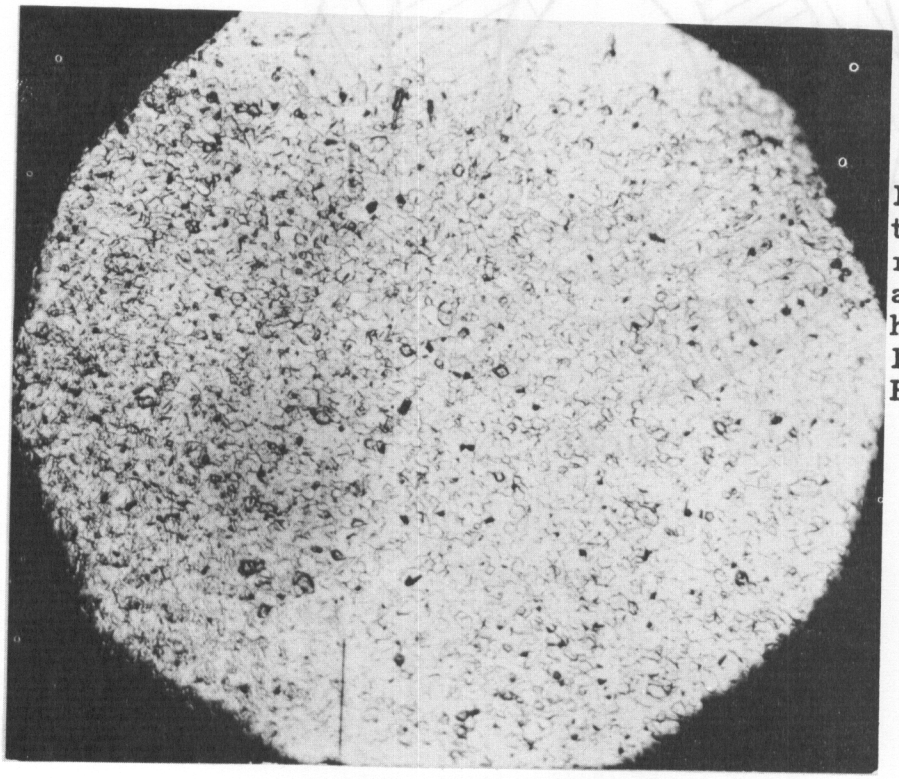

Fig. 12 Iodide titanium cold-rolled 97% and annealed for three hours at 1000°F. Etchant: $HNO_3$-HF-$H_2O$. X 250

## 3.8% Aluminum-Titanium

The texture of the cold-rolled 3.8% aluminum-titanium alloy was described as (0002) [ $10\bar{1}0$ ], Figure 3. Annealing one hour at 1500°F changes this texture to (0002) [ $11\bar{2}0$ ], Figure 13. Both the ($10\bar{1}0$) and ($10\bar{1}1$) pole figures show large amounts of scatter in the rolling direction. Pole figures which were obtained for a specimen annealed one hour at 1300°F showed both (0002) [ $10\bar{1}0$ ] and (0002) [ $11\bar{2}0$ ].

Grain size determinations, made by counting the number of grains

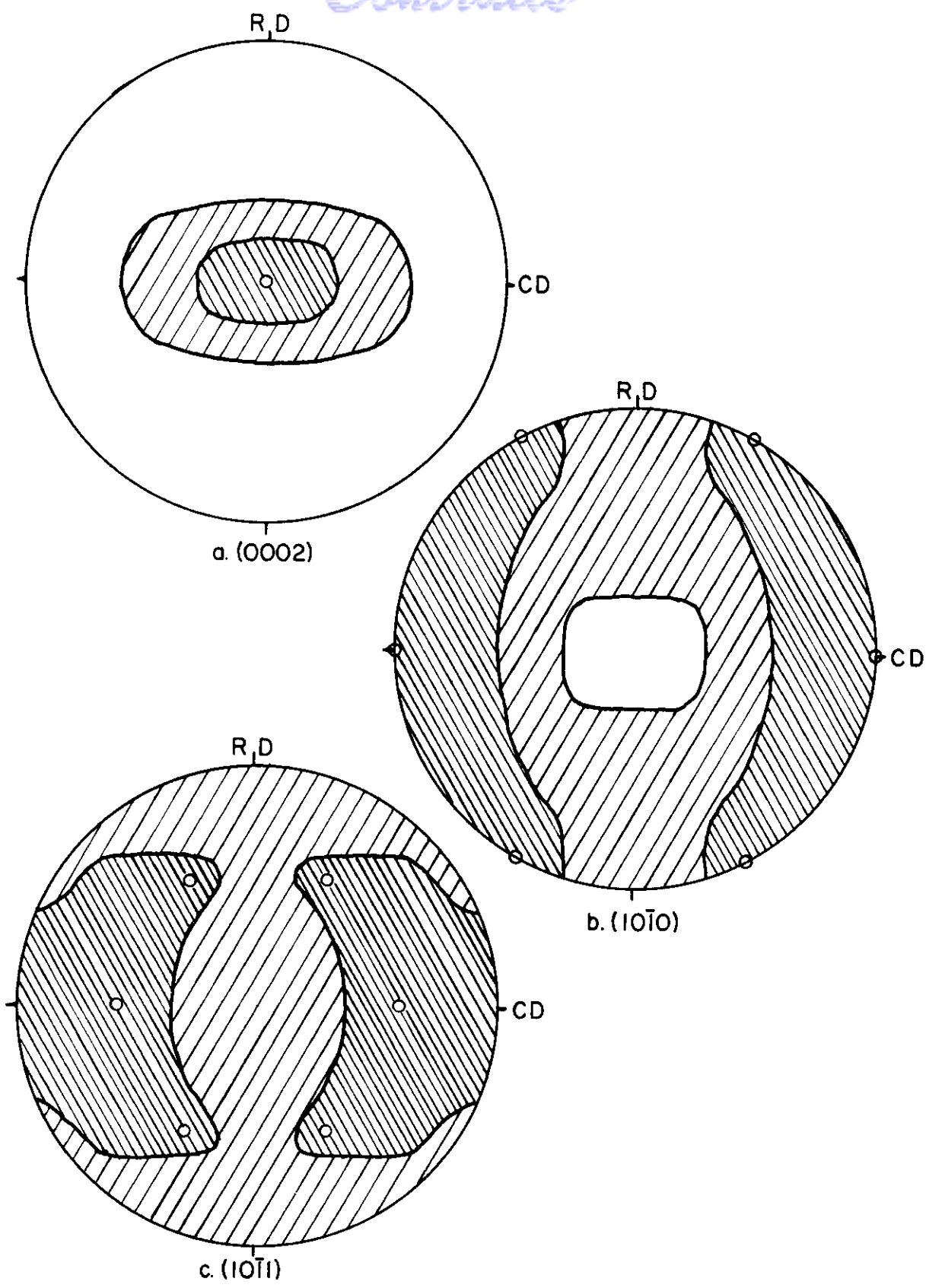


Fig.13 Texture of 3.8% Al-Ti alloy cold-rolled 94% and annealed one hour at 1500°F. o = (0002) [11$\bar{2}$0].

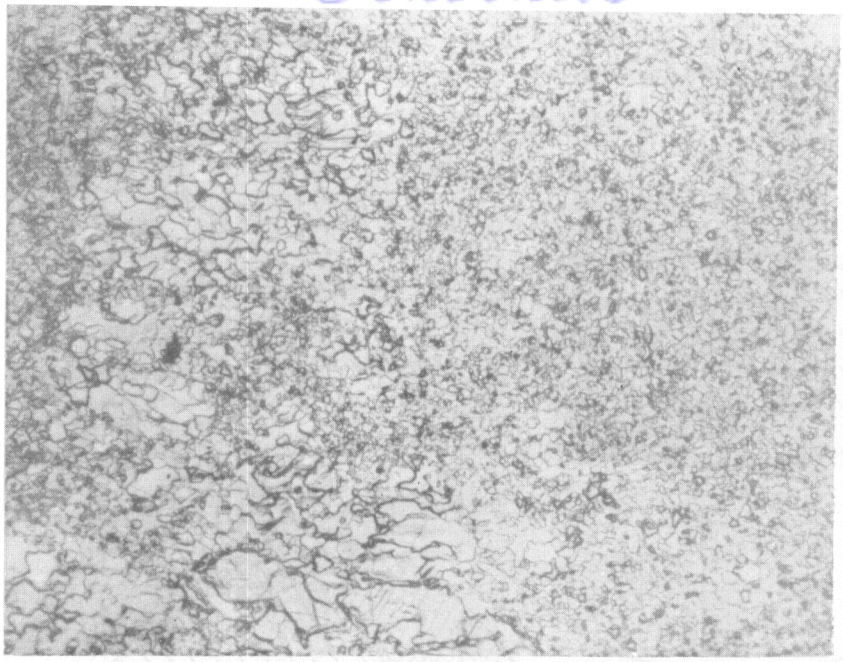

a. X83

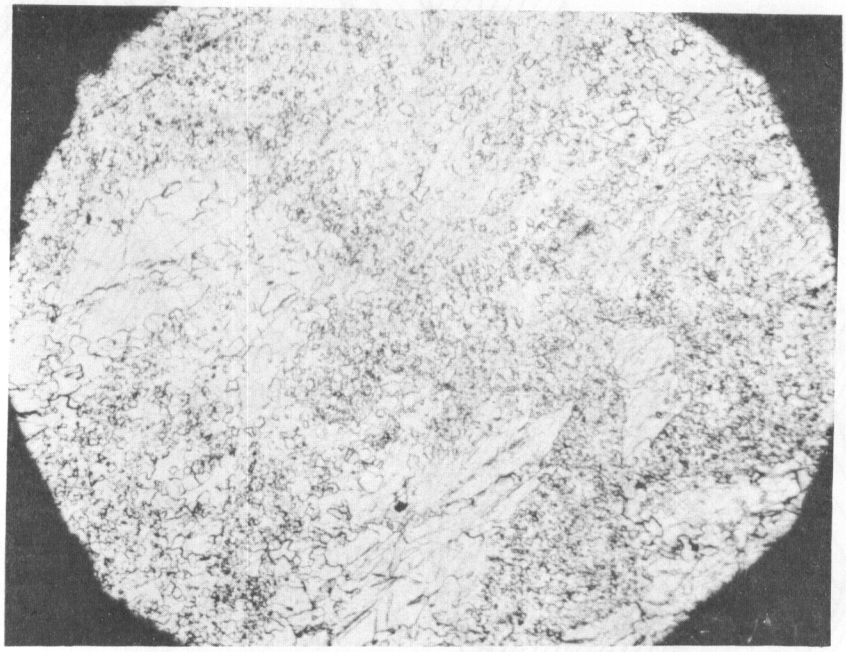

b. X100

Fig. 14 3.8% Al-Ti cold-rolled 94% and annealed one hour at 1300°F; a and b are same specimen but different areas. Etchant: $HNO_3$-HF-$H_2O$.

in a representative area of a photomicrograph, gave average grain diameters of 0.015 mm and 0.02 mm for the titanium-aluminum alloy annealed at 1300° and 1500°F, respectively, Table 4. The microstructures of these specimens annealed at 1300°F were characterized by duplex grain structure, Figure 14. After annealing at 1300°F the grain boundaries were not clearly delineated in some cases but areas corresponding to grains showed slight differences in intensity of reflected light. Also, the grain structure of the specimen annealed at 1300°F was such as to suggest a growth of certain grains at the expense of the matrix. This was even more pronounced for the one hour at 1500°F anneal in that the larger grains appeared to follow paths of faster growth and to isolate the regions of almost similar orientations. On the basis of reflectivity, these regions appeared to differ but slightly from the surrounding matrix, Figure 15.

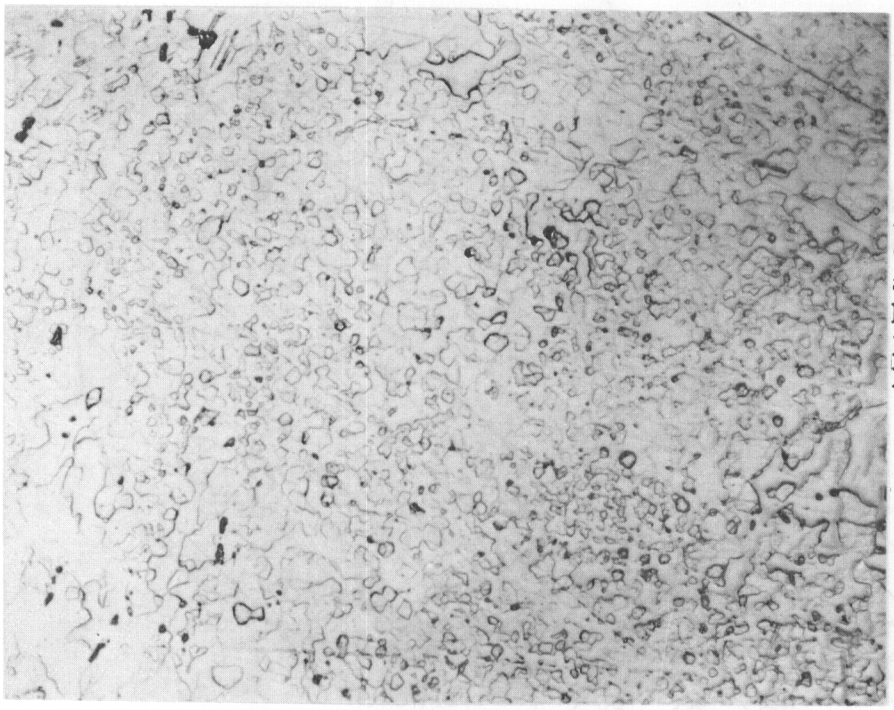

Fig. 15 3.8% Al-Ti cold-rolled 94% and annealed one hour at 1500°F. Etchant: $HNO_3$-HF-$H_2O$. X 100

## 3.6% Columbium-Titanium

In Figure 16 are presented the pole figures of 3.6% columbium-titanium alloy annealed one hour at 1500°F. These figures can be described in terms of a duplex texture, both components having the basal planes tilted approximately 40° to the rolling plane. The stronger component has $[10\bar{1}0]$ directions parallel to the rolling direction while the weaker has $[11\bar{2}0]$ directions aligned with the rolling direction. This alloy annealed one hour at 1300°F had a tilted $(0002)$ $[10\bar{1}0]$ texture as did the cold-rolled specimen.

Metallographic examinations of the 1300°F annealed specimen showed large areas sub-divided into regions of apparently slightly

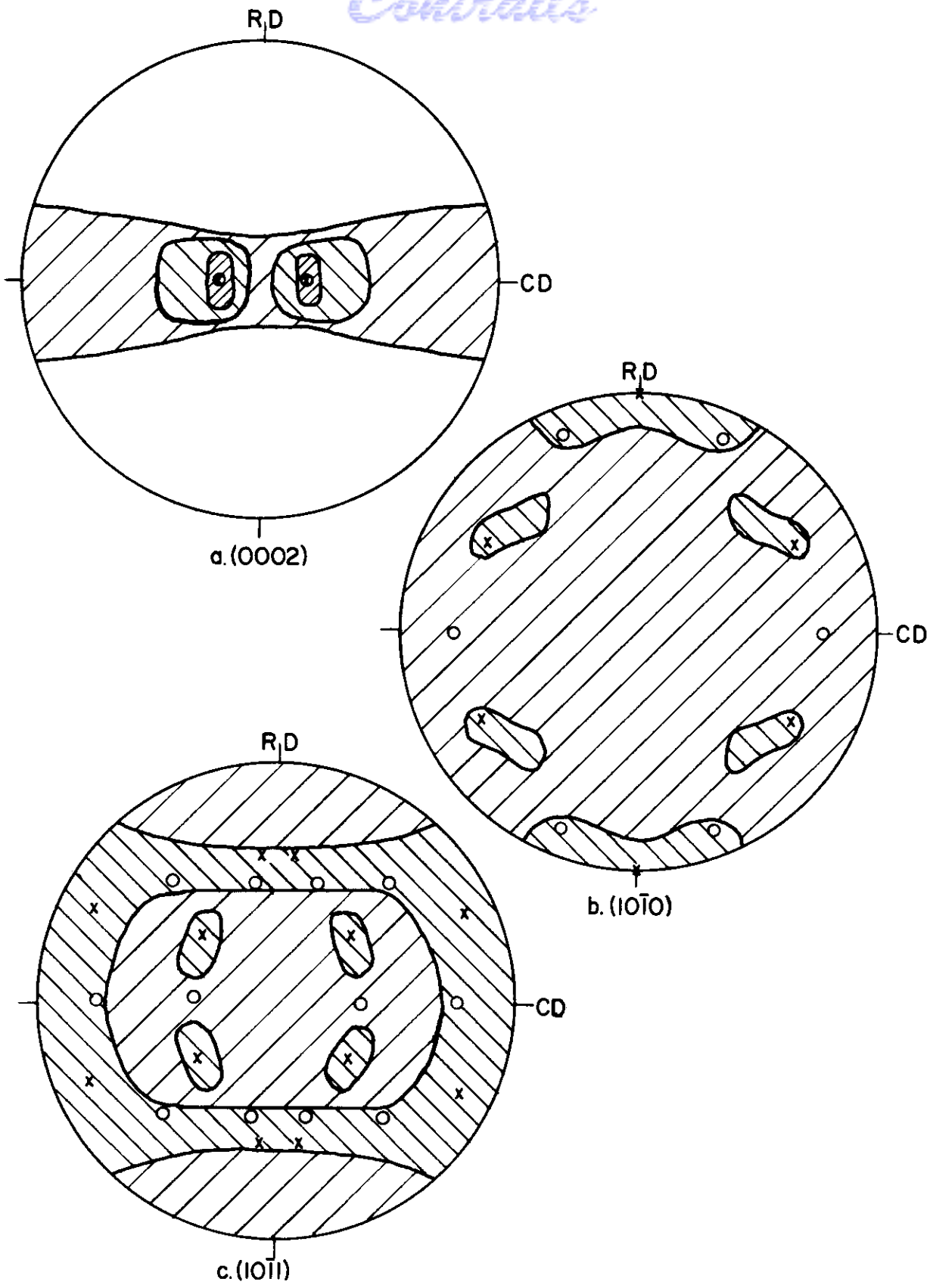


Fig.16 Texture of 3.6% Cb–Ti alloy cold-rolled 94% and annealed one hour at 1500°F. x = (0002) rotated 20° from R.P. [10$\bar{1}$0], o = (0002) rotated 20° from R.P. [11$\bar{2}$0].

different orientations. The irregular network of the boundaries of these larger regions was similar in appearance in many cases to that of ordinary grain boundaries. In other cases, no clear boundary was observed, but a change in the intensity of the reflected light of the microscope was noted. The average size of these sub-regions was found to be on the order of 0.002 mm.

The microstructure of the 1500° F specimen showed a number of grains with sharp boundaries intermingled with small areas similar to those sub-regions in the before mentioned 1300° F annealed specimens. The average grain size of the grains with sharp foundries was 0.010 mm and that of the smaller grains of poorly delinated boundaries 0.004 mm.

3.6% Tantalum-Titanium

Annealing the specimens of the 3.6% tantalum-titanium alloy for one hour at 1300° or 1500°F produced no significant changes in orientation from the cold-rolled texture, (0002) [$10\bar{1}0$]. Pole figures for the 1500° F treatment are shown in Figure 17. The grains or sub-grain regions of these specimens were too small and poorly defined for grain size measurements.

Strips of this alloy annealed for one hour at 1600°F showed a duplex texture, Figure 18. Both components of the texture have the basal planes tilted approximately 30° to the rolling plane toward the transverse direction. The stronger component has [$11\bar{2}0$] directions parallel to the rolling direction, whereas the minor component has the [$10\bar{1}0$]directions aligned with the rolling directions.

The average grain size for the 1600°F annealed specimen was 0.015 mm. However, it was noted that there were many grains as large as 0.030 mm and others as small as 0.002 mm.

7.1% Zirconium-Titanium

Annealing the 7.1% zirconium alloy for one hour at 1300°F produced the duplex texture shown in Figure 19. Again the components of this texture can be described as tilted (0002) [$10\bar{1}0$] and tilted (0002) [$11\bar{2}0$]. The one hour anneal at 1500° F produced a texture containing only the latter component, Figure 20.

An average grain size of 0.015 mm was observed for the 1300°F annealed specimen and 0.040 mm for the 1500°F annealed specimen. Their grain boundaries were fairly easily delineated. The 7.1% zirconium alloy annealed for one hour at 1300°F showed a rather uniform grain size, Figure 21, but polarized light indicated the grains to have varying orientations.

## C. DISCUSSION OF RESULTS

It is without doubt that the film technique used in this investi-

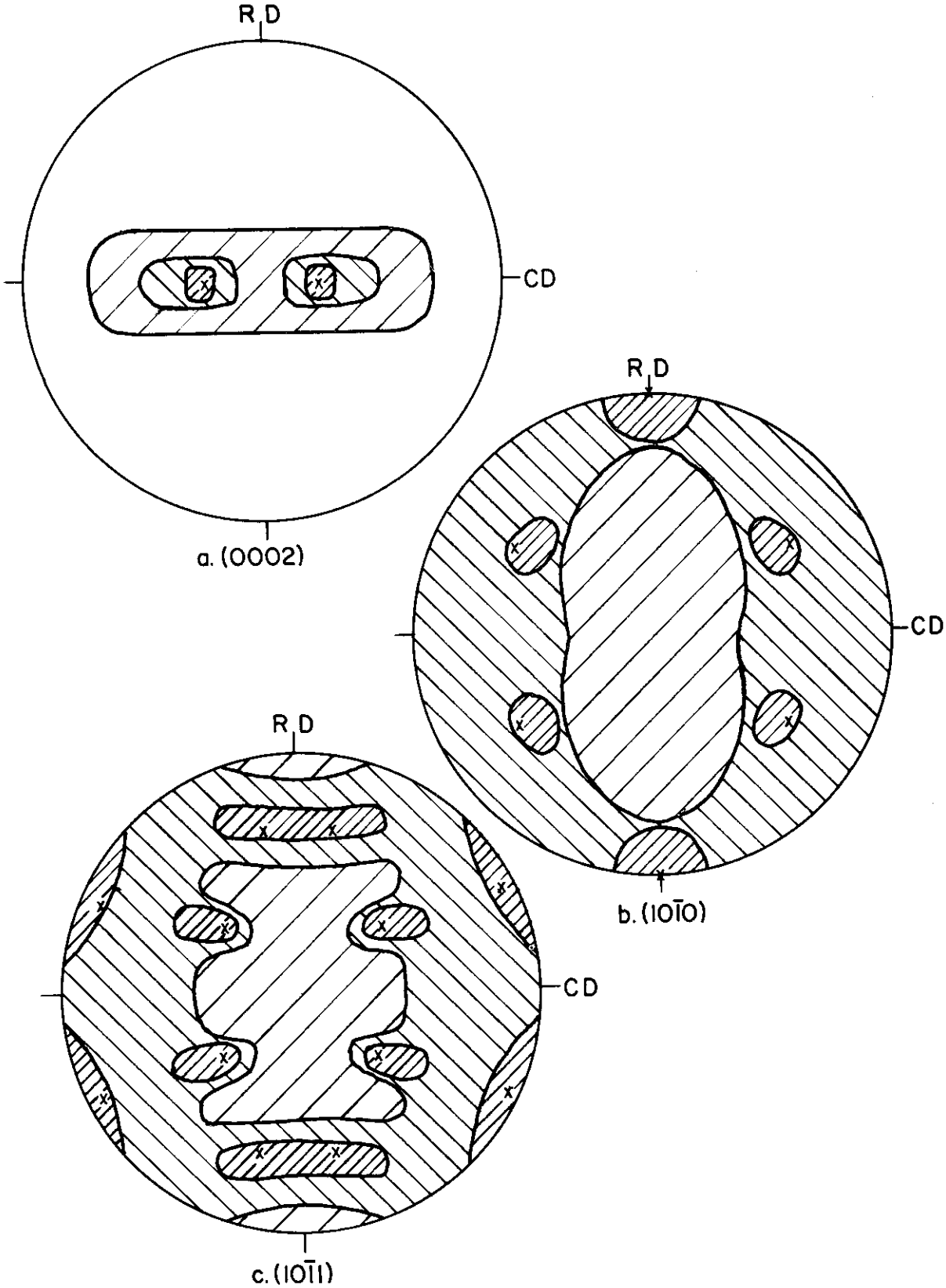


Fig.17 Texture of 3.6% Ta-Ti alloy cold-rolled 94% and annealed one hour at 1500°F. x = (0002) rotated 30° from the R.P. [10$\bar{1}$0].

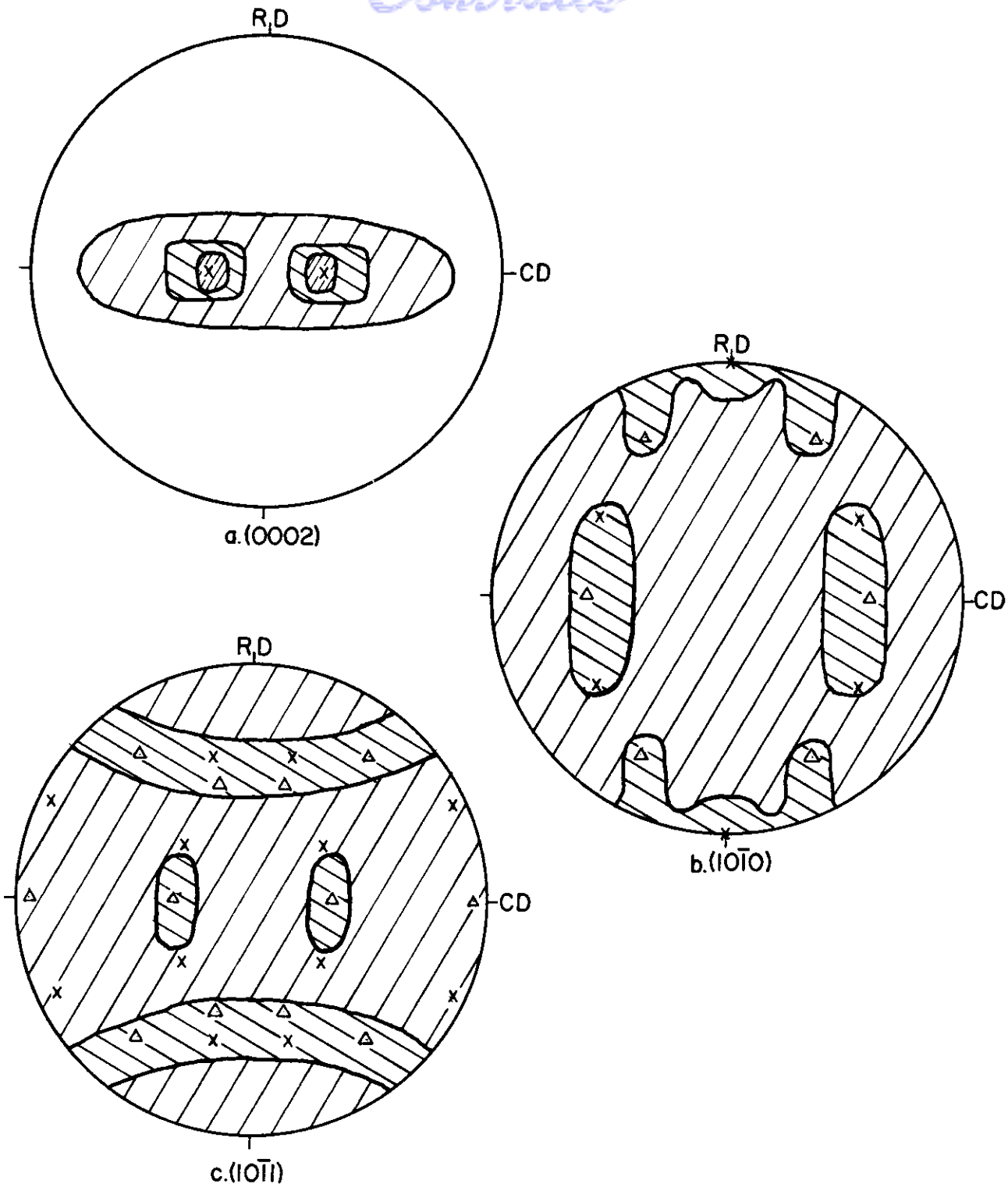


Fig.18 Texture of 3.6% Ta-Ti alloy cold-rolled 91% and annealed one hour at 1600°F. x = (0002) rotated 30° from R.P. [10$\bar{1}$0], Δ = (0002) rotated 30° from R.P. [11$\bar{2}$0].

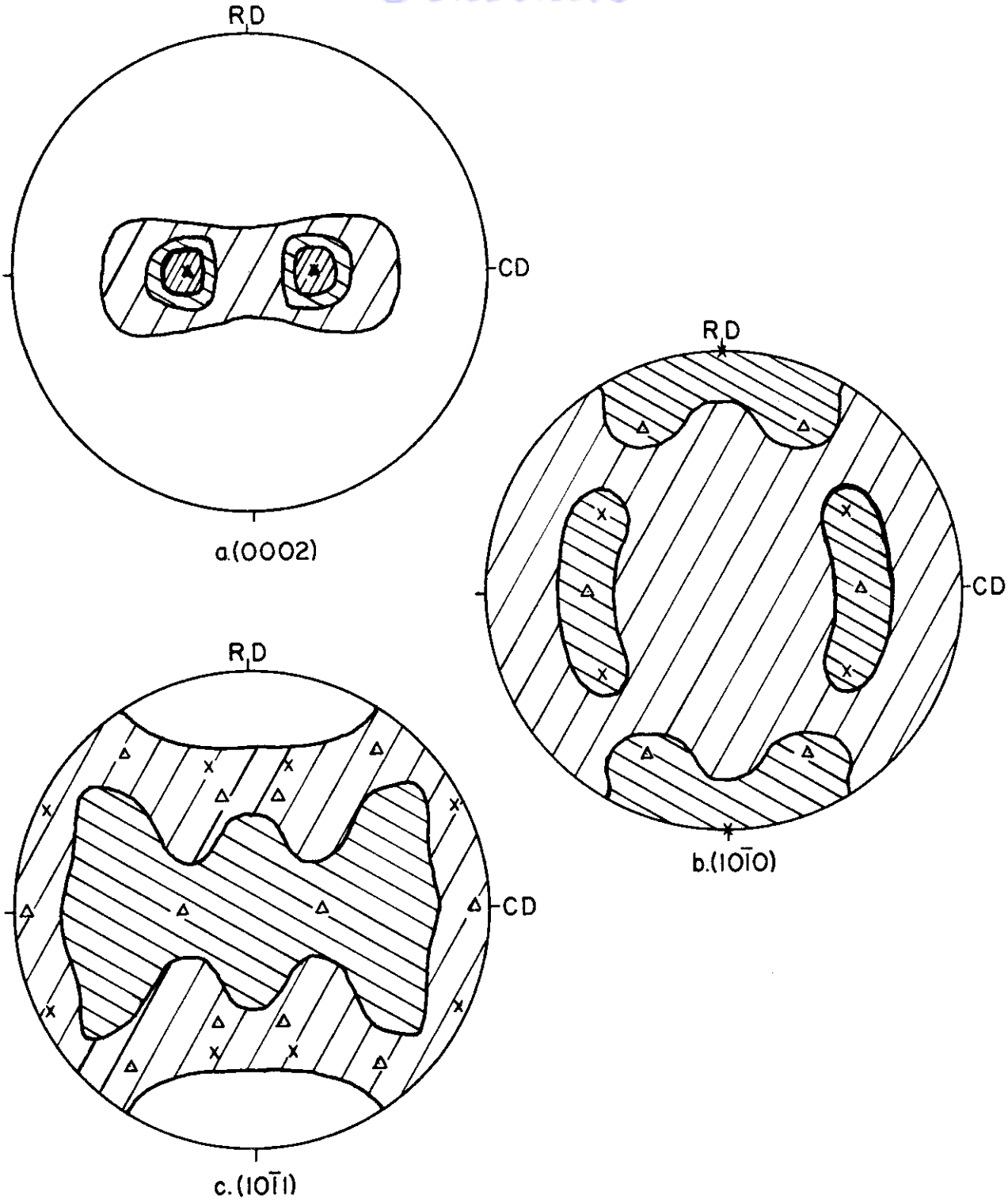


Fig.19 Texture of 7.1% Zr – Ti alloy cold-rolled 91% and annealed one hour at 1300°F. x = (0002) rotated 30° from R.P. [10$\bar{1}$0], Δ = (0002) rotated 30° from R.P. [11$\bar{2}$0].

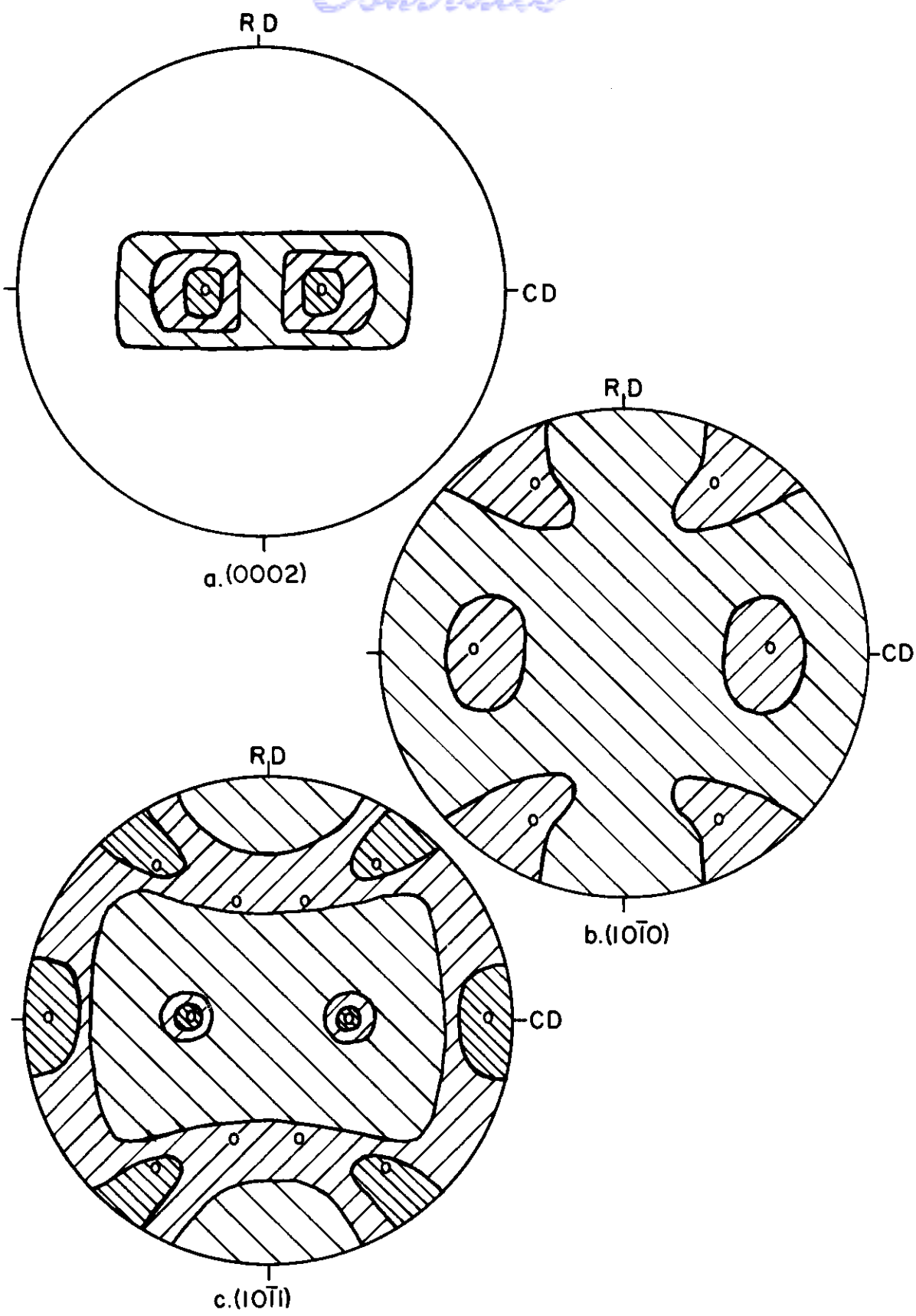


Fig. 20 Texture of 7.1% Zr – Ti alloy cold-rolled 94% and annealed one hour at 1500°F. o = (0002) rotated 27° from R.P. [11$\bar{2}$0].

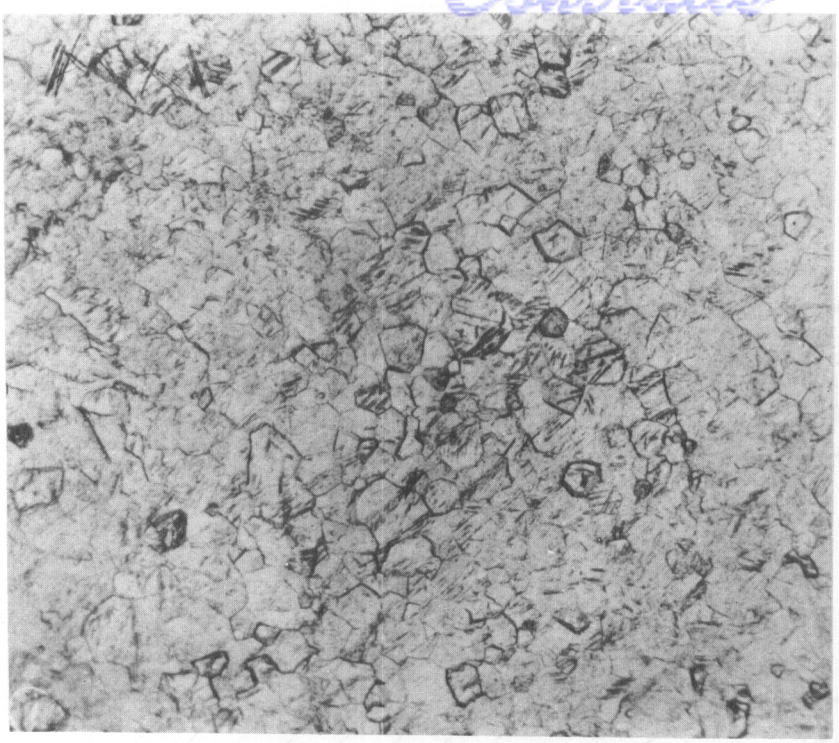

Fig. 21 7.1 % Zr-Ti cold-rolled 94% and annealed one hour at 1300 °F. Etchant: $HNO_3$-HF-$H_2O$. X 250

gation does not record the detail in pole figures obtainable with an X-ray Geiger counter spectrometer. Thus, the annealed textures described as having the $[11\bar{2}0]$ direction parallel to the rolling direction may actually have this direction symmetrically oriented a small amount away from the rolling direction (22), such as is the case for zirconium (17). Nevertheless, the results point to certain significant features which warrant discussion.

As can be seen from Figures 2,3,5 and 6, the cold-rolled textures of titanium and its solid solution alloys can be described as tilted $(000\bar{1})$ $[10\bar{1}0]$ with the exception of the 4% Al-Ti alloy, which has a non-split basal texture. On low annealing titanium (at 1000 °F for one hour) the deformation texture was retained with a slight sharpening of the basal poles but an increased randomness of the $(10\bar{1}0)$ poles, Figure 8. The microstructure of the titanium annealed for one hour at 1000 °F revealed a fine uniform grain size of approximate 0.002 mm in diameter. This texture was indicative of a 'recrystallization in situ' condition or a polygonized state of well delineated low-angle boundaries. The same results were observed on annealing the 3.6% Cb-Ti alloy for one hour at 1300 °F. On the other hand, annealing of titanium at 1300 ° F for one hour resulted in a partially reoriented texture and increased grain size. The effect of the columbium addition was to raise the temperature at which reorientation from the deformation texture occured. This same result was observed for additions of tantalum, where the annealing temperature at 1600 °F was required before reorientation occurred with one hour annealing. In all cases, the reorientations that were achieved on annealing at successively high temperatures tended toward a texture having the $[11\bar{2}0]$ parallel to the rolling direction.

The annealing texture as described above is, therefore, related to the deformation texture by a rotation of 30° about the C-axis. This is observed to be true for both split and non-split basal textures and results in an annealed texture which is best described as a (0001) rotated approximately 30° from the R.P. with [11$\bar{2}$0] 11 R.D.

TABLE 4

SUMMARY OF ANNEALING RESULTS

| Specimen | Treatment | Texture | Grain Diameter in mm |
|---|---|---|---|
| Iodide Ti | C.R. 97% | (0001) 30°R.P.[10$\bar{1}$0] | * |
| Iodide Ti | 1 hr. @ 1000°F | (0001) 30°R.P.[10$\bar{1}$0] | 0.002 |
| Iodide Ti | 3 hrs. @ 1000°F | (0001) 30°R.P.[11$\bar{2}$0] | 0.01 |
| Iodide Ti | 1 hr. @ 1300°F | (0001) 30°R.P.[10$\bar{1}$0]+[11$\bar{2}$0] | 0.015 |
| Iodide Ti | 1 hr. @ 1500°F | (0001) 30°R.P.[11$\bar{2}$0] | 0.05 |
| 3.8%Al-Ti | 1 hr. @ 1300°F | (0001) [10$\bar{1}$0]+[11$\bar{2}$0] | 0.015 |
| 3.8%Al-Ti | 1 hr. @ 1500°F | (0001) [11$\bar{2}$0] | 0.02 |
| 3.6%Cb-Ti | 1 hr. @ 1300°F | (0001) 40°R.P.[10$\bar{1}$0] | 0.002 |
| 3.6%Cb-Ti | 1 hr. @ 1500°F | (0001) 40°R.P.[10$\bar{1}$0]+[11$\bar{2}$0] | 0.01 |
| 3.6%Ta-Ti | 1 hr. @ 1300°F | (0001) 30°R.P.[10$\bar{1}$0] | * |
| 3.6%Ta-Ti | 1 hr. @ 1500°F | (0001) 30°R.P.[10$\bar{1}$0] | * |
| 3.6%Ta-Ti | 1 hr. @ 1600°F | (0001) 30°R.P.[10$\bar{1}$0]+[11$\bar{2}$0] | 0.015 |
| 7.1%Zr-Ti | 1 hr. @ 1300°F | (0001) 30°R.P.[10$\bar{1}$0]+[11$\bar{2}$0] | 0.015 |
| 7.1%Zr-Ti | 1 hr. @ 1500°F | (0001) 30°R.P.[11$\bar{2}$0] | 0.04 |

*Too fine for measurement

Though there are several theories of nucleation, there is general agreement now with the proposal by Cahn (23) that recrystallization nuclei form by a process of polygonization. This method of polygonization has been used to account for recovery and the formation of subgrains in deformed and annealed metals. One can account for the low temperature annealing effect where there is a slight sharpening of tex-

ture with the theory of polygonization, ascribing this effect to subgrain formation and relief of strain. The mechanism of preferential absorption (24) may be responsible for the large reorientations that take place in the (0001) pole figure on annealing titanium at 1000°F. This reorientation relates to the removal of material orientated at approximately 30° from the main component in the cross direction (a tilt of 30° between C-axes). This accounts for absorption of small grains that are oriented considerably from the dominating texture as a result of the greater mobility of their higher energy boundaries.

When the gross reorientation of the grains takes place on further annealing either at higher temperature or longer times in such a manner as to give a wholly different texture with respect to the deformation texture, there is usually an association of grain growth. This aspect of the oriented growth theory shall be dealt with in detail.

For explaining the relationship between the annealed texture and the deformation texture, two general theories have been put forth. They are 'oriented nuclei' and 'oriented growth'. Both theories have accounted for most of the observed recrystallization textures in metals, in general. In order to explain the annealing texture, the theories must account for the lack of grains oriented in any position other than that found for the annealed texture.

The 'oriented nucleation' theory formerly generally accepted proposes that the recrystallization textures are determined by the formation of nuclei in the deformed matrix in such a manner that they have the orientation of the recrystallized or annealed texture with respect to the matrix (25-27). On the other hand, the 'oriented growth' theory as described by Beck and co-workers (28-33), predicts an annealing texture related to the deformation texture in a manner such that the recrystallized grains are oriented for maximum misfit energy with respect to the 'recrystallization in situ' texture. The dependency of the grains for growth upon their disregistry with neighboring grains prevails even though there may be other randomly orientated grains which will compete for growth.

Both of the mechanisms introduced above will account for the annealing reorientations observed in titanium and its solid solution alloys. The oriented nuclei are obtained by the mechanisms proposed by Burgers et al (25) and by Cahn (23) using the high energy clock theory. These nuclei are formed by the passing of two slip planes close to each other but not transversing the entire grain in such a manner as to create an area of 'local curvature' which is oriented with respect to the matrix grain by a rotation parallel to the active slip plane and perpendicular to the active slip direction.[1/] For titanium and its solid

1/ A similar orientating of potential nuclei, e.g., a rotation about an axis in the slip plane normal to the slip direction would be obtained also by kink banding and other mechanisms of distorsion.

solution alloys, the slip has been shown to occur predominately on $(10\bar{1}0)$ $[11\bar{2}0]$. Thus, on annealing one would expect from this theory the relationship between the deformation and annealing textures to be a rotation about the C-axis. This has been observed to be the case. However, this mechanism has not always been found to be applicable (34-36) for the explanation of textures resulting from annealing of cold-worked metals.

In applying the oriented growth theory to the resulting textures for annealed titanium, the orientation of maximum misfit between neighboring grains must be known. This has been stated for the case of hexagonal close-packed metals to be a relationship between grains of a 30° rotation about the C-axis (29). This can be intuitively felt since a 30° rotation about the C-axis is half-way between two positions of perfect match. Hence, a $[10\bar{1}0]$ direction lying 30° to another $[10\bar{1}0]$ direction would be a situation of maximum boundary mismatch. There is opposition to the oriented growth theory in that grain boundary mismatch energy is used to determine the relationship of fastest growth (37), along with the fact that there is no completely quantitative data available relating grain growth with orientation parameters. However, qualitative data is available and it indicates an orientation relationship as stated above (32,38). Another mechanism, discussed by Kronberg and Wilson (27), accounts for the relationship observed on annealing with rotations about the $[111]$ for face-centered cubic metals and about the (0001) in the hexagonal close-packed metals. The mechanism proposed by Kronberg and Wilson could be used to explain the relationship between the growing grain and matrix by reason of smallest magnitude and coordinated nature of the atom movements for certain relationships. There are certainly other facts which should be understood in order to apply completely the orientated growth theory. Some of these are grain size required for favorable combination of deorientation for growth and mechanism of nuclei formation.

One of the most frequent observations made in investigations aimed at determining orientated growth mechanisms is the increase in grain size which accompanies reorientation during annealing. The work of Beck and Hu (28) on aluminum associated the lack of grain growth on annealing with the recrystallization in situ texture. That McGeary and Lustman found a reorientation of the deformation texture up to the stage where about 40 % of the annealed texture had formed without appreciable subgrain or domain growth was significant (15). It is noted from the work on aluminum (28) that short annealing periods were used at temperatures where complete recovery of hardness takes place within five minutes. The major part of the data on the annealing reorientations in zirconium (15) was acquired in a range of temperatures where hardness recovery was completed only in times much in excess of five minutes. At the highest temperature of annealing zirconium (1112°F), the time required for complete hardness recovery was more than one hour, and the time for formation of the fully annealed texture was greater than 50 minutes (15). Thus, it should be noted that the temperatures of annealing used on aluminum were much

higher with respect to its recrystallization range than were the temperatures employed on annealing zirconium with respect to its recrystallization range. It was observed in the present work on titanium that on annealing one hour at 1000°F- a temperature and time at which the hardness is not fully recovered, Figure 22-the 'recrystallization in situ'texture resulted. On increasing the time to three hours, at 1000°F, there was approximately a five fold increase in grain diameter over that for one hour at 1000°F and a practically complete reorientation in texture. Increasing the temperature of annealing to 1300°F for one hour, resulted in a grain size somewhat larger that that observed on annealing for three hours at 1000°F, yet there was less reorientation of the texture for the larger grain size. From the interpretations of the preferred growth mechanisms, however, a larger grain size would indicate more growth of grains oriented for greatest growth with respect to the matrix material. On annealing at 1500°F for one hour, the average grain size was considerably larger than at 1300°F and the fully annealed texture prevailed. It is thus concluded here that the consideration of temperature and time of annealing will determine whether or not larger grain size is always associated with greatest reorientation of the deformation textures.

In this connection, it can be stated that annealing mechanisms are largly dependent upon temperature. Longer times at lower temperatures tends toward the fully annealed textures. Low temperatures of annealing titanium are believed to cause a somewhat different mechanism of reorientation than the higher annealing temperatures. This difference is explainable on the basis of availability of nuclei for growth between the lower and higher temperatures of annealing. The effect of this is observed when annealing at higher temperatures a larger grain size is evident, but less reorientation of the material to the fully annealed texture has taken place than for a longer time at a lower temperature. Conversely, smaller grain size at the lower temperatures of annealing with longer times may give greater reorientation to the annealing texture than the larger grained, higher annealed specimens. A combination of 'oriented growth' theory and 'oriented nucleation' would seem to better satisfy the results instead of either of the theories alone. The 'oriented nuclei' mechanism may be more prodominate at the lower temperatures of annealing and the 'oriented growth' theory may prevail at the higher temperatures where grain growth is prominent.

The alloying elements studied here have no effect on what will be the crystallographic relationship between the cold-rolled and fully annealed texture. The grain size of the annealed material decreases with refractorness of the alloying element. The temperature at which the fully annealed texture is developed increases with the melting point of the solid solution alloy additions. The addition of zirconium to titanium did not decrease the grain size of the annealed material nearly as much as did the elements which have different crystalline structures, Table 4. For example, aluminum has a much lower melting point than zirconium but a face-centered cubic structure as compared to hexagonal close-packed for both zirconium and titanium. However,

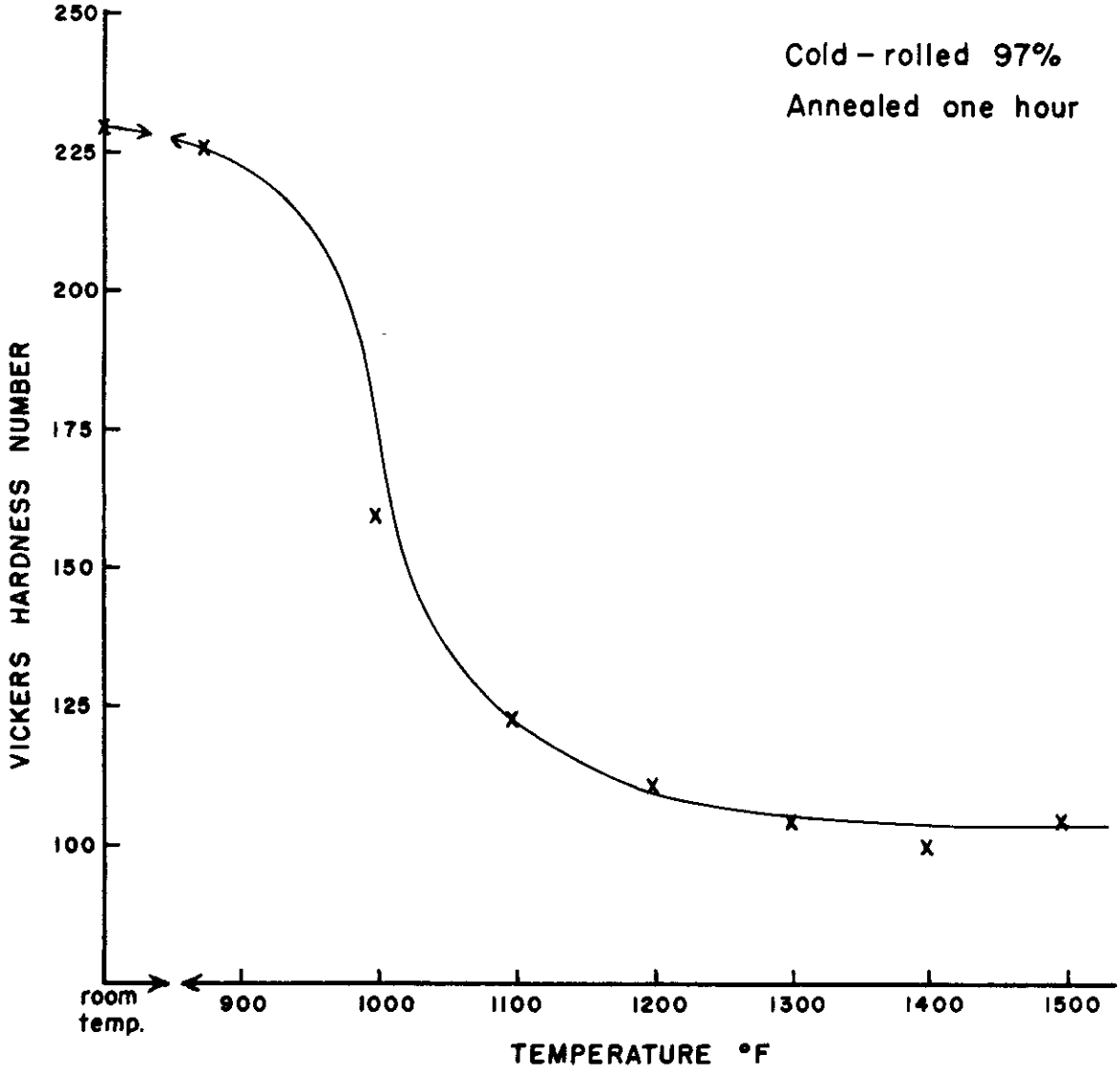


Fig. 22 Hardness vs Temperature for one hour vacuum anneal of cold – rolled Iodide Titanium sheet.

for the same time and temperatures of annealing, the Ti-Zr alloy had much the larger grain size. Evidently, the effect of zirconium on decreasing grain size in the annealed material is not great since the chemical properties and crystal structure are similar.

## SECTION VI

## TEXTURES OF TITANIUM-MOLYBDENUM ALLOYS

### A. INTRODUCTION

The titanium-molybdenum alloys studied included those of alpha, alpha plus beta, and beta structures which are stable at room temperature. This study was conducted as a part of the work on the effects of a number of variables on the textures of titanium. The effects of a second phase were investigated for the alpha and beta structures. All the titanium-molybdenum alloys were amenable to large reduction by cold rolling. The textures observed in these Ti-Mo alloys have followed the pattern of textures found in other metals of similar crystal structure.

### B. RESULTS AND DISCUSSION OF COLD-ROLLED TEXTURES IN THE ALPHA, BETA, AND ALPHA PLUS BETA REGIONS

#### Cold-Rolled Sheet Texture, Alpha Region

The alpha alloy containing 0.38% molybdenum was cold reduced 93% reversing the rolling direction 180° after each pass.

The pole figures for the hexagonal alpha phase are shown in Figure 23. They closely resemble the pole figures of cold-rolled titanium except that there is more spread of the basal poles in the cross direction. The basal planes are tilted approximately 30° in the cross direction with the $[10\bar{1}0]$ direction parallel to the rolling direction.

Molybdenum along with columbium has less alpha solid solubility than the other alloying elements, aluminum, tantalum and zirconium, used in these investigations. Molybdenum (39) and tantalum, Figure 47*, give decreasing c/a ratios with increasing concentration. The body-

* An asterisk following a Figure denotes that those figures are located in the Appendix.

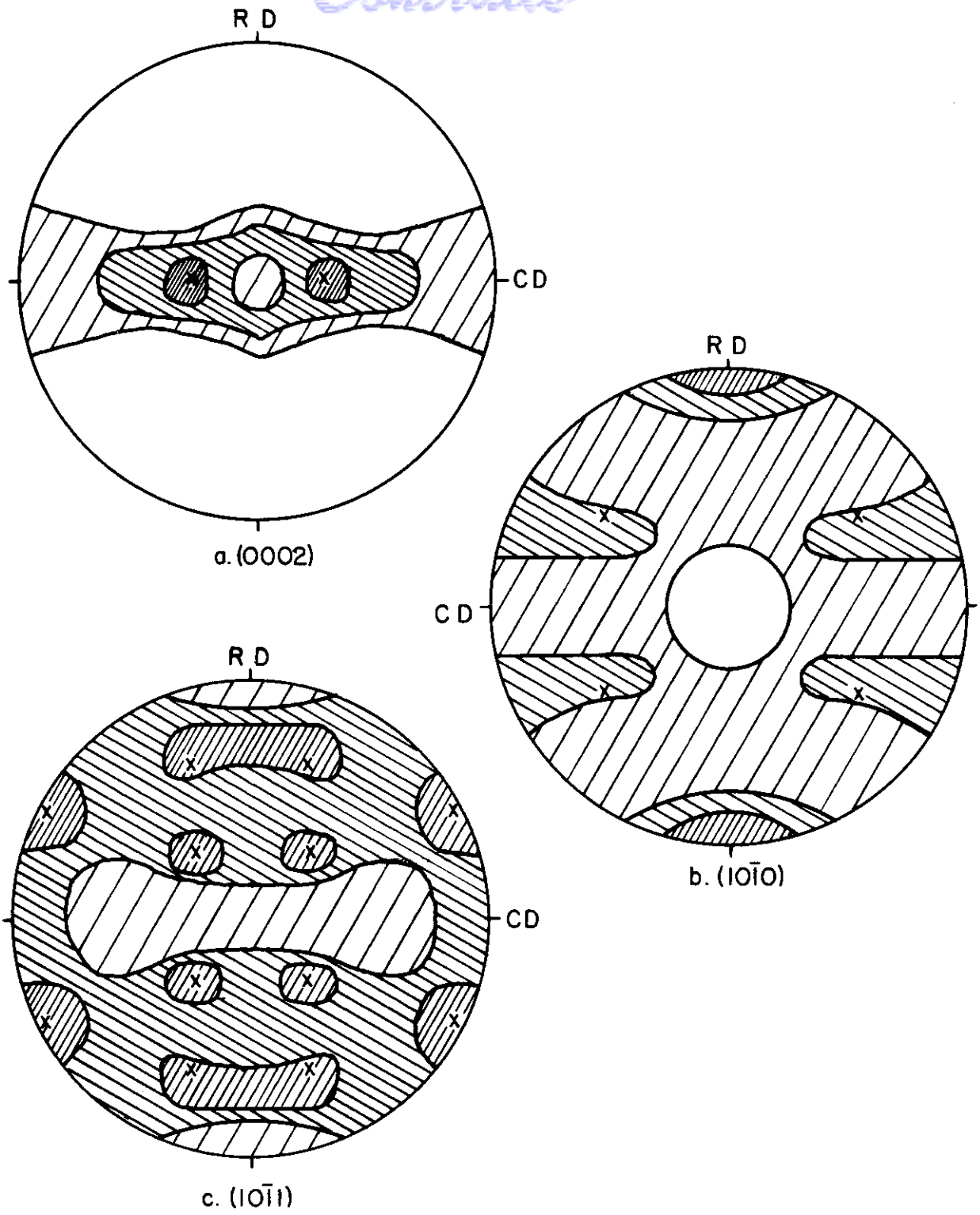


Fig23 Texture of 0.38% Mo-Ti alloy cold-rolled 93%, x = 30° rotated basal (0002) [10$\bar{1}$0].

centered alloying elements Mo, Ta and Cb give essentially the same cold-rolled textures in alpha titanium. Molybdenum gives more scatter in the cross direction of the (0002) pole figure than Ta and Cb, this being the only distinguishable feature among them. Thus, the texture of the 0.38%Mo-Ti alloy has followed the pattern of other alpha solid solution alloys of this investigation, which have no correlatable dependency upon c/a ratio.

## Cold-Rolled Sheet Texture, Beta Region

The texture of the body-centered cubic alloy (containing 31.8%Mo) is shown in Figure 24. This texture is adequately represented by the ideal orientation (100) [110]. The amount of spread from this orientation is much less than that observed for other body-centered cubic metals (40), and it is necessary to use only this one component to describe the texture.

The textures of body-centered cubic iron (41), vanadium (42), and molybdenum (43) can be described with more than one ideal orientation, namely, (100) [110](112) [110] and (111) [112]. However, the most prominent orientation is the (100) [110]. Carbon increases the scatter in iron. The 31.8 pct Mo-Ti alloy had very little contamination, and it exhibited but little scatter.

## Cold-Rolled Sheet Textures, Alpha plus Beta Region

The texture of the beta phase in the alpha plus beta alloy (containing 14.3% Mo) is shown in Figure 25. The effect of the alpha phase on the body-centered beta phase can be seen by comparing Figures 24 and 25.

The beta phase in the alpha plus beta alloy has markedly more spread in the cross direction. The beta phase of this alloy has a texture described by the orientations (100) [110] and minor (112) [110].

Due to the inability of resolving the alpha Debye rings because of differences in intensity and lack of $\theta$ value differences, the alpha texture was not determined.

The alpha plus beta alloy has approximately a composition of 50% alpha and 50% beta, assuming near equilibrium was obtained on cooling. The texture of the beta phase is nearly the same as for other body-centered cubic metals. The texture of the beta phase of this alloy differed from the texture of the all beta alloy (31.8%Mo) in that more scatter was evident in the cross direction of the (110) pole figure. Since the beta phase of the alpha plus beta alloy has about the same composition as the all beta alloy, the results would seem to indicate that restraint, due to the alpha phase, is causing the increased scatter.

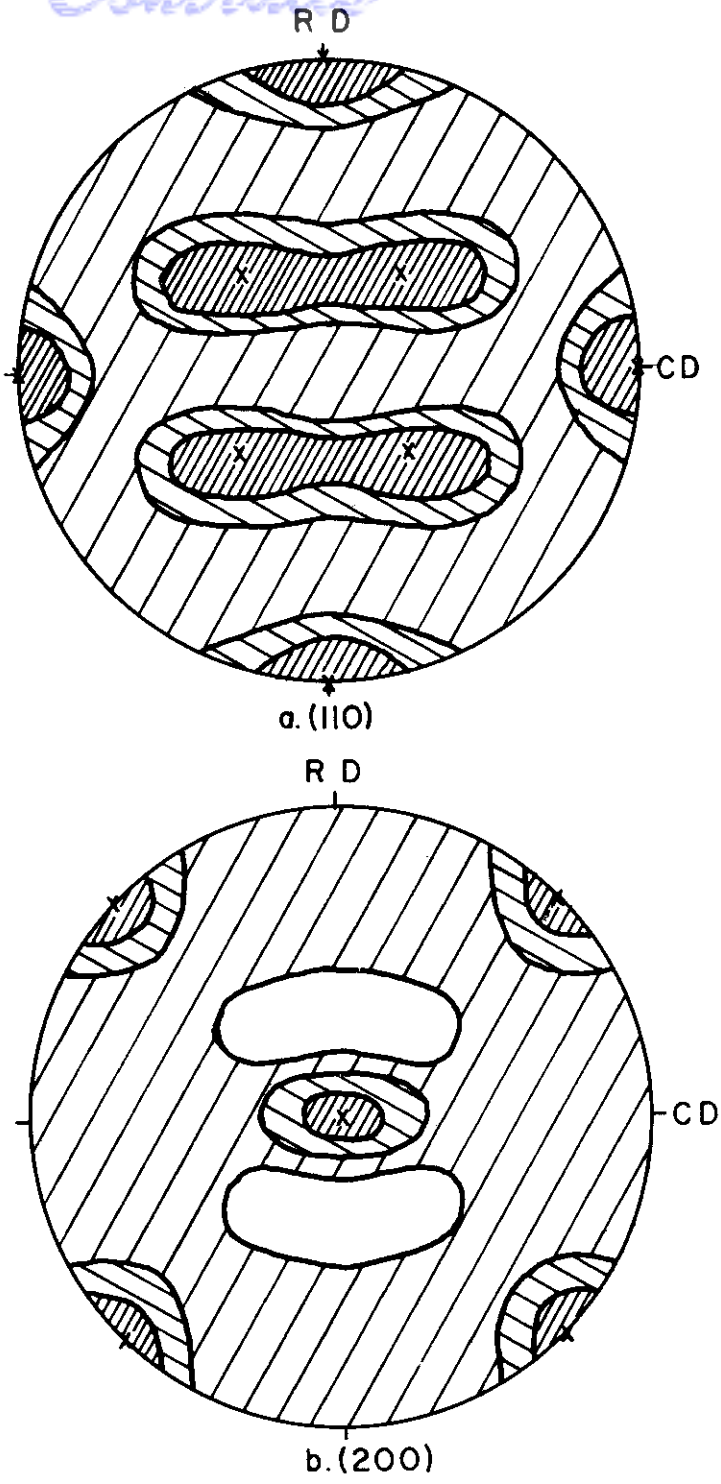


Fig. 24 Texture of 31.8% Mo - Ti alloy cold - rolled 93%, x = (200) [110].

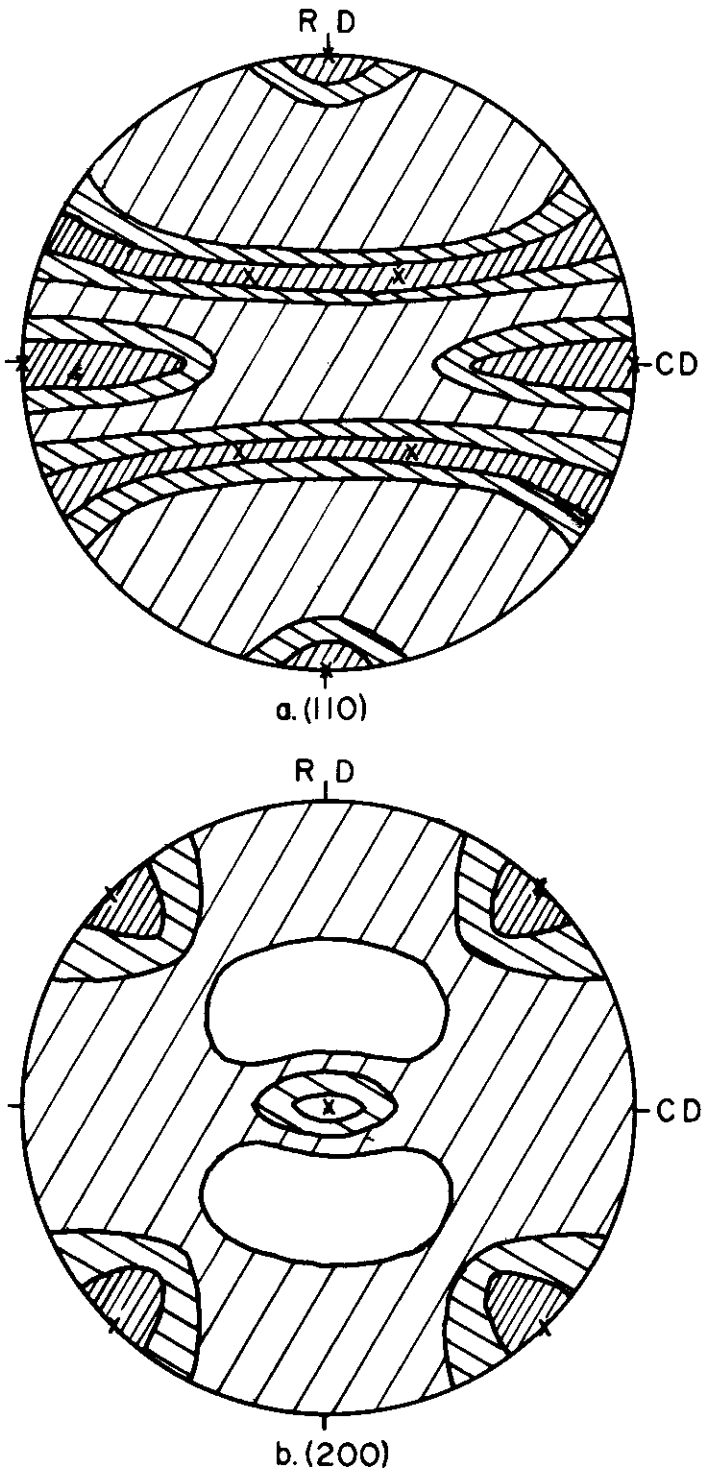


Fig. 25 Texture of beta phase of 14.3% Mo - Ti alloy cold-rolled 93%, x = (200) [110].

## C. RESULTS AND DISCUSSION OF ANNEALING TEXTURES IN THE ALPHA AND BETA REGIONS

### Annealed Textures in the Alpha Region

The pole figures for the alloy containing 0.38% Mo annealed for one hour at 1500°F are presented in Figure 26. The (0002) pole figure shows the tilted basal at 30° from the center towards the cross direction. The $(10\bar{1}0)$ pole figure shows the average $[11\bar{2}0]$ direction to be parallel to the rolling direction. The X of Figure 26 represents 30° rotations about basal normals while ⊛ corresponds to 20° and 40° rotations. The texture is best described by the 20° and 40° rotations.

A sharpening of the texture in the (0002) pole figure due to decrease in scatter in the cross direction is observed to result from annealing the alpha alloy at 1500°F. The rotations about the normal to the close-packed plane resulting from annealing has also been observed in iodide titanium, although the rotations were approximately 30° as opposed to the 20° and 40° rotations indicated in the present case. Zirconium on annealing at 1112°F was found to have a rotations of 20° and 40° about the normal to the close packed plane (15). McGeary and Lustman concluded that this annealing texture was not developed by oriented nucleation and growth, but through preferred growth of grains due to maximum misfit of neighboring grains. This would seem to apply for the Ti-Mo alpha alloy in the annealed state as was discussed for other alloys in Section V.

### Annealed Textures in the Beta Region

The texture of the body-centered cubic alloy containing 31.8%Mo as annealed at 1500°F for one hour is shown in Figure 27. The annealing tends to sharpen the texture over the cold-rolled texture of Figure 24. This is shown by less spread in the (110) pole figure from the ideal orientation (200) [110]. It has been reported that iron (41) and vanadium (42) have a 15° rotation upon annealing, but Semchyshen and Timmons reported that molybdenum retained its cold-rolled texture on annealing (43). In order to check these findings for body-centered cubic metals, the 31.8% Mo-Ti alloy was annealed at 2000°F for one hour. The grains were so large that much difficulty was experienced in obtaining data for the pole figures; however, enough data was obtained to show that the (200) poles rotated approximately 20° about the [100] direction normal to the rolling plane, as a result of annealing for one hour at 2000°F.

The sharpening of the texture due to the 1500°F anneal can be ascribed to the mechanism of preferred absorption of small grains with orientations deviating considerably from those of the dominating texture of (200) [110] as a result of the greater mobility of their higher energy boundaries (24). This could account for the removal of the major proportion of the cross direction spread in the (110) pole figure.

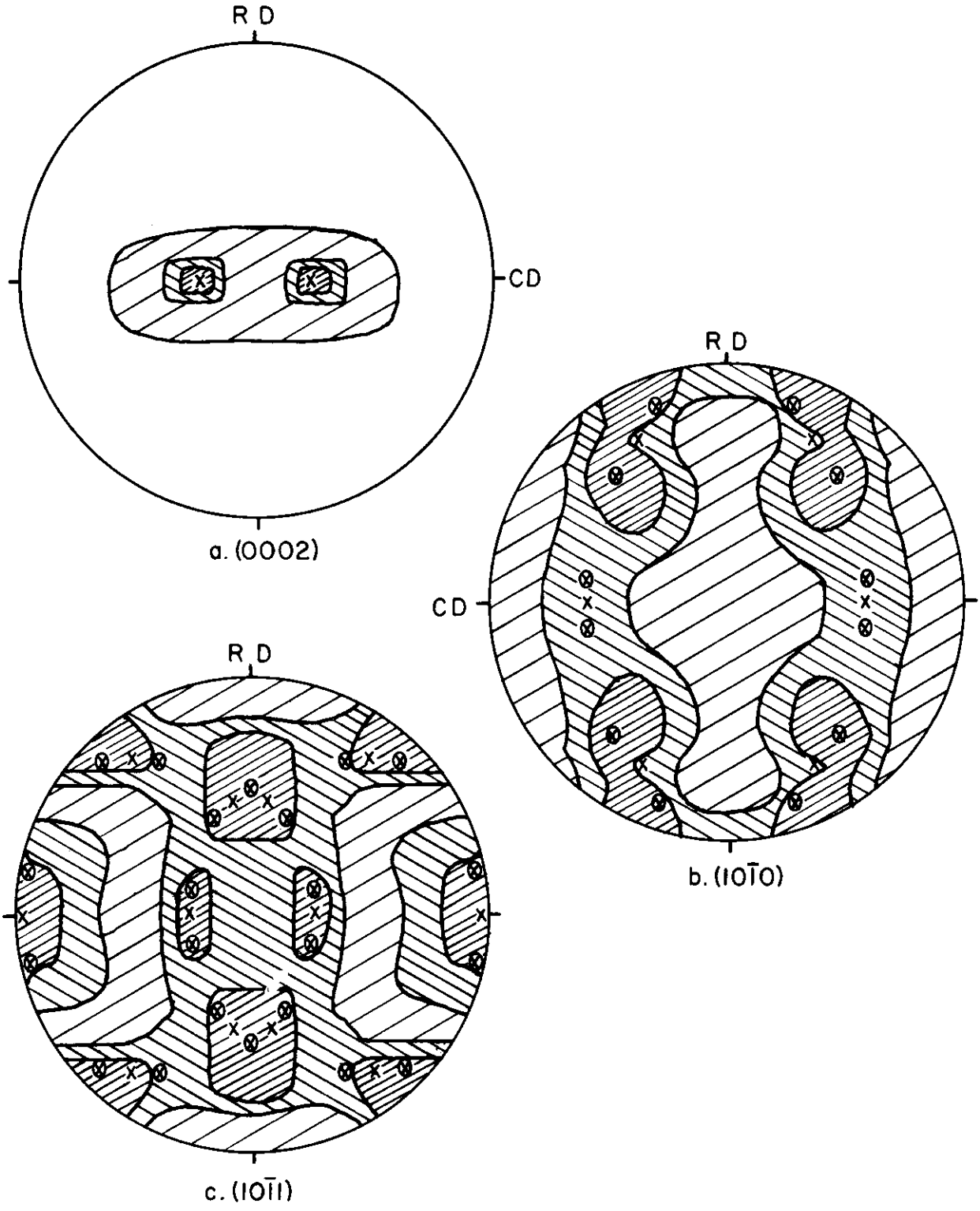


Fig. 26 Texture of 0.38% Mo-Ti alloy cold-rolled 93%, annealed one hour at 1500°F. x = (0002) [11$\bar{2}$0], ⊗ = cold-rolled texture rotated 20° and 40°.

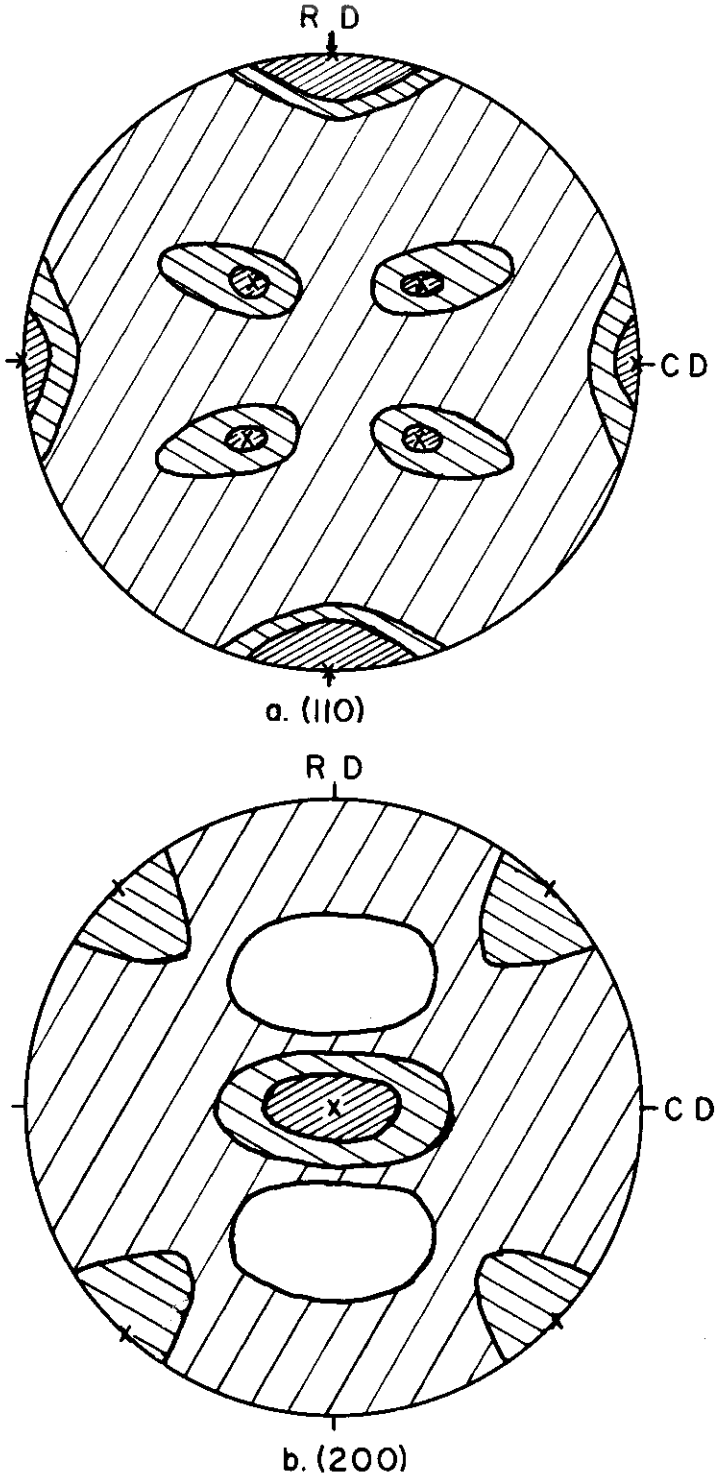


Fig. 27 Texture of 31.8% Mo-Ti alloy cold-rolled 93%, annealed one hour at 1500° F., x = (200) [110].

During the 2000°F anneal the (200) poles were rotated 20° about the [100] perpendicular to the rolling plane. This would indicate that preferred growth of those grains located for maximum misfit with other grains would take place at the expense of the major portion of the oriented matrix.

In conclusion it may be stated that molybdenum changes the annealing characteristics of titanium by raising the temperature at which the preferred growth mechanism becomes operative or where the fully annealed texture is developed. Thus, molybdenum is similar in this respect to the other solid solution additions studied in this work.

## SECTION VII

## THE HOT-ROLLED TEXTURES OF TITANIUM AND TITANIUM ALLOYS

### A. INTRODUCTION

When a metal is hot-rolled the resulting texture may be ascribed to several different effects. Certainly the mechanisms of deformation at the rolling temperature will play an important role in the outcome. Time at temperature will influence the texture as in effect it will constitute intermittent annealing. Since alloying affects the annealing time and/or temperature of annealing, it will be a factor as will be the mechanisms of recrystallization.

Previously reported hot-rolled textures are those of low carbon steel sheet (44), zirconium (16), and beryllium (26). Goss reported that a low carbon steel rolled at room temperatures developed a (001) [110] texture while that rolled in the region of 700°F developed a (110) [001] texture (44). Rolling at intermediate temperatures produced some degree of randomness as one texture shifted to the other. Both zirconium and berryllium were reported to have developed the same basic textures for rolling at temperatures up to 1475°F as at room temperature, differing only by an increase in the spread of the basal planes toward the transverse direction as the temperature of deformation was increased.

The preparation of the alloys for this study and the x-ray techniques have been described in a previous section.

Rolling was carried out using 2-high 4 in. dia. rolls. The strips

were heated in air to a temperature 50°F greater than the desired rolling temperature between each pass through the rolls.

## B. RESULTS

### Unalloyed Titanium

The texture of unalloyed titanium resulting from hot rolling 95% at 1050°F is presented in the pole figures of Figure 28. The texture can be described in terms of the "ideal" orientation, tilted (0002) $[10\bar{1}0]$. The basal maxima is spread $\pm 27°$ in the cross direction. On comparing this texture with that of cold-rolled titanium, Figure 2, it is apparent that less material is scattered beyond the intense areas in the cross direction for the hot-rolled material.

Also, this texture is more random in orientations about the C-axis in that considerable material is aligned with $[11\bar{2}0]$ directions parallel to the rolling direction.

Hot rolling titanium at 1450°F to a reduction of 95% results in the texture shown in Figure 29. The randomness of the texture in the specimen rolled at 1450°F is greater than that rolled at 1050°F. The split basal has lost its identity to an average position aligning (0002) planes parallel to the rolling direction with maximum scatter of $\pm 30°$ in the rolling direction and $\pm 40°$ in the cross direction. In this texture, no one direction appears to be preferentially aligned parallel to the rolling direction.

### 14.75% Zirconium-Titanium

Pole figures for an alloy containing 14.75% zirconium reduced in thickness 90% by rolling at 1050°F are shown in Figure 30. The texture can be described as (0002) tilted 30° R.P., $[10\bar{1}0]$, the same as the cold-rolled texture of this material. There is a larger amount of scatter from this orientation, particularly with regard to the direction aligning with the rolling direction, than for the cold-rolled sheet.

Figure 31 contains the pole figures for the same alloy reduced in thickness 90% by rolling at 1450°F. The basal pole figure shows an increase in the amount of material oriented parallel to the rolling plane and at the same time an increase in the spread toward the transverse direction. Figure 31b shows the $[10\bar{1}0]$ and $[11\bar{2}0]$ directions aligned with the rolling direction. Thus, it appears that this texture contains as its components the orientations (0002) $[10\bar{1}0]$, tilted (0002) $[10\bar{1}0]$ and tilted (0002) $[11\bar{2}0]$.

### 3.8% Aluminum-Titanium

Pole figures for an alloy of titanium with 3.8% aluminum reduced in thickness 90% at 1050°F are shown in Figure 32. These figures show a relatively sharp (0002) $[10\bar{1}0]$ texture. The only significant

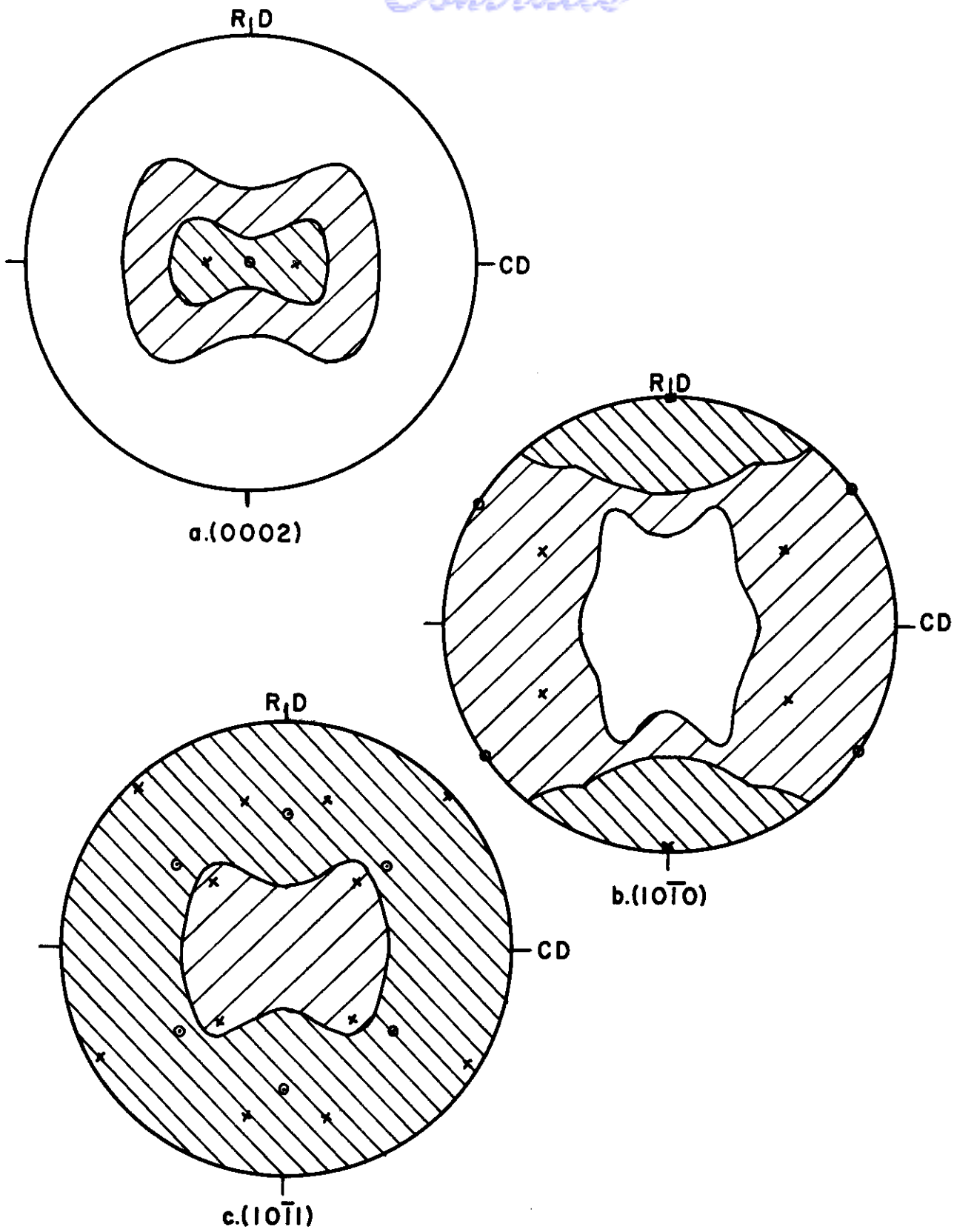


Fig. 28 Texture of Iodide Titanium rolled 95% at 1050°F. o = (0002) [10$\bar{1}$0].

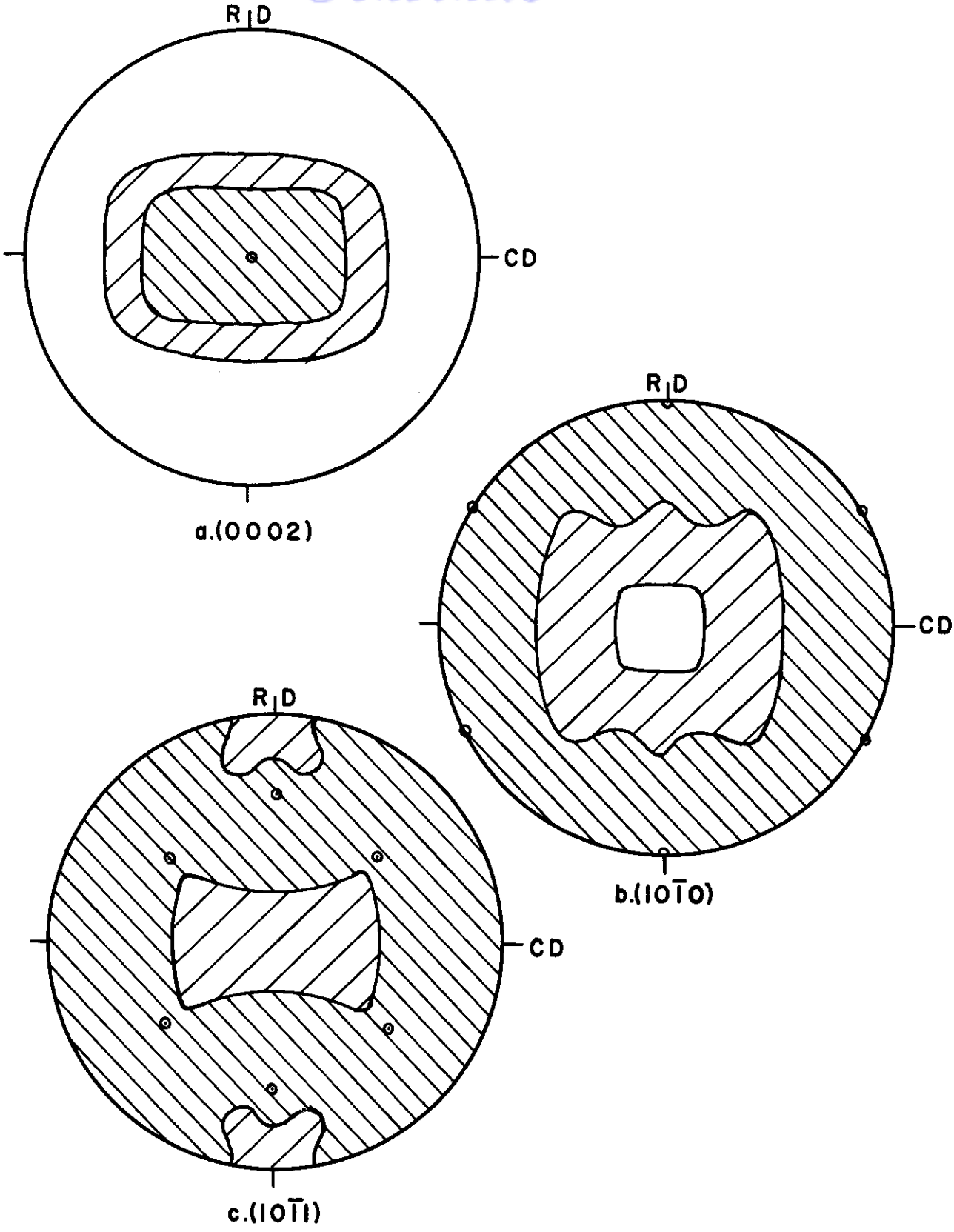


Fig. 29 Texture of Iodide Titanium rolled 95% at 1450°F. o = (0002) [10$\bar{1}$0].

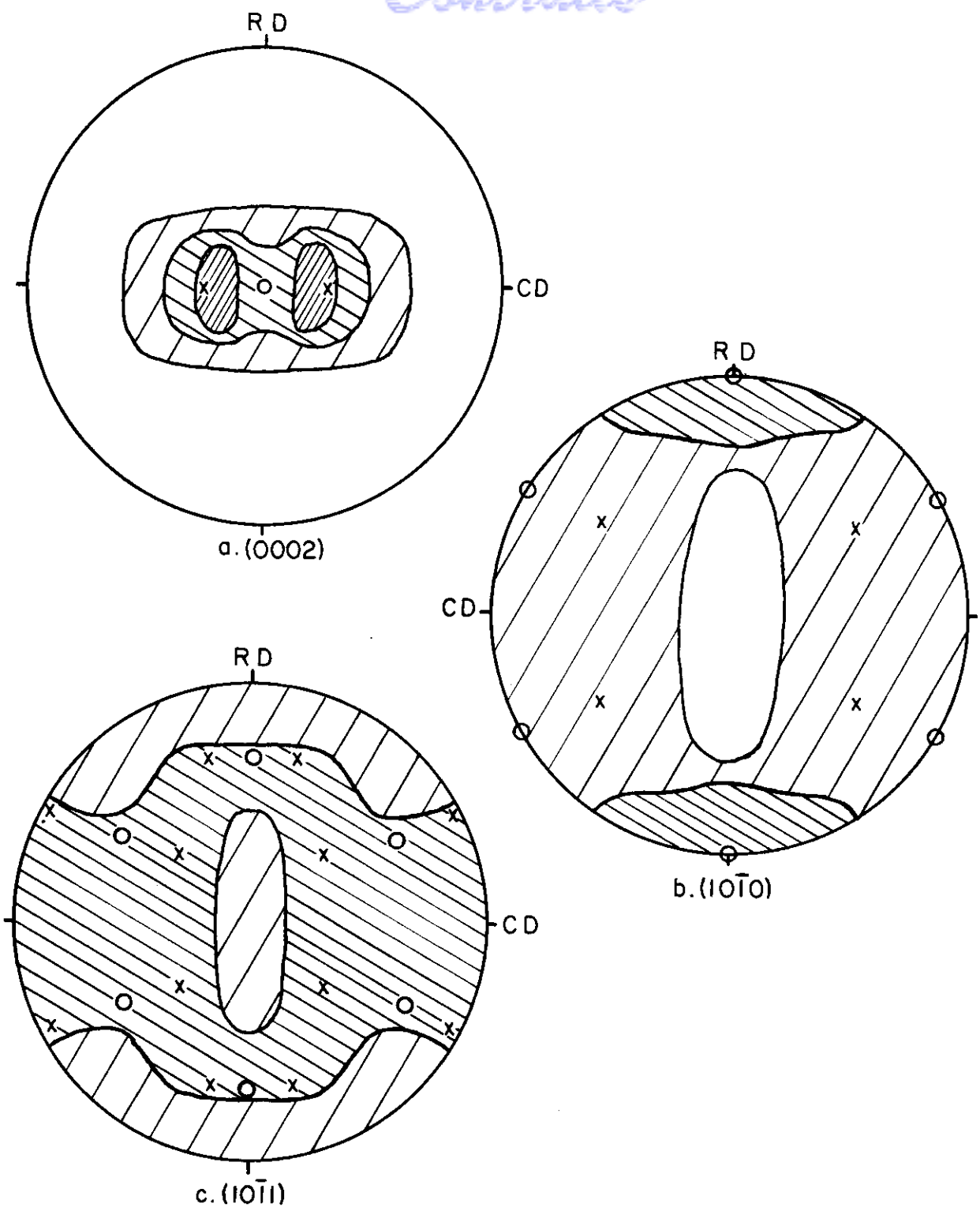


Fig. 30 Texture of 14.7% Zr-Ti alloy rolled 90% at 1050° F.
O = (0002) [10$\bar{1}$0]; x = (0002) rotated 27°, [10$\bar{1}$0].

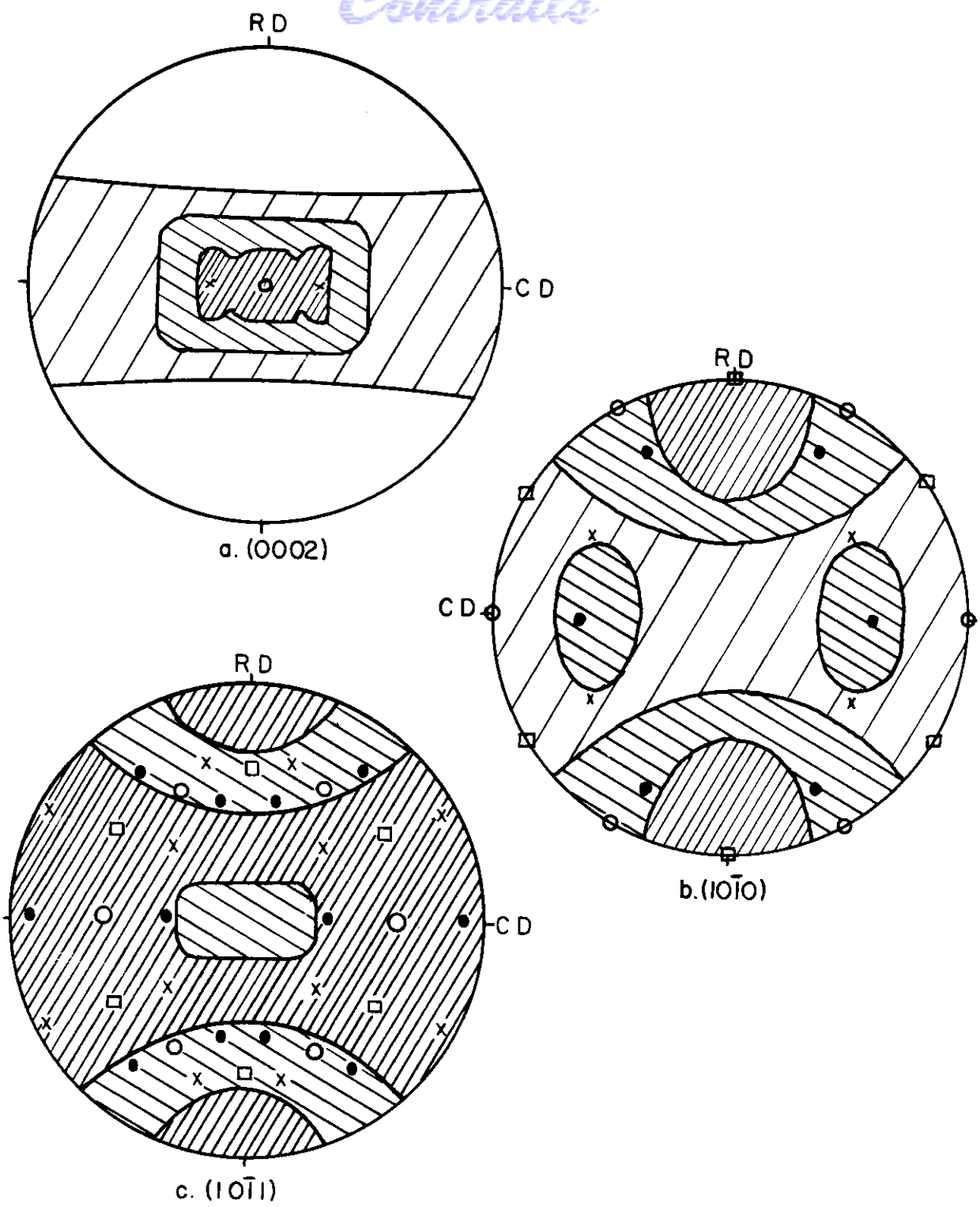


Fig. 31 Texture of 14.7% Zr-Ti alloy rolled 90% at 1450°F. □ = (0002) [10$\bar{1}$0]; x = (0002) rotated 27°, [10$\bar{1}$0]; 0 = (0002) [11$\bar{2}$0]; ● = (0002) rotated 27°, [11$\bar{2}$0].

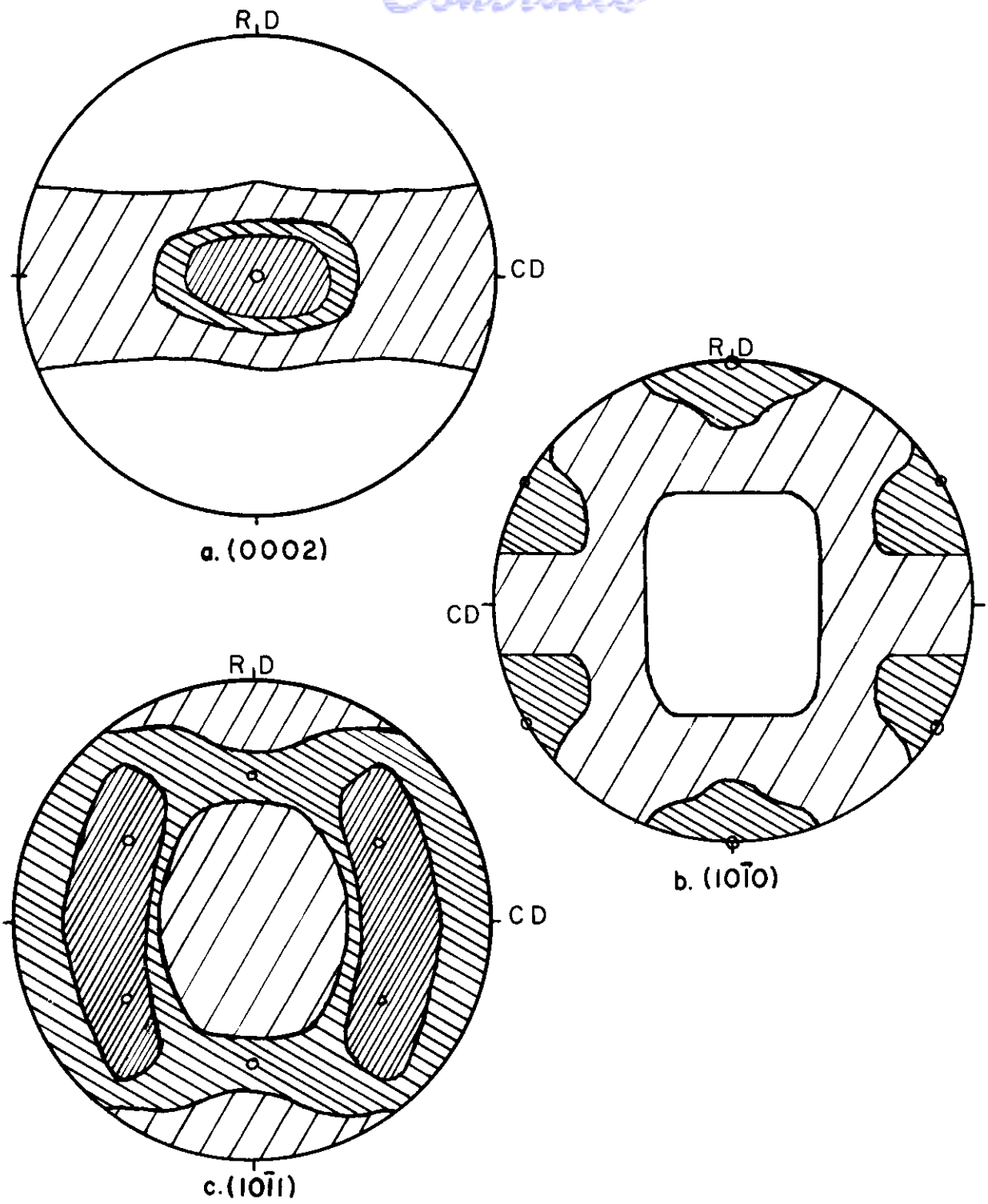


Fig.32 Texture of 3.8% Al-Ti alloy rolled 90% at 1050°F.
0 = (0002) [10$\bar{1}$0]

difference between this texture and the cold-rolled texture of this alloy is the extent of the region of low intensity in the cross direction.

This titanium-aluminum alloy rolled at 1450°F, Figure 33, also gave a sharp (0002) [$10\bar{1}0$] texture. The scatter of the major intensity region in the cross direction is greater than for this material rolled at the lower temperature.

The pole figures for this alloy rolled at 1600°F, Figure 34, show that the (0002) [$10\bar{1}0$] texture developed by rolling at lower temperatures has been replaced by a texture described by (000$\bar{2}$) [$11\bar{2}0$]. The texture observed on rolling at 1600°F was sharper than those noted in specimens rolled at 1050° and 1450°F.

15.4% Tantalum-Titanium

The texture of the alloy containing 15.4% tantalum rolled at 1050°F is shown by Figure 35. As in the above cases these pole figures are adequately described by the same orientation as those for the cold-rolled alloy, namely (0002) tilted 27°, [$10\bar{1}0$].

Rolling this alloy at 1450°F introduced another variable inasmuch as the alloy was in the alpha plus beta region at this temperature. Figure 36a shows a marked increase in the degree of scatter of the basal planes. Figure 36b and 36c show that despite the scatter of the basal plane, the [$10\bar{1}0$] and [$11\bar{2}0$] directions are concentrated parallel to the rolling direction.

## C. DISCUSSION OF RESULTS

A discussion of data regarding the deformation mechanisms of titanium and titanium alloys in relation to deformation textures is given in Section VIII.

Although the detailed mechanisms of texture formation in hot rolling are not entirely clear, the results can be rationalized in terms of two separate discernable processes. In each case reported, rolling at 1050°F resulted in a texture similar to that developed by cold rolling. Accordingly, it would appear that the deformation elements that operate at this temperature, at least, may not be widely different to those operating at room temperature. In addition to deformation, there is the influence of thermal effects on the textures. It is suggested that the affect of temperature for 1050°F rolling is to cause low-angle boundary migration. However, neither small alterations in deformation mechanisms nor low-angle boundary migration produces a significant change in the texture.

The appearance of the component containing the [$11\bar{2}0$] directions parallel to the rolling direction at the higher rolling temperature can be explained on the basis of an annealing effect due to temperature of rolling. A previous section on annealed textures of titanium shows that

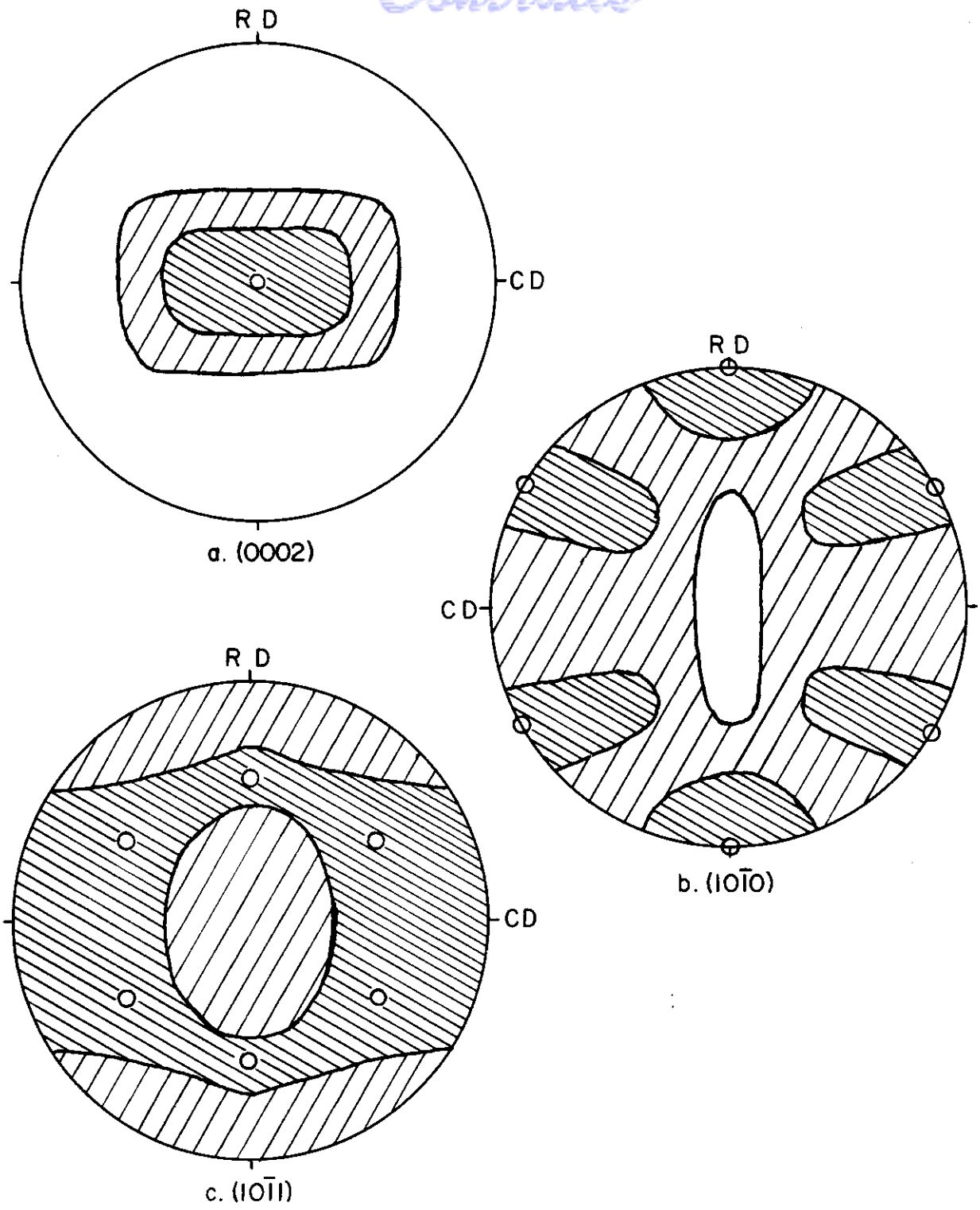


Fig. 33 Texture of 3.8% Al-Ti alloy rolled 90% at 1450° F.
0 = (0002) [10$\bar{1}$0]; x = (0002) rotated 27°, [10$\bar{1}$0].

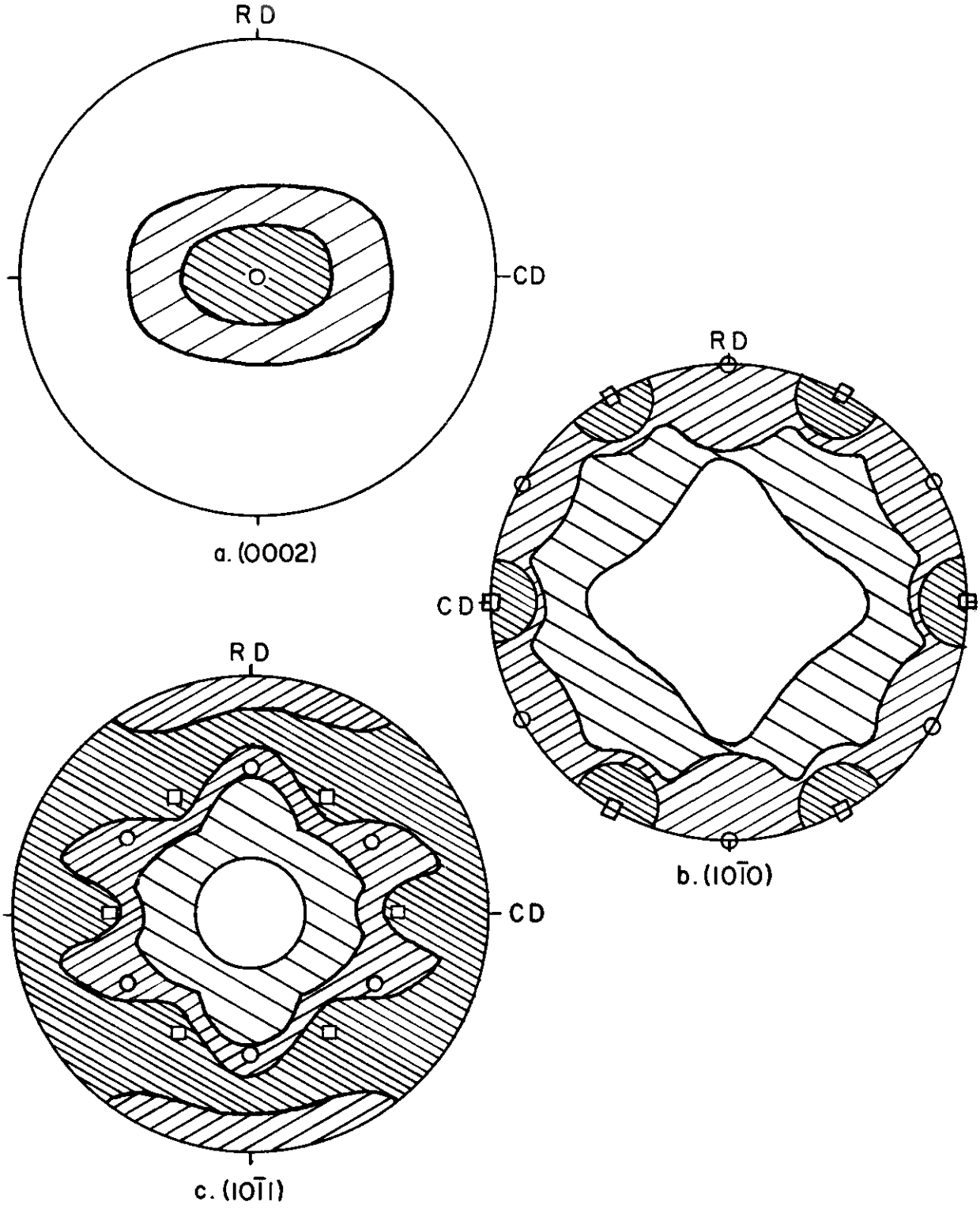


Fig.34 Texture of 4% Al-Ti alloy rolled 91% at 1600°F.
O = (0002) [10$\bar{1}$0]; □ = (0002) [11$\bar{2}$0].

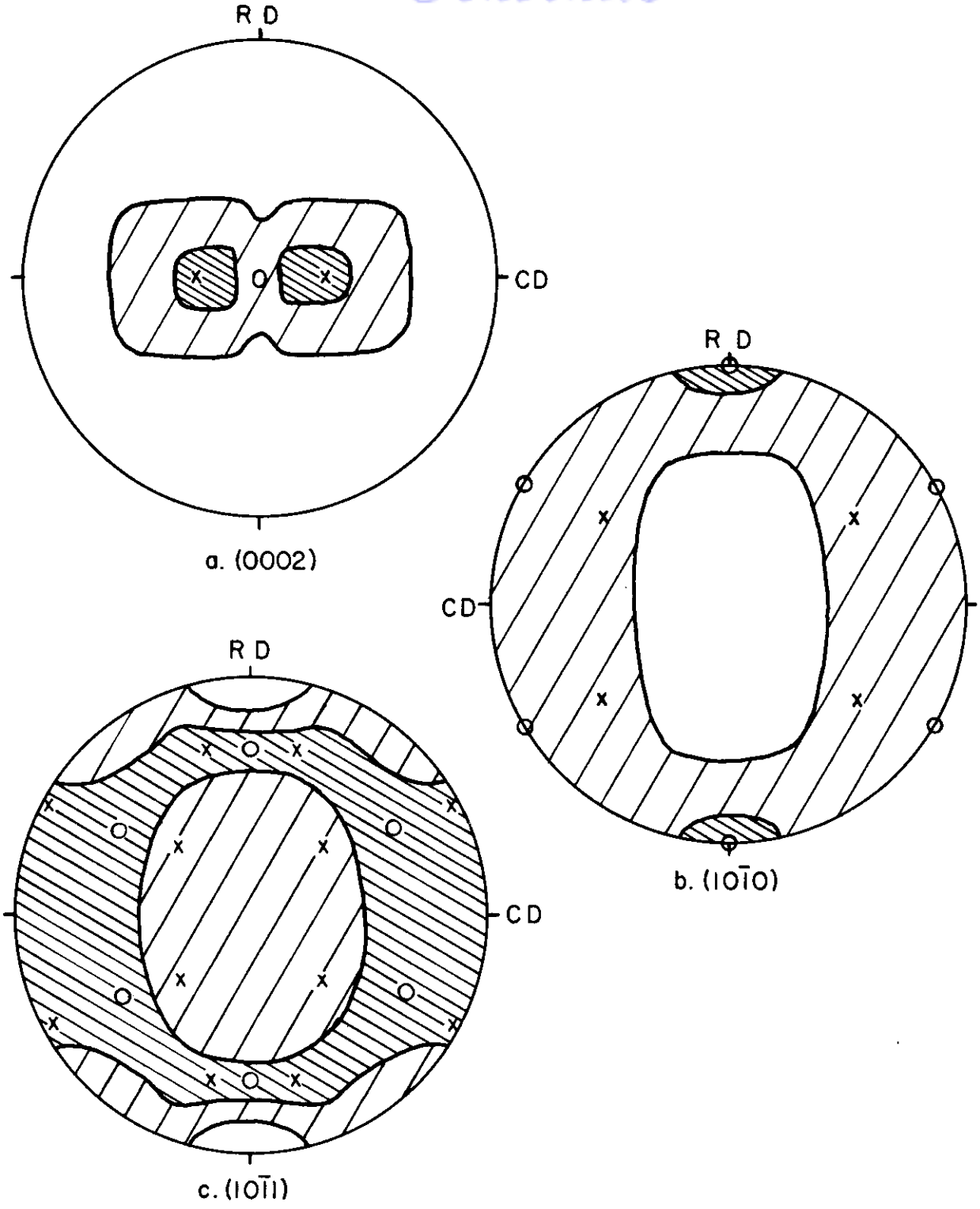


Fig. 35 Texture of 15.4% Ta - Ti alloy rolled 90% at 1050°F.
O = (0002) [10$\bar{1}$0]; x = (0002) rotated 27°, [10$\bar{1}$0].

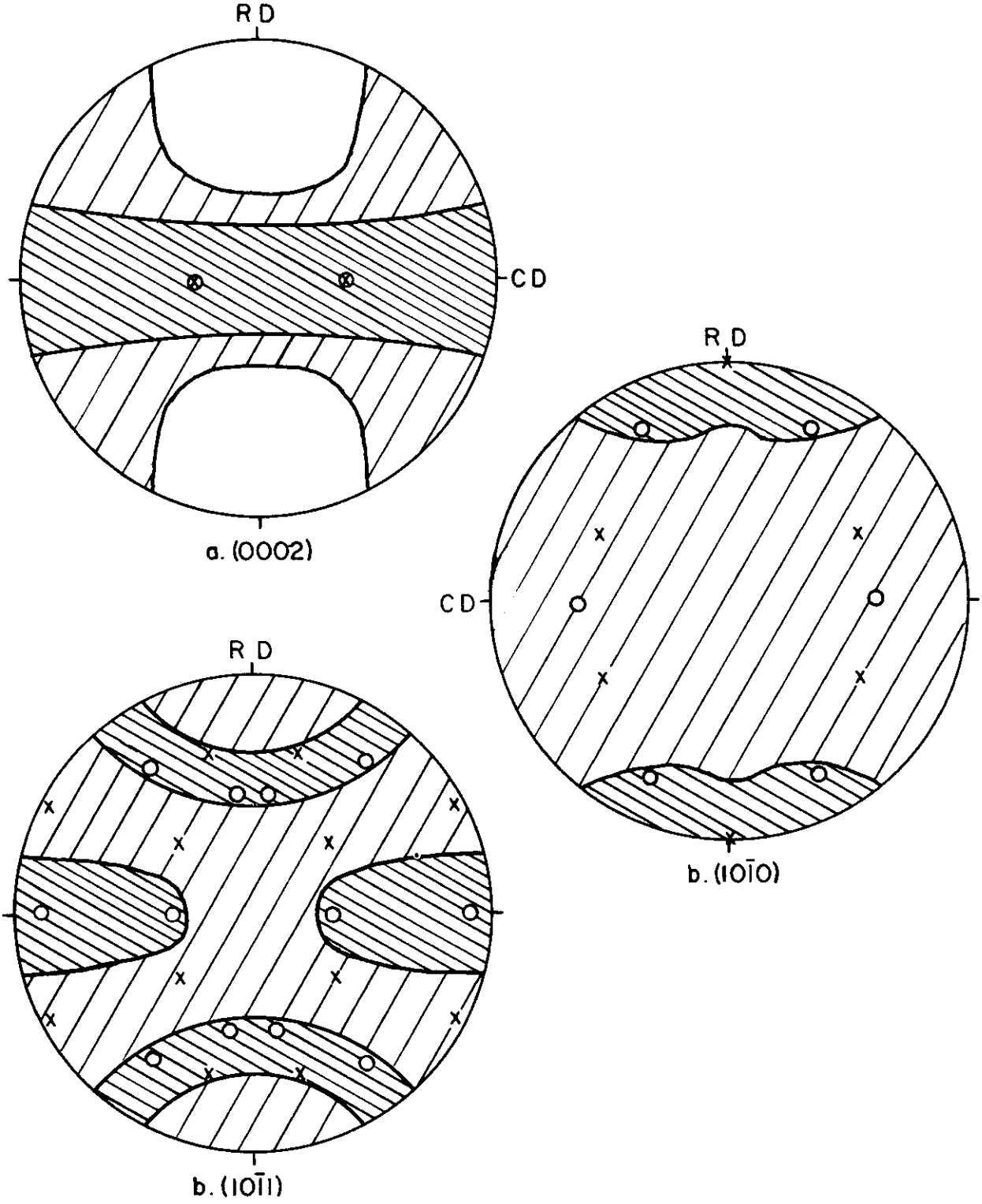


Fig. 36 Texture of 15.4% Ta - Ti alloy rolled 90% at 1450°F. O = (0002) rotated 27°, [11$\bar{2}$0]; x = (0002) rotated 27°, [10$\bar{1}$0].

at the higher annealing temperatures the [ 11$\bar{2}$0 ] direction is aligned parallel to the rolling direction. Those textures which exhibited the [ 11$\bar{2}$0 ] directions parallel to the rolling direction were called the fully annealed textures and were best related to the cold-rolled textures by a 30° rotation about the C-axis. This resulting relationship is believed to be caused by preferred growth (as discussed in Section V on annealing textures). Thus, the influence of higher temperatures on hot rolling is to cause an annealing effect which tends to alter the texture from that with the [ 10$\bar{1}$0 ] aligned parallel to the rolling direction to a texture that has the [ 11$\bar{2}$0 ] aligned in the rolling direction.

Hence, the tilted (0002) [ 10$\bar{1}$0 ] components of the 14.7% zirconium-titanium and the 15.4% tantalum-titanium alloys would be due to deformation and the tilted (0002) [ 11$\bar{2}$0 ] components would be growth components. This is also true for the iodide titanium rolled at 1450°F where both [ 10$\bar{1}$0 ] and [ 11$\bar{2}$0 ] directions are aligned in the rolling direction. In the 3.8% aluminum-titanium alloy, apparently the full annealing temperature is higher. Because of this, as is seen in Figure 33, the texture developed by rolling the Ti-Al alloy at 1450°F is (0002) [ 10$\bar{1}$0 ]. It is necessary to roll at 1600°F before the (0002) [ 11$\bar{2}$0 ] texture is found in this alloy, Figure 34. It is generally noted here that the alloying additions increased the temperature of hot rolling necessary to develop the [ 11$\bar{2}$0 ]11 to the rolling direction.

The randomness that is quite evident in the hot-rolled textures in comparison to the cold-rolled textures could be attributed partially to the annealing effect since the annealed textures generally were more random than the cold-rolled textures, and in particular for rotations about the C-axis. However, the non-split basal exhibited by titanium on hot rolling at 1450°F is not comparable to the annealed texture since the split basal is definitely retained on annealing. This matter is discussed more fully with regard to the deformation mechanisms operating at the higher temperature in Section VIII.

It is noted that in the 14.7% zirconium-titanium alloy rolled at 1450°F there may be components described as tilted (0002) [ 10$\bar{1}$0 ] and tilted (0002) [ 11$\bar{2}$0 ]. It is not clear whether the appearance of the high intensity region at the center of the (0002) pole figure is the result of the increased scatter or is indicative of a true component of the texture. If a component is taken such that the basal plane is parallel to the rolling plane, a satisfactory explanation cannot be offered without further knowledge of the deformation mechanism involved.

The very large amount of scatter in the pole figures of the alloy containing 15.4% tantalum rolled at 1450°F may be caused by rolling in a two phase region.

In summary, the alloying additions Al, Ta and Zr do not greatly effect the resulting hot-rolled texture of titanium. The effect of hot rolling at progressively higher temperatures is to cause a tendency toward the fully annealed texture.

# DEFORMATION MECHANISMS IN TITANIUM AT 1500°F AND ITS SOLID SOLUTION ALLOYS AT ROOM TEMPERATURE

## A. INTRODUCTION

The room temperature deformation elements have been determined for unalloyed titanium by other investigators, (12, 45). Additional information relative to deformation mechanisms was needed in order to account for the textures of the alloys of titanium resulting from cold and hot rolling. Hence, the deformation mechanisms for titanium were determined at 1500°F and for its solid solution alloys of 4% Al, 15% Zr and 10% Ta at room temperature. The alloying elements were chosen for the greatest variance in c/a ratio. These results should indicate how sensitive the textures are to the changes in mechanisms of plastic flow and aid in rationalizing the differences between cold and hot-rolled textures. Also, knowledge of deformation mechanisms would help in formulating opinions on annealing texture formation.

The deformation mechanisms of titanium were determined for room temperature deformation by two independent investigators. The work by Rosi, Dube, and Alexander (12) was conducted on sponge titanium with grains averaging between 0.08 to 0.32 in. in diameter. Their results were $(10\bar{1}0)$ and $(10\bar{1}1)$ slip with $(11\bar{2}1)$, $(10\bar{1}2)$ and $(11\bar{2}2)$ as twinning planes. The planes of predominate action are listed first. The results of Anderson, Jillson and Dunbar (45) on iodide titanium crystals averaging about one inch in length, gave $(10\bar{1}0)$ and (0001) as the slip planes with $(10\bar{1}2)$, $(11\bar{2}1)$ and $(11\bar{2}2)$ twinning. Another investigation, on titanium flakes produced by fused salt electrolysis, gave the two additional twinning planes $(11\bar{2}3)$ and $(11\bar{2}4)$ besides those previously mentioned (46). It has been observed that many metals undergo changes in the slip systems when deformed at temperatures other than room temperature. Some of the materials which have been reported to change slip systems are aluminum, magnesium, beta-tin, molybdenum and iron-silicon alloys (47).

Magnesium was reported to have (0001), $(10\bar{1}0)$ and $(10\bar{1}2)$ slip planes above 482°F by Schmid (48). Bakarian and Mathewson found (0001), and $(10\bar{1}1)$ but no $(10\bar{1}2)$ slip at 626°F (49). Twinning has not been observed to occur on any additional planes at elevated temperatures. On the contrary, twinning has been found to be less frequent as the temperature of deformation increases. Only $(10\bar{1}2)$ twinning has been noted for the hexagonal metals (50) except titanium, which has $(10\bar{1}2)$, $(11\bar{2}1)$ and $(11\bar{2}2)$ twinning (12, 45). Only slight twinning occurs on the last mentioned plane.

There is but little mention made in the literature of the effect of solid solution additions upon the mechanisms of plastic flow. Most work has been pointed toward determining changes in critical shear stress with concentration of soluble or insoluble additions. However, there are a few alloyed metals on which deformation studies have been conducted. The strong trend is that alloying additions have very little to no effect on the operative slip planes of the unalloyed metal and in no case have been known to change the slip direction. On twinning there is even a lesser amount of information. Barrett, Ansel and Mehl (51) gave information on iron-silicon alloys which indicated an increase in twinning with increasing silicon content. It was stated for cadmium (52) that with slight purity changes and increased strain hardening twinning stress remains about the same.

## B. PRODUCTION OF LARGE GRAINS

Due to the allotropic transformation which takes place on cooling titanium from the melt to room temperature, it was impossible to grow alpha single crystals from the liquid. Previous attempts to grow large grains in titanium have met with considerable success. The cyclic anneal used by Anderson, et al (45) produced the largest titanium grains of any method on record. The strain anneal method used by Rosi, et al (12) was successful but not to the extent of the cyclic anneal method. All heat treatments used in growing the large grains were in vacuum. The cyclic anneal method consisted of heating 0.2 x 0.2 x 2.0 inch specimens to around 2192°F for four hours and then holding at just below the transformation temperature (1562°F) from three to five days. This cycle was then repeated three or more times. The grains were between 0.25 in. and 2.0 in. long (45). For strain annealing largest grains were produced when the specimen consisted of uniformly coarse grains, strong preferredness in orientation and a prestrain of 1.5%. The prestrained specimens were heated in vacuum from 752°F at a rate of approximately 302°F per day, and then given a final anneal of two days at 1544°F. The grains produced in this manner were from 0.08 to 0.32 in. in diameter (12).

As a starting point for growing large grains in titanium, the strain anneal method was used. These grains were to be used for determining the high temperature deformation mechanisms on pure titanium. After having prepared the iodide titanium ingot, described in Section I Preparation of Alloys, they were cold-rolled about 70% to a final thickness of 0.05 in. The specimens, measuring 3 in. x 0.25 in., were sealed in quartz capsules and annealed at 1450°F for one hour, giving relatively fine, equiaxal grains with an average diameter of 0.00157 in. The specimens were then strains in tension 1 to 3% by bending. Best results were achieved with a prestrain of 1.5% in tension. Only two usable grains were produced from seven strain annealed specimens. The cyclic anneal method was tried and all except the above two grains were produced in this way. The cyclic treatment consisted of heating the cold-rolled strips to 1562°F for 24 hours and then to 2012°F for 4 hours and back again to 1562°F for 24 hours. This

cycle was repeated several times, ending with 24 hours at 1562°F. This produced grains of 0.5 in. in length.

The three solid solution alloys of titanium were made into specimens of the same size as that for the iodide titanium, 3 x 0.25 x 0.050 inches. Four specimens of this size were fabricated from each 25-gram button. At least four buttons were made for each alloy. The cyclic anneal method was tried using the same procedure as described by Anderson, et al (45). The upper temperature was 2200°F, but the lower temperature, which was chosen to be just below the transformation temperature, varied with the alloy. For the 4%Al-Ti alloy, the latter temperature was 1652°F, whereas, for the 15% Zr-Ti it was 1382°F and for the 13% Ta-Ti alloy it was 1112°F. These specimens were found to have attained a beta grain size of about 0.5 in. in diameter but on the last transformation formed alpha grains of about 0.04 in. in diameter. Because of the resulting small grain size, they were replaced in evacuated quartz tubes and recycled twice. The 15% Zr-Ti alloy contained several grains between 0.25 and 0.36 inches in diameter. However, these grains were so brittle that deformation mechanisms could not be determined. This specimen was found to contain 0.93 % silicon, being contaminated by the quartz tube. Future specimens consequently were wrapped in tantalum foil and separated from the tantalum with titanium rings. Another group of specimens were prepared and cycled using the tantalum foil with still no grains suitable for use. However, during the transfer of the specimens from the furnace to the other furnaces of lower temperature, a quartz tube containing a 4% Al-Ti specimen was accidentally broken. The result was grains almost an inch in length. While a minimum of time in the alpha plus beta region during cooling was indicated to be desirable, this particular specimen was brittle and unsuitable for use. Since the 13% Ta-Ti alloy consistently had smaller grains than the other two alloys, its composition was changed to 10% tantalum so as to raise the alpha phase region and narrow the alpha plus beta region. Thus a wide alpha plus beta region in these alloys was believed to be the factor detrimental to the growth of the large grains.

In order to decrease the time in the alpha plus beta region or the time for formation of nuclei, it was decided to cool the specimens from the high temperature of 2200°F to about 400°F, instead of to a temperature slightly below their respective transformation temperatures. Then, the temperature was raised to just below the transformation temperature. However, this procedure did not noticably increase the size of the grains over those of the previous processes.

A more drastic quench was tried by immersing the specimens at 2200°F and sealed in quartz into water and oil at room temperature. Whereas, both treatments increased the grain size materially, the tubes were often broken by the water quench. The alpha grains resulting from the oil quench were of about the same size as those from the water quench and were less serrated. The grains had a diameter of about 0.0787 in. with the largest grain being 0.157 in. The speci-

mens were resealed in evacuated quartz tubes and heated to just below the transformation temperature for three days without any apparent increase in size.

It had been noticed that the alpha grain size was larger when associated with larger beta grains. To increase the beta grain size it was decided to try a cyclic anneal solely in the beta range. This was to decrease the refinement in the final alpha grains which resulted in previous treatments by cycling through the transformation. Although the strain energy produced by cycling through the transformation was absent, the beta grain size was larger and resulted in larger alpha grains. This method was adopted for growing the grains for this investigation. Thus, the procedure used in producing large grains was to heat the specimens to 2200°F for four hours, transfer immediately to a furnace at 1750°F and hold for three days, reheat to 2200°F for four hours and repeat the cycle three to five times. The last step was to quench from 2200°F in oil at room temperature, reseal specimens as necessitated and heat to just below the transformation for one to three days. The specimens treated in this manner produced as many as five grains per specimen that were from 0.10 to 0.30 inches in diameter.

While the above mentioned work on cyclic annealing was being done, several specimens were strain annealed. The strain was varied between 1/2 and 6%, giving grain sizes varying from 0.00157 to 0.039 inches in diameter. The specimens sealed in evacuated quartz tubes were placed in a furnace at 500°F, heated at rates varying between 50°F/day and 300°F/day to just below the transformation temperature and held for three to five days. This method did not produce satisfactory grains. The largest grains were hardly more than 0.039 in. in diameter. Thus, the grains grown by the cyclic annealing were used in the deformation studies.

In final analysis, the 4% Al-Ti alloy produced the largest grains, and the 15% Zr-Ti the smallest. The 10% Ta-Ti grains were more serrated than the others. It was found in many cases that a few very small grains existed in a large grain and in some instances their difference in orientation could only be distinguished by polarized light. The 15% Zr-Ti solid solution alloy appeared to have considerable material as a second phase and to be more brittle than the other two.

## C. EXPERIMENTAL METHOD

The grains were polished and slightly etched prior to taking x-ray back-reflection shots using a Unican camera with optical goniometer. Radiation from a tungsten tube operated at 35 KV and 17 ma was used. Great care was taken not to blemish the surface of the grains in any way during this and the subsequent operations. A Southwark-Emery 60,000-pounds capacity testing machine was fitted with a furnace for the high temperature deformation tests on iodide titanium. Loading was at the rate of 0.1 in./min. free head speed. The furnace was resist-

ance-wound, input was through two variacs and a micromax recorder-controller. The heating was done in a dried argon (99.98%) atmosphere to a temperature of 1500° F ±5°. The specimen surfaces remained bright during heating.

The solid solution alloys of titanium were pulled in tension in the same testing machine at room temperature. When specimens could not be gripped by the specimen holders, they were deformed by bending about a radius. Audible clicks could be heard during the deformation due to twinning. The tension axis of all the grains examined are plotted in Figures 37 and 38.

The deformation markings were read with reference to a mark on the specimen surface that was used in aligning the specimen for orientation determination by x-rays. The normal to the tracings on the grain surface were plotted on a stereographic projection of the grain as a great circle passing through the center. A tentative identification of the deformation elements were made by noting which poles of planes fell on the trace normals. The slip and twinning planes were then determined by the method of Bowles (53) for plotting one surface traces.

Slip and twinning traces could be distinguished by polishing carefully until complete removal of the deformation markings is achieved and then etching again to reveal the twin markings. Careful study was required here as some twin markings were not contrasted with the surface on etching but were only in relief as was revealed by oblique lighting. About 30% of all grains were such as to allow use of the two-surface method of analysis for a unique determination of the deformation elements.

## D. RESULTS AND DISCUSSION

The major deformation elements for titanium at elevated temperature and those of the solid solution alloys at room temperature are listed in Tables 5,6,7 and 8. On only one crystal was the direction of slip determined for the solid solution alloys. This was on the Ti-4% Al-¼ crystal which from geometrical considerations of glide gave the $[11\bar{2}0]$ as the slip direction for $(10\bar{1}0)$ slip. The slip direction was found to be $[11\bar{2}0]$ for the high temperation deformation of unalloyed titanium for grain AG. Inasmuch as every hexagonal close-packed metal investigated to date has the $[11\bar{2}0]$ as the slip direction and that in no case has the direction of slip been found to change for any metal due to alloying additions or temperature change plus the knowledge that at room temperature titanium has the $[11\bar{2}0]$ as the slip direction (12,45), it is assumed here that the slip direction is $[11\bar{2}0]$ irrespective of the slip plane for all of the materials investigated in this work.

Titanium Deformed at 1500°F.

The results of fourteen grains studied in tension at 1500°F are summarized in Table 5 and their tension axes are plotted in Figure 37.

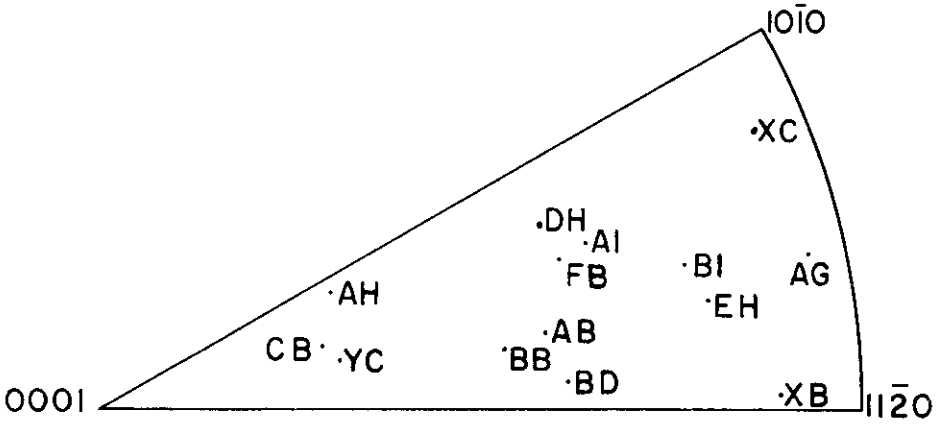


Fig.37 Orientations of titanium grains deformed in tension at 1500°F.

Two slip planes, $(10\bar{1}0)$ and $(10\bar{1}1)$, and two twin planes, $(11\bar{2}1)$ and $(11\bar{2}2)$, were observed to be active at 1500°F for unalloyed titanium.

Slip on $(10\bar{1}0)$ planes apparently dominated at the temperature of testing, but it appeared that $(10\bar{1}1)$ slip occurred more frequently than at room temperature. Rosi and co-workers (12) reported slip on $(10\bar{1}1)$ only in crystals which exhibited a complex slip process, whereas Anderson, et al (45) failed to note its occurrence at all. It is significant that all the slip in three grains, EH, BI and FB, occurred on $(10\bar{1}1)$ planes. No basal slip was observed.

TABLE 5

DEFORMATION ELEMENTS OF TITANIUM CRYSTALS DEFORMED AT 1500° F IN TENSION

| Grain | Slip Planes | Twin Planes |
|---|---|---|
| BB | --------- | $(11\bar{2}2)$ |
| XC | $(10\bar{1}0) + (10\bar{1}1)$ | $(11\bar{2}1)$ |
| DH | $(10\bar{1}0) + (10\bar{1}1)$ | $(11\bar{2}1)$ |
| EH | $(10\bar{1}1)$ | $(11\bar{2}1)$ |
| CB | $(10\bar{1}0)$ | $(11\bar{2}1)$ |
| AI | $(10\bar{1}0) + (10\bar{1}1)$ | ---- |
| BI | $(10\bar{1}1)$ | $(11\bar{2}1) + (11\bar{2}2)$ |
| YC | $(10\bar{1}0)$ | $(11\bar{2}1)$ |
| FB | $(10\bar{1}1)$ | $(11\bar{2}1)$ |
| AB | $(10\bar{1}0)$ | $(11\bar{2}1)$ |
| BD | $(10\bar{1}0)$ | ---- |
| XB | $(10\bar{1}0)$ | $(11\bar{2}2)$ |
| AH | $(10\bar{1}0)$ | $(11\bar{2}1)$ |
| AG | $(10\bar{1}0)$ | ---- |

In the present study, no twinning was observed on the $(10\bar{1}2)$ reportedly favored by other hexagonal metals. Twinning was on the $(11\bar{2}1)$ and $(11\bar{2}2)$ planes. Twins were found in all but three grains; however, twinning was not as pronounced as that at lower temperatures. In three grains $(11\bar{2}2)$ type twins were observed and in two of these $(11\bar{2}2)$ accounted for all of the twinning. The reasons for the differences in twinning behavior of titanium and other hexagonal metals are not apparent.

Over the temperature range of 78°F to 437°F, the change in $a$ is $11.0 \pm 0.3 \times 10^{-6}$ and in $c$ is $8.8 \pm 0.3 \times 10^{-6}$ for titanium (53). Hence, as the temperature increases the c/a ratio for titanium decreases. Rosi, Dube and Alexander suggest that the complexity of the slip systems increases as the c/a ratio decreases (12). Because of

the decrease in c/a ratio, the atomic density of the $(10\bar{1}0)$ and $(10\bar{1}1)$ planes increases relative to the density of the (0001) as temperature is increased. Apparently, the relative density of packing of the $(10\bar{1}1)$ planes increases with temperature and causes an increase in tendency for slipping on $(10\bar{1}1)$ planes at higher temperatures.

After hot rolling polycrystalline titanium at 1050°F both $(10\bar{1}2)$ and $(11\bar{2}1)$ twins are observed. However, on hot rolling at 1450°F only the $(11\bar{2}1)$ twins are present. Thus, the disappearance of $(10\bar{1}2)$ twinning occurs in the temperature range of 1050°F to 1450°F.

4% Al-Ti Alloy Deformed at Room Temperature

Table 6 indicates the prominence of $(10\bar{1}0)$ slip for the 4% Al-Ti alloy. The $(10\bar{1}2)$ plane is still the predominate twinning plane though twinning occurs also on the $(11\bar{2}1)$ and $(11\bar{2}2)$ planes. The tension axis of the grains are plotted in Figure 38a. The c/a ratio for 4% Al-Ti is 1.600 compared to 1.588 for pure iodide titanium. This increase in c/a ratio means the relative atomic density of the (0001) plane is greater for the alloy than for pure titanium. Rosi, et al (12) reports no basal slip, whereas, Anderson, et al (45) reports basal slip in titanium. The latter investigator attributed the difference to the small crystal size, the orientation of the grains and impurities of the material used by Rosi, et al. The size of the grains used for this work were more similar to those used by Rosi, et al. Although the one surface trace method indicated the presence of (0001) slip in two instances, the solution was not definite. Figure 39 shows a deformed grain with $(10\bar{1}0)$ and $(10\bar{1}2)$ deformation markings.

TABLE 6

DEFORMATION ELEMENTS OF 4% AL-TI ALLOY DEFORMED IN TENSION

| Grain | Slip Plane | Twin Plane |
|---|---|---|
| IA | $(10\bar{1}0)$ | ---- |
| IB | $(10\bar{1}0)$ | $(10\bar{1}2)$ |
| IIC | ---- | $(10\bar{1}2)$ |
| IID | $(10\bar{1}0) + (0001)$ | $(10\bar{1}2)$ |
| IIF | $(10\bar{1}0)$ | $(10\bar{1}2) + (11\bar{2}1)$ |
| IIG | ---- | $(11\bar{2}2) + (11\bar{2}1)$ |
| III | $(10\bar{1}0)$ | ---- |
| IIIK | $(10\bar{1}0)$ | $(11\bar{2}1) + (10\bar{1}2) + (11\bar{2}2)$ |
| IIIL | $(10\bar{1}0)$ | ---- |
| VX | $(10\bar{1}0)$ | ---- |
| VY | ---- | $(10\bar{1}2)$ |

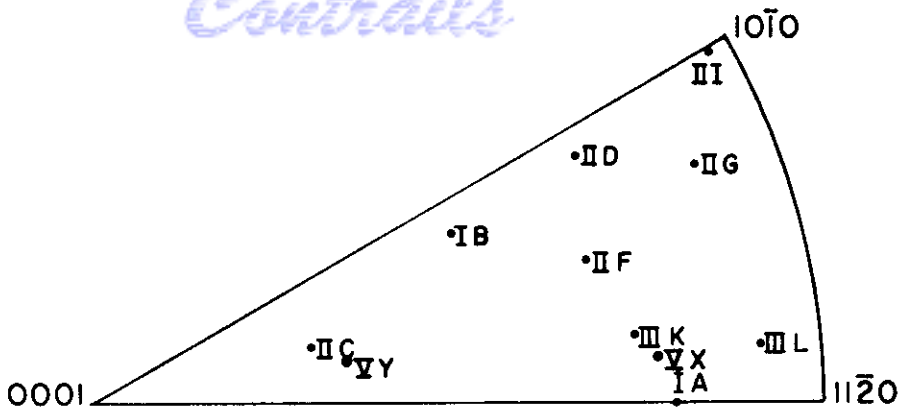


a. Ti – 4%Al

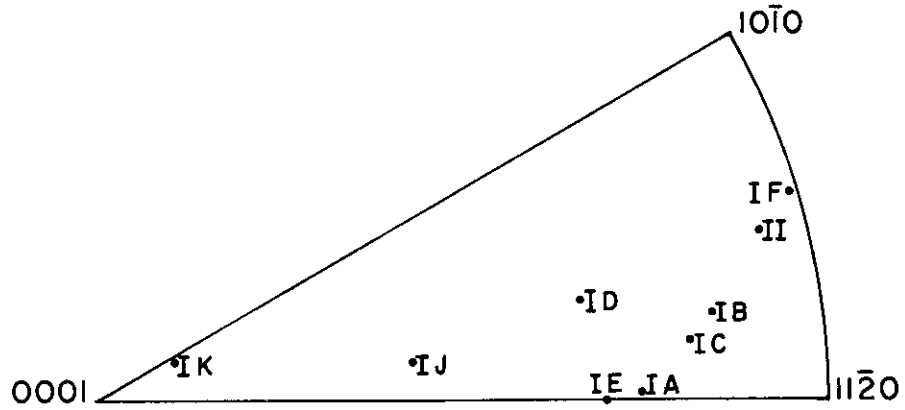


b. Ti – 10%Ta

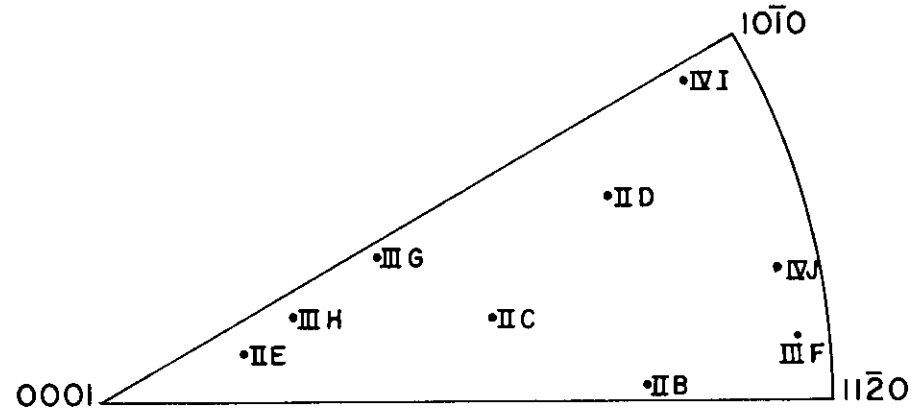


c. Ti – 15%Zr

Fig. 38 Tension axis of Titanium alloy grains deformed at room temperature.

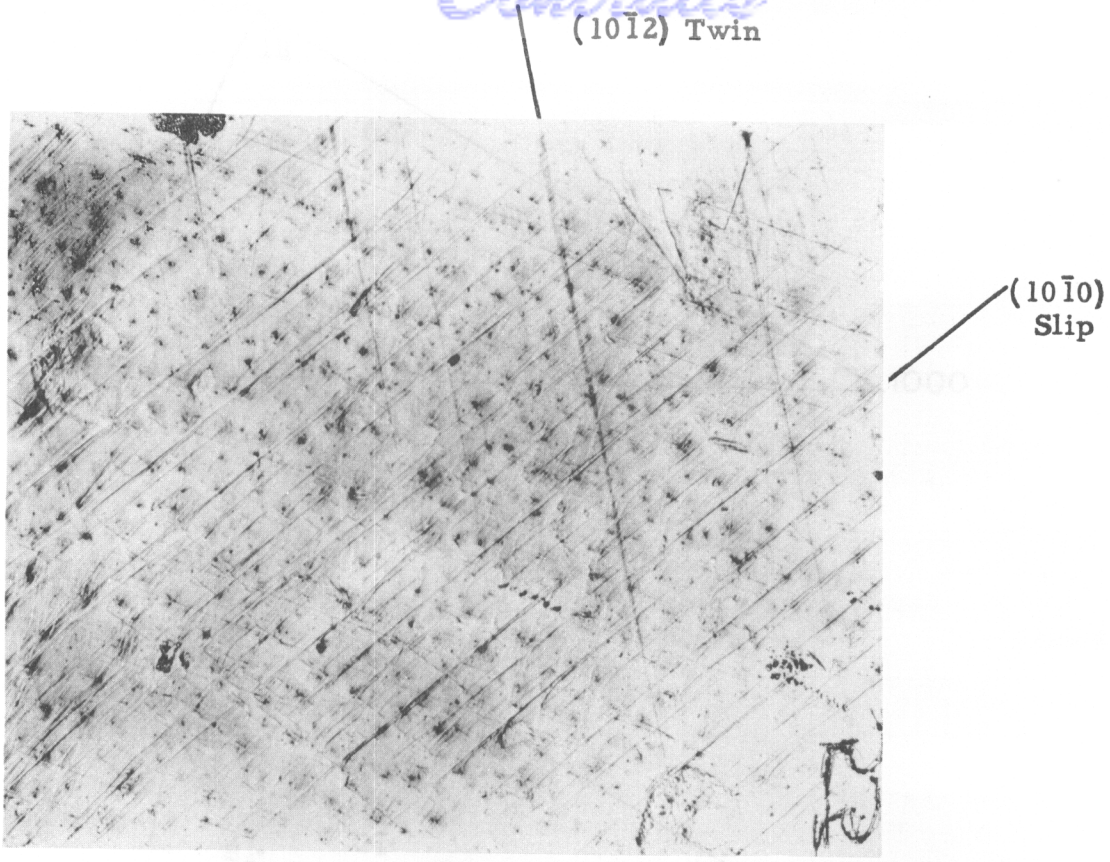


Fig. 39 4% Al-Ti grain No. II D deformed in tension showing (10$\bar{1}$0) slip and (10$\bar{1}$2) twin markings. X 150

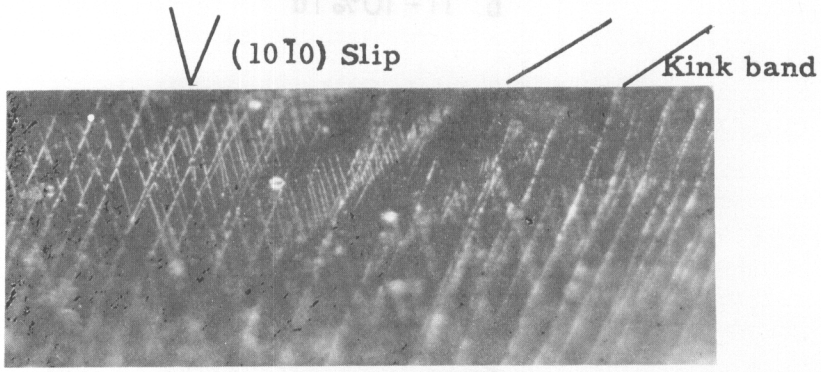


Fig. 40 4% Al-Ti grain No. I B deformed in tension showing (10$\bar{1}$0) slip, kink band formation and then slip on another (10$\bar{1}$0) type plane. Polarized light X 250

Their deformation characteristics were believed to be complicated because of the small size of the crystals on which this work was performed. In many instances, the grain under study was completely surrounded by other grains. On a few of the grains, some of the deformations markings could not be attributed to low indices planes. Such is a case for grain IIC where slip lines display a cross connecting pattern. When this crystal was extended further $(10\bar{1}0)$ slip was prominent. From Figure 38a, the tension axis of grain IIC is shown to be located in that region where Anderson, Jillison and Dunbar report finding the majority of basal slip. The presence of $(10\bar{1}1)$ slip was indicated in three of the eleven grains studied; however, since some doubt existed as to their true identity they are not listed in Table 6.

Kink band formation was observed to occur only in two grains, and in each case there was no evidence of twinning, Figures 40 and 41. The observations in kink band formation were the same as made by Rosi (54) in that they occurred in connection with $(10\bar{1}0)$ slip with $(11\bar{2}0)$ the bend plane. Figure 40 shows an interesting kink band formation where slip first occurred on a $(10\bar{1}0)$ plane then the kink bands formed and were followed with slip on another type $(10\bar{1}0)$ plane. The second type $(10\bar{1}0)$ slip lines split just as they intersect the bend plane. Also, the kink bank is associated with only one of the $(10\bar{1}0)$ slip systems, the most favored one.

Thus, the deformation mechanisms of 4% Al-Ti are not widely different from those reported for unalloyed titanium. The complexity of deformation observed for the 4% Al-Ti alloy here is attributed in part to the large-grained polycrystalline aggregate on which the study was conducted, as opposed to the results one might expect from single crystals.

TABLE 7

DEFORMATION ELEMENTS OF 15% ZR-TI ALLOY DEFORMED IN TENSION

| Grain | Slip Plane | Twin Plane |
|---|---|---|
| II B | ---- | $(11\bar{2}1)$ |
| II C | $(10\bar{1}1)$ | $(11\bar{2}1)$ |
| II D | $(10\bar{1}1)$ | $(11\bar{2}2)$ |
| II E | ---- | $(11\bar{2}1) + (10\bar{1}2) + (11\bar{2}2)$ |
| III F | ---- | $(11\bar{2}2) + (10\bar{1}2)$ |
| III G | ---- | $(11\bar{2}1)$ |
| III H | ---- | $(11\bar{2}1) + (11\bar{2}4)$ |
| IV I | $(10\bar{1}0)$ | $(11\bar{2}1) + (11\bar{2}2)$ |
| IV J | ---- | $(11\bar{2}1) + (11\bar{2}2)$ |

Like the 4% Al-Ti alloy, the 15% Zr-Ti alloy has a c/a ratio greater than that of titanium being 1.602. The results of deforming

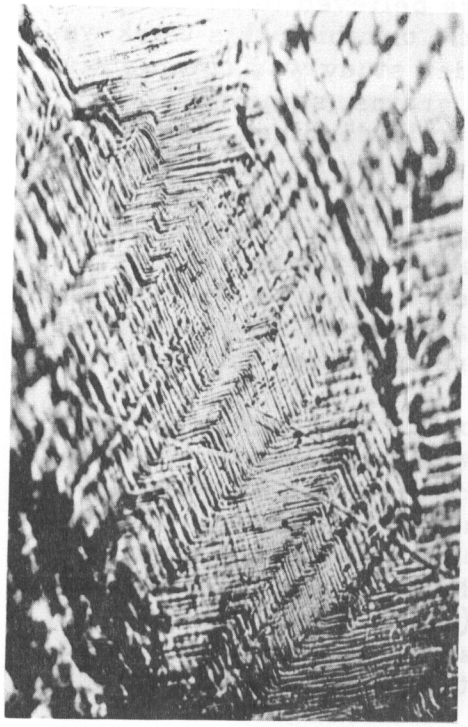

Fig. 41 4% Al-Ti grain no. II I deformed in tension showing a series of kink bands formed with $(10\bar{1}0)$ slip and bend plane $(11\bar{2}0)$. X 250


Fig. 42 15% Zr-Ti grain no. III G deformed in tension showing three traces of $(11\bar{2}1)$ twin planes and a veined all alpha structure. X150

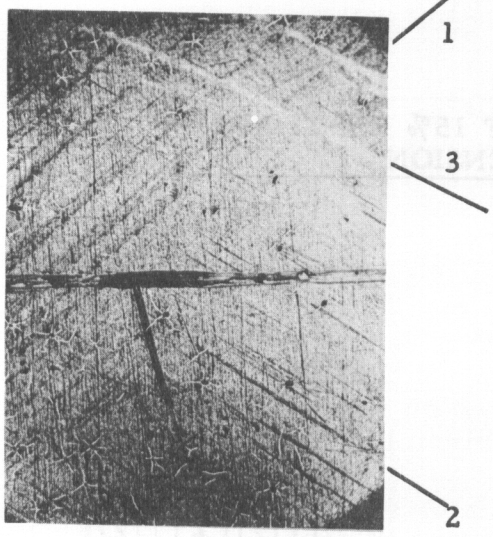


a. Surface


b. 90° Edge

Fig. 43 10% Ta-Ti grain no. I K deformed in tension showing three $(10\bar{1}2)$ twin markings in two surfaces 90° apart. X 25

nine grains in tension are shown in Table 7. Their tension axis is plotted in Figure 38c. This alloy was found to deform almost entirely by twinning except where the grains are made to undergo larger amounts of deformation. This effect may be attributed to solution hardening of zirconium addition and possibly contamination of the specimens resulting from prolonged heating at elevated temperatures. The embrittlement of the 15% Zr-Ti alloy occurred despite the precautionary measures which left the 4% Al-Ti and 10% Ta-Ti alloys very ductile. The contaminant is believed to be silicon from the quartz tubes. The lack of elongation in tension was the only measure of its brittleness. As mentioned previously for cadmium (52) and silicon-ferrite (51), the critical shear stress for twinning does not seem to be effected by solution hardening, whereas it is certain that the critical shear stress for slip is greatly increased by solution hardening. Thus, the critical shear stress for slip is increased in relation to that which is necessary for twinning.

Since the 4% Al-Ti alloy has about the same c/a ratio as the 15% Zr-Ti alloy, the difference in frequency of deformation elements is not explainable there. Also, it may be noted that the initial 15% Zr-Ti alloy was amenable to 90% cold reduction as were the other alloys. In spite of the embrittlement of the cyclic annealed 15% Zr-Ti specimens, the elements of deformation were the same except for an additional twinning plane of the type $(11\bar{2}4)$ and the frequency of occurance of the deformation elements. The additional twinning plane was among those reported by Liu and Steinberg (46) for titanium crystals formed from fused salts by electrolysis. Figure 42 is an illustration of the major twin plane $(11\bar{2}1)$ found in the 15% Zr-Ti alloy. The wide band markings are transformed beta and are due to the transformation on cooling . They correspond to $(10\bar{1}0)$ planes. Cleavage was found to occur along these lines.

10% Ta-Ti Alloy Deformed at Room Temperature

This was the only solid solution alloy with a c/a ratio less than that for unalloyed titanium, 1.580 compared to 1.588. The deformation elements are listed in Table 8 below.

Of the nine grains studied, no additional deformation elements were found. The results indicate no major change from the observations on the other alloys. The only effect that can be attributed to the addition of tantalum is that twinning becomes more frequent than that in unalloyed titanium. This may result from an increase of critical shear stress for slip relative to that for twinning.

An appearance of more $(10\bar{1}1)$ slip for this alloy than observed for 4% Al-Ti may be explained by the increase in density of the $(10\bar{1}1)$ planes relative to the (0001) with decreasing c/a ratio. In agreement with the results of Rosi (54) and Anderson, et al (45) on unalloyed titanium, grain IK was found to deform by $(10\bar{1}2)$ twinning alone. From Figure 38b, it can be seen that the tension axis is located near the (0001).

Figure 43 shows the three $(10\bar{1}2)$ type deformation markings in two surfaces 90° apart. Variance in the position of the twin plane with respect to the tension axis is depicted by the width of the twinned areas. The smaller the angle between tension axis and pole of the plane the greater the width of the twinned area.

TABLE 8

DEFORMATION ELEMENTS OF 10% TA-TI ALLOY DEFORMED IN TENSION

| Grain | Slip Planes | Twin Planes |
|---|---|---|
| IA | ---- | $(10\bar{1}2)$ |
| IB | ---- | $(10\bar{1}2) + (11\bar{2}2) + (11\bar{2}1)$ |
| IC | $(10\bar{1}1)$ | $(11\bar{2}2)$ |
| ID | $(10\bar{1}0)$ | $(10\bar{1}2) + (11\bar{2}1)$ |
| IE | ---- | $(11\bar{2}1) + (10\bar{1}2) + (11\bar{2}2)$ |
| IF | $(10\bar{1}0) + (10\bar{1}1)$ | $(11\bar{2}2)$ |
| II | $(10\bar{1}0)$ | $(11\bar{2}2) + (11\bar{2}1)$ |
| IJ | $(10\bar{1}1) + (0001)$ | ---- |
| IK | ---- | $(10\bar{1}2)$ |

Here again, the modes of deformation are essentially the same as for unalloyed titanium. The only noticeable difference was an increase in twinning relative to slip.

## E. DISCUSSION AND CONCLUSIONS

Having seen the deformation textures for cold-and hot-rolled unalloyed titanium and the cold-rolled textures of titanium alloyed with Al, Ta and Zr, the differences in textures will now be treated in terms of differences in deformation mechanisms. The conditions of deformation in these determinations of the flow mechanisms more closely approximate that which is found in polycrystalline metal than in single crystals. Still, the deformation mechanisms determined from large-grained polycrystalline material with small deformations may not be entirely suitable when used in predicting the deformation textures which result when severely deforming fine-grained material. In general, however, the predictions of deformation textures from the metal's deformation mechanisms have been good. Still, the predicted pole figures are only general in nature and lack considerable detail.

Assuming the deformation mechanisms determined by Rosi, et al (12) and rotation data from Anderson, et al (45) for titanium the cold-rolled texture of titanium has been accounted for (55) using the theory of Hibbard and Yen (56) and Calnan and Clews (57). The predicted results were in good agreement with the experimentally determined pole figures. Williams and Eppelsheimer (14), also using the data of Rosi,

et al (12) and Anderson, et al (45), derived the cold-rolled texture for titanium using the theory of Calnan and Clews. Their resulting pole figures also were in good agreement with the experimental texture. However, both investigations generally concluded that suitable choice of slip and twin elements, their relative frequency of operation and the sequence of their operation had much to do with the degree of success. However, whereas, Williams and Eppelsheimer chose $(10\bar{1}1)$ $[11\bar{2}0]$, $(0001)$ $[11\bar{2}0]$ and $(10\bar{1}0)$ $[11\bar{2}0]$ in order of prominence and increasing relative critical shear stress, the present work used $(10\bar{1}0)$ $[11\bar{2}0]$ and $(10\bar{1}1)$ $[11\bar{2}0]$. Both used the same twinning planes. It is noted that Williams and Eppelsheimer concluded that $(10\bar{1}0)$ slip was not necessary, but that $(0001)$ slip was necessary in the theoretical development of the textures. The fact that in the present work the same texture was developed without considerations of slip on the $(0001)$ plane shows the theory of Calnan and Clews is quite flexible when the end result is known.

Only certain of the textures that were developed on annealing or hot rolling had a direction other than $[10\bar{1}0]$ parallel to the rolling direction. The theoretical development of the cold-rolled texture of titanium showed that the aligning of the $[10\bar{1}0]$ parallel to the rolling direction was due to tensive and compressive slip. The only noticeable difference between the pole figures besides the tendency of $[11\bar{2}0]$ 11R.D. on annealing or hot rolling was in the basal pole figures. The split basal varied from 27° to 40° in the cross direction and from a split to a non-split condition. In the discussions of the application of the Calnan and Clews theory, both investigations credited twinning with removal of $(000\bar{1})$ poles from the rolling plane normal. Tension twinning on the $(10\bar{1}2)$ was postulated to remove all $(0001)$ poles within approximately 29° of the rolling direction to a position near the transverse axis. Compression twinning on $(11\bar{2}2)$ and $(11\bar{2}1)$ will remove the $(0001)$ poles within 30° of the rolling plane normal to a region near the circumference of the pole figure. The presence of the $(000\bar{1})$ poles in the rolling plane normal are attributed to compressive stress with slip on the $(0001)$ by Williams and Eppelsheimer, while the present work attributes it to compressive twinning on the $(10\bar{1}2)$ and tension twinning on the $(11\bar{2}1)$ or $(11\bar{2}2)$. These mechanisms for $(0001)$ pole placement are postulated due to the complex nature of the stress system in polycrystalline material and the inhomogenities of deformation. Here again the question arises as to which sequence is correct.

Since there seems to be some ambiguity in the prediction of the deformation textures from the deformation mechanism, there can only be speculation as to the reasons for the differences in textures arising from known differences in deformation mechanisms.

On comparing the deformation elements of 4%Al-Ti, 15%Zr-Ti and 10%Ta-Ti, it is seen that $(10\bar{1}1)$ slip was absent from all 4%Al-Ti grains, whereas it was definitely detected in the other alloys. This does not imply that $(10\bar{1}1)$ slip does not occur in the 4%Al-Ti alloy in texture formation but indicates that its frequency of occurrence may be less than for the other alloys. Since, according to the theory of

Calnan and Clews, $(10\bar{1}1)$ slip rotates the (0001) poles 58° from the compression axis, the lack of it, with other things being equal, would tend toward more (0001) poles in the center of the (0001) pole figure. Also, (0001) slip would have a tendency to create a non-split basal since the (0001) poles would rotate toward the normal to the rolling plane. The deformation elements of titanium at 1500°F consisted of considerable $(10\bar{1}1)$ slip and the experimental pole figure showed a non-split basal for a rolling temperature of 1450°F, Figure 29. Hence, the slip mechanism $(10\bar{1}1)[11\bar{2}0]$ would have doubtful value in the determination between split and non-split basal textures.

Compression twinning on the $(10\bar{1}2)$ in the early stages of deformation and tension twinning on the $(11\bar{2}1)$ and $(11\bar{2}2)$ would result in a tendency for a non-split basal. The reverse of this, tension twinning on the $(10\bar{1}2)$ plane, would result in removal of the (0001) poles from the center of the (0001) pole figure as would compression twinning on the $(11\bar{2}1)$ or $(11\bar{2}2)$. From the theory of Calnan and Clews, no definite prediction could be made about the effect of the twinning planes on the split basal texture since the twinning sequence is arbitrary. Still the spread of the basal planes in the transverse direction can be accounted for by $(10\bar{1}2)$ or $(11\bar{2}1)$ twinning. However, the observation of only $(10\bar{1}2)$ twinning in the hexagonal close-packed metals Zn, Cd and Mg where (0001) slip is prominent does not account for spread in the transverse direction of the basal pole figure. Consequently, $(10\bar{1}2)$ tension twinning would have had to be predominantly operative in the later stages of deformation. Assumption of tension twinning on the $(10\bar{1}2)$, seems to be the most logical. This is borne out by the observations of Rosi (54) when he found more profuse $(10\bar{1}2)$ and $(11\bar{2}1)$ twinning for crystals deformed in compression. Due to the extension of the C-axis for $(10\bar{1}2)$ twinning, it certainly would not be expected to occur in the later stages of deformation. Since lack of $(10\bar{1}2)$ twinning was obvious in the deformation of titanium at 1500°F and a non-split basal pole figure resulted, it may be concluded that $(10\bar{1}2)$ twinning, or lack thereof, is not related to the splitting of the basal planes.

In the alloys of titanium studied for deformation mechanism, $(11\bar{2}1)$ and $(11\bar{2}2)$ were the most porminent twinning planes for the 10% Ta-Ti and 15% Zr-Ti while the $(10\bar{1}2)$ was most pronounced for 4% Al-Ti. Twinning on these planes in compression will remove the (0001) poles from the normal to the rolling plane toward the circumference. Then greater frequency of operation on these twin mechanisms would result in less (0001) poles in the center of the (0001) pole figure. That the 4% Al-Ti alloy has a non-split basal texture on cold rolling in contrast to the split basal texture of the Ti-Zr and Ti-Ta alloys could be related to the occurrence of $(11\bar{2}1)$ and $(11\bar{2}2)$ twinning for the latter alloys. However, the hot rolling of titanium at 1450°F results in a non-split basal texture though the deformation elements were more inclined to $(11\bar{2}1)$ and $(11\bar{2}2)$ twinning than even the cold-rolled Ti-Ta and Ti-Zr alloys, which have split basal textures. Many hexagonal metals show increase in randomness on hot rolling so that the seemingly non-split texture could be attributed to this general randomness Hence, frequency of operation of $(11\bar{2}1)$ and $(11\bar{2}2)$ twinning seems to

be doubtful as a determinant between split and non-split basal textures.

Since basal slip rarely occurred for the grains deformed in this investigation, its effect on split basal was at first neglected. Now, it seems that it should be considered. Those hexagonal metals previously mentioned which slip on the (0001) and twin on the $(10\bar{1}2)$ have basals tilted in the rolling direction and in some cases they are split in the rolling direction. Since beryllium has (0001) and $(10\bar{1}2)$ deformation elements and displays a deformation texture similar to cold-rolled titanium with exception of the splitting of the basal (20), (0001) slip possibly is not the determining factor.

In a latter section the effect of varying concentrations of aluminum on the split basal texture of cold-rolled titanium will be shown. As the aluminum content increases, the spread of the basal poles in the cross direction decreases. At one intermediate stage, the basal pole figure shows a high intensity region surrounding a lower intensity region in the center. At this stage, it could be expected that $(11\bar{2}1)$ or $(11\bar{2}2)$ twinning resulting from tension stresses are removing the basal poles toward the surface of the stereographic projection.

In conclusion, it can be stated that the deformation mechanisms for 4% Al-Ti, 10% Ta-Ti and 15% Zr-Ti at room temperature and of iodide titanium at 1500°F were very similar. The frequency of twinning at room temperature was probably greater in relation to slip for the alloyed titanium than the unalloyed. The 4% Al-Ti alloy had a greater portion of $(10\bar{1}2)$ twinning than the other alloys. Iodide titanium at 1500° F was found to twin only on the $(11\bar{2}1)$ and $(11\bar{2}2)$ without any occurrence of $(10\bar{1}2)$. The slip planes for titanium and its alloys are $(10\bar{1}0)$, $(10\bar{1}1)$ and (0001) in decreasing frequency of occurrence. The theory of Calnan and Clews cannot predict changes in the deformation textures, from the small alterations of deformation mechanisms as determined by the methods employed. Moreover, it has been shown that there is considerable contradiction between deformation textures predicted from their theory and small changes in deformation mechanisms. Why there is a split basal spread in the cross directions for titanium and some of its alloys and a non-split basal in others is not understood from a comparison of deformation mechanisms.

SECTION IX

# EFFECTS OF THE ALPHA-BETA-ALPHA TRANSFORMATION ON TEXTURES

It can be seen in Figure 44 that a sharp texture is present after the double transformation alpha-beta-alpha. This texture can be described by the 27° tilted basal plane with the $[11\bar{2}0]$ direction parallel to the rolling direction. This is the same orientation reported for iodide titanium annealed at 1500°F.

One specimen of cold-rolled titanium sheet was cycled five times between the alpha and beta regions, and x-ray shots were made to determine if any change in the texture resulted. The procedure was to heat the cold-rolled material to 1650°F for five minutes then slowly cool to room temperature. The only difference noted was a slight increase in the spread of the basal planes in all directions; otherwise, the sharp texture of Figure 44 was retained.

The presence of this sharp texture indicates that definite crystallographic orientation relationships exist between alpha and beta during transformation. Moreover, since the texture is essentially the same as the high temperature annealing texture, it would appear that the same specific crystallographic relationships operate between conjugate grains both during transformation to beta and back again to alpha. Either this would appear to be the case, or only specific planes of a family must be permitted to function in the first place. Once in the beta field, the grains had little opportunity for growth or other change from the initial transformed orientation.

There are 72 geometrically possible orientations for the final alpha grains resulting from an alpha-beta-alpha transformation according to the Burgers relationship (58). There have been several factors used to account for the retention of the texture. One of the most recent states that the simple dislocations present in the parent phase can only return to simple dislocations after a second transformation if the original orientation returns (59). Sub-microscopic inclusions in nucleating transformation could be responsible for similar results.

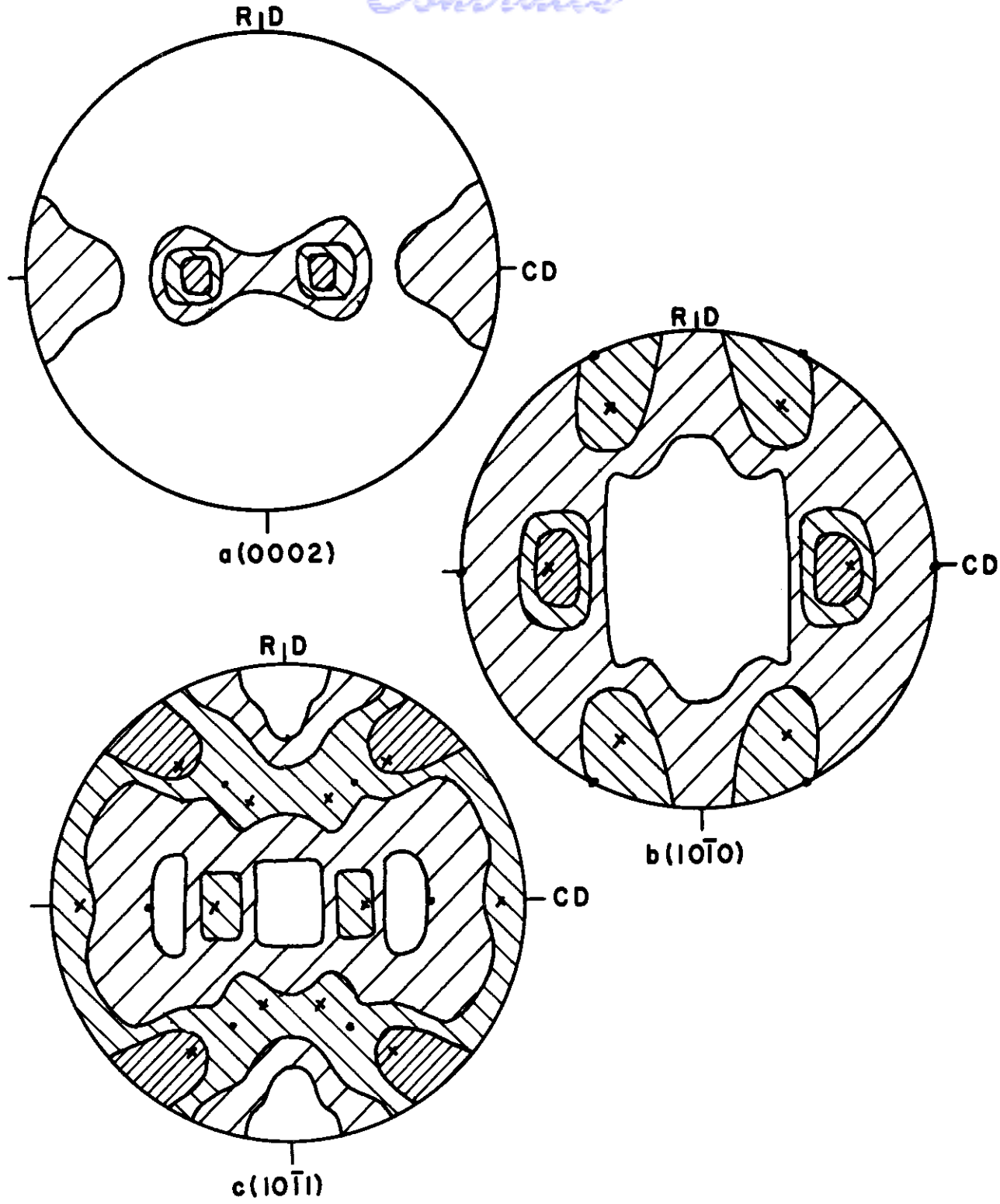


Fig.44 Texture in Iodide Titanium Cold-rolled 97%, Heated Above The $\alpha \rightarrow \beta$ Transformation Temperature and Slowly Cooled. •=(0002)[11$\bar{2}$0] X (0002) Rotated 25° About Rolling Direction, [11$\bar{2}$0] Parallel to Rolling Direction.

SECTION X

# LAYER STUDIES AND BEND TESTS

## A. INTRODUCTION

The formation of layer structure was studied on cold-rolled, annealed and hot-rolled Ti-75A forgings furnished by the Allegheny Ludlum Steel Corporation. These forgings were sectioned and cold-reduced 60,70, and 80% in thickness with a 10% reduction per pass and reversing the rolling direction 180° after each pass. An etchant was used to remove the surface layers one side at a time while the other side was protected with wax. Layer studies and bend tests were conducted on materials that had none, 0.005 and 0.010 inches of surface material removed from each side. The relationship of preferredness of texture to bendability was determined from this data.

## B. LAYER STUDIES, RESULTS AND DISCUSSION

Since reflection x-ray shots do not give data for the entire pole figures, the limits of the outer intensities of Figures 49* to 56* could not be shown. In order to make sure that the texture for sponge-type material is the same as for the iodide titanium, a few transmission exposures were made on material etched to a final thickness of 0.005 inches. These results indicated that the same basic texture is present in both types of material, differing only in the degree of preferredness for different amounts of cold work.

A study of Figures 49*, 50* and 51* shows that the degree of spread of the basal plane increases in the rolling direction for all reductions as the center of the specimen is approached. For example, the spread of the region of maximum intensity of the (0002) plane in the rolling direction increases from $\pm$ 15° at the surface of the specimen cold-rolled 80% to $\pm$ 38° at the center of the same specimen. The spread in the transverse direction of the regions of high intensity remains approximately the same at all levels for the specimens studied.

The same cold-rolled specimens annealed one hour at 1000°F, Figures 52* to 54*, showed textures which were very similar in all respects. Microstructures indicate that 'recrystallization in situ' had taken place in all cases and grain growth was not excessive.

The specimens hot-rolled 80% at 1050° F and 1450° F in both cases showed an increase in the spread of the higher intensity region of the (0002) plane as the center was approached in both the rolling and cross directions, Figures 55* and 56*.

* An asterisk following a figure denotes that those figures are located in the Appendix.

Figure 56* is similar to Figure 29 which shows the texture of iodide titanium rolled at 1450°F. These pole figures show that the basal planes in the hot-rolled sheets are parallel to the rolling plane, and that there are no significant differences in the textures at the surface and the center of the specimen. The annealed specimens had textures similar to those of iodide titanium annealed at the same temperature and variances between surface and center were small.

Although the reasons for a surface texture differing from an inner texture is uncertain, several possible explanations have been advanced. One possibility is that the flow of metal at the surface may be different from the flow of metal in the interior. Another idea is that the texture at the surface may be produced by the partial recrystallization of the surface layers.

Hu, Sperry, and Beck (60) observed a layer effect in aluminum when strips of this material were rotated 180° between successive passes through the rolls. However, straight rolling did not produce this effect. Strips of brass and copper, on the other hand, had similar textures throughout the specimens regardless of the rolling technique. These investigators attributed the change in the aluminum texture to the alteration of the rolling procedure.

In a progress report of an investigation conducted by Anderson and Jillson (61), it was reported that in one instance different textures were observed at the surface and at a sub-surface layer in arc-melted iodied titanium rolled at room-temperature. The texture at the surface was similar to the high-temperature annealing texture described earlier in the present report, and the sub-surface texture was said to be that reported here as the cold-rolled texture. However, the same authors report that two other specimens from the same ingot failed to show this effect. The only difference in the treatment of the specimen which showed the layer effect and those which did not, was that the former was not allowed to cool between passes, whereas, the latter specimens were.

In the course of the present investigation, it was noted that considerable heating of the specimens occurred for even relatively small reductions per pass. For this reason, reductions of only 10% per pass were used, and the strips were allowed to cool between passes. Since the recrystallization temperature decreases with increasing amounts of cold work, and since the reported surface texture of titanium was similar to the fully annealed texture, it is suggested that this reported layer texture was caused by partial recrystallization. It is concluded that the cold-rolled sheet texture of titanium reduced 80% to a final thickness of 0.030 in. is the same at the surface and center of the sheet.

## C. BEND TESTS, RESULTS AND DISCUSSION

Duplicate bend tests were made on specimens in both the transverse and the longitudinal directions. The test is similar to that used by Fuller and Edmunds in studying zinc (62,63). The specimen is

bended by hand in a large arc, then placed in a press and the bending continued until the first signs of cracking appear. In order to eliminate the effects of change of thickness due to the removal of the surface material, the minimum radius for bending to failure was reported in terms of the sheet thickness. The common region of failure is the outer-bend radius which is deformed in tension. The bend test is used here to point out the significance of differences in surface textures on the ability of the rolled sheet to deform in tension.

The data obtained from the bend tests are presented in Table 9. It will be noted from the table that in every case, except the surface of the specimen rolled at 1450°F, the radius of bend was smaller for the specimen taken with the long dimension parallel to the transverse direction than the one with the long dimension parallel to the rolling direction. It is believed that the one exception mentioned might have been related to surface contamination produced during the heating to temperature and rolling at 1450°F.

In every case studied, the capacity for bending increased as the more highly preferred material was removed from the surface. For example, in the specimen cold-rolled 80%, the radii changed from 1 3t for the transverse specimen and 20t for the longitudinal specimen at the surface to 3.5t and 15t, respectively, for specimens with 0.010 in. etched away.

The bending properties of the annealed specimens were much better than those for the cold-rolled ones. There was little difference in results between annealed specimens that had been rolled 60, 70 and 80%.

TABLE 9

RESULTS OF BEND TEST*

| Treatment | Surface TD | Surface LD | 0.005 in. TD | 0.005 in. LD | 0.010 in. TD | 0.010 in. LD |
|---|---|---|---|---|---|---|
| CR 60% | 6.0t | 10.0t | 4.0t | 8.0t | 2.0t | 8.0t |
| CR 70% | 7.5t | 18.0t | 4.5t | 17.0t | 3.0t | 13.0t |
| CR 80% | 13.0t | 20.0t | 7.5t | 20.0t | 3.5t | 15.0t |
| CRR 60% | 3.0t | 3.7t | 2.0t | 2.3t | 180°abt 1t | 1.5t |
| CRR 70% | 3.0t | 3.7t | 2.0t | 2.5t | 1.0t | 1.3t |
| CRR 80% | 3.0t | 4.0t | 2.0t | 2.7t | 1.0t | 1.0t |
| HR 80% 1050°F | 2.0t | 3.0t | 2.0t | 2.7t | 1.2t | 1.5t |
| HR 80% 1450°F | 2.9t | 2.5t | 2.0t | 2.5t | 180°abt 1t | 1.3t |

* All results are the average of determinations on two specimens.

The bend properties of the hot-rolled specimens were slightly better than the others at the surface but were comparable to the annealed material at the 0.005 in. and 0.010 in. depths. Both annealed and hot-rolled specimens were superior to those cold-rolled.

## SECTION XI

## SUMMARY

1. The cold-rolled fiber texture for iodide titanium is described as having the $[10\bar{1}0]$ direction parallel to the wire axis with all azimuthal positions possible. On annealing at 1000°F for 40 minutes, the fiber texture is best described as having the $[11\bar{2}0]$ direction tilted $\pm$ 11° from the wire axis. An addition of 3.8% aluminum to titanium did not change the cold-rolled fiber texture; however, annealing this alloy resulted in a fiber texture best described as $[11\bar{2}0]$ lying along the wire axis.

2. Iodide titanium cold-rolled 97% has a preferred orientation described as (0002) rotated 27° in the cross direction with the $[10\bar{1}0]$ parallel to the rolling direction. This is similar to results reported by other investigators. An addition of 3.8% aluminum to titanium results in a non-split (0002)$[10\bar{1}0]$ texture. The amount of aluminum necessary to cause titanium to display a non-split basal texture is about 1.5%

3. Additions of 3.6% columbium, 3.6 and 15.4% tantalum, and 7.1 and 14.75% zirconium changes the texture of cold-rolled iodide titanium only with respect to the amount of spread of the basal poles in the cross direction. It is concluded that the observed changes in textures may not be attributable to the small changes in c/a ratio.

4. Low temperatures of annealing (1000°F for one hour) of titanium and its solid solution alloys resulted in a sharpening of the cold-rolled textures and was described in terms of polygonization. A gross reorientation of some of the basal poles by 30° was ascribed to preferred absorption.

5. Higher temperatures of annealing (>1300°F for one hour) produce a texture related to the cold-rolled texture by a rotation of approximately 30° about the C-axis. The development of the annealing textures from the cold-rolled matrix is believed to be caused by 'oriented nucleation' and 'oriented growth' with the former being the more predominant at

the lower temperatures and longer times of annealing.

6. Additions of 3.8% aluminum, 3.6% tantalum and 7.1% zirconium do not affect the crystallographic relationship of the annealed material with the cold-rolled matrix though they do decrease grain size and raise the temperature of recrystallization. The degree of influence appears to be dependent on melting points and similarity of chemical properties of the alloying additions with titanium.

7. Alpha alloys of titanium containing molybdenum were found to have cold-rolled and annealing textures similar to the unalloyed titanium. The beta alloy (31.8% Mo) has a cold-rolled texture best described as (100) [110] and on annealing one hour at 1500°F the texture is sharpened. Annealing the beta alloy one hour at 2000°F resulted in a texture related to the cold-rolled texture by rotations of about 20° around the [100].

8. The alpha-beta alloy of titanium containing 14.3% Mo has a cold-rolled beta texture similar to the all beta alloy but with markedly more spread in the cross direction and an additional minor component described as (112) [110]. It was concluded that the effect of the alpha phase was to increase scatter of the texture.

9. The texture of iodide titanium hot-rolled at 1050°F is best described as (0002) rotated 27° in the cross direction, [$10\bar{1}0$]. This is the same as the cold-rolled texture that had been annealed for one hour at 1000°F. Hot rolling at 1450°F results in a loss of the split basal texture and a random orientation of the basal poles about the normal to the rolling surface with both [$10\bar{1}0$] and [$11\bar{2}0$] components aligned parallel to the rolling direction.

10. The hot-rolled textures of titanium alloys containing 3.8% Al, 15.4% Ta and 14.75% Zr are basically the same as hot-rolled unalloyed titanium.

11. The effect of hot rolling on the textures of unalloyed titanium and it solid solution alloys can be ascribed to the thermal effect in that hot rolling produced results similar to that of annealing. This observation was corroborated by the fact that the deformation mechanisms at 1500°F were found to be practically the same as those at room temperature, and hence, unable to account for the difference between hot- and cold-rolled textures.

12. The best procedure found in this investigation for growing large grains in the solid solution alloys of titanium is to cycle solely in the beta region and then rapidly cool to well below the transformation temperature. The success of this method is believed to be derived from the removal of the grain refinement effect of the transformation through the wide alpha-beta region.

13. The deformation mechanisms of iodide titanium deformed at 1500°F were ($10\bar{1}0$), ($10\bar{1}1$) slip and ($11\bar{2}1$), ($11\bar{2}2$) twinning. The absence of

$(10\bar{1}2)$ twinning was the only major difference from the deformation mechanisms determined at room temperature by other investigators.

14. The deformation mechanisms of the 4% Al-Ti alloy at room temperature were $(10\bar{1}0)$, (0001) slip and $(10\bar{1}2)$, $(11\bar{2}1)$, $(11\bar{2}2)$ twinning. The absence of $(10\bar{1}1)$ slip in this alloy is the only major difference in deformation mechanisms between it and unalloyed titanium.

15. The 15% Zr-Ti alloy was found to have a much greater frequency of occurance of twinning relative to slip than unalloyed titanium and the other alloys studied. This is attributed to impurities.

16. The room-temperature deformation mechanisms of the 10% Ta-Ti alloy were similar to those of unalloyed titanium. The presence of $(10\bar{1}1)$ slip was greater in this alloy than in the other two investigated.

17. The influence of solid solution additions on the deformation mechanisms of unalloyed titanium is an increase in the frequency of occurance of twinning relative to slip.

18. Using the theory of Calnan and Clews, the cold-rolled texture of unalloyed titanium can be predicted from its deformation mechanisms. However, the theory of Calnan and Clews is quite flexible when the end result is known and could not account for minor changes in textures using minor differences in deformation mechanisms.

19. Cycling cold-rolled titanium through the alpha-beta transformation temperature by heating to 1650°F for five minutes and slowly cooling results in a sharpening of the texture present on annealing at 1500°F.

20. The degree of preferredness of the sheet textures of titanium varied from the surface toward the center. There was increasing scatter of the texture from the surface in.

21. The greater the amount of total cold or hot reduction, the less the difference in texture scatter between surface and interior for rolled titanium sheet.

22. The capacity for bending of rolled titanium sheet increased with (1) removal of highly preferred material from the surface, (2) decreasing amounts of reduction, (3) increasing temperatures of hot rolling and (4) annealing. Also, titanium has greater bendability in the transverse than longitudinal direction in all cases studied.

## REFERENCES


1. Tinsley, M.L. An Investigation of the Titanium Rich End of the Titanium--Copper System. Thesis, University of Kentucky, 1950. pp. 18.

2. Battelle Memorial Institute. Research and Development of Titanium Alloys. United States Air Force Technical Report No. 6218, Part 2, United States Air Force, Air Material Command, 1950.

3. Smith, D.W. Symposium of Radiography and X-Ray Diffraction. A.S.T.M., Philadelphia, 1937.

4. Sutcliffe, D.A. and Reynolds, J.A. Electrolytic Polishing of Titanium. Metallurgia. March 1950. pp. 210.

5. Burgers, W.G., Fast J.D. and Jacobs, F.M. On the Sheet Texture of Zirconium. Ztsch Metallkunde. Vol. 29. 1937. pp. 410.

6. Morell, L.G. and Hanawalt, J.D. Studies of Plastic Working of Mg Alloys. Jnl. Appl. Phys. Vol 3. 1932. pp. 161.

7. Taylor, A. Introduction to X-Ray Metallography. John Wiley and Sons. New York, 1949.

8. Brick, R.M., Martin D.L., Angier, R.P. Effect of Various Solute Elements on the Hardness and Rolling Textures of Copper. Transaction of the A.S.M. Vol. 31. 1943. pp. 675.

9. Bakarian, P.W. Preferred Orientation in Rolled Magnesium and Magnesium Alloys. Transaction of the A.I.M.E. Vol. 147. 1942. pp. 266.

10. Fuller, M.L. and Edmunds, G. Crystal Orientations Developed by Progressive Cold Rolling of an Alloyed Zinc. Transactions of the A.I.M.E. Vol. 111. 1934. pp. 146.

11. Cagliot, V. and Sachs, G. The Rolling Texture of Zinc and Magnesium. Metallwirtschaft. Vol. 11. 1932. pp. 1.

12. Rosi, F.D., Dube, C.A. and Alexander, B.H. Mechanism of Plastic Flow in Titanium-Determination of Slip and Twinning Elements. Transactions of the A.I.M.E. Vol. 197. 1953. pp. 257.

13. Clarke, H.T., Jr. Textures of Cold-Rolled and Annealed Titanium. Transactions of the A.I.M.E. Vol. 188. 1950. pp. 1154.

14. Williams, D.N. and Eppelsheimer, B.S. The Cold Rolled Texture of Titanium. Transactions of the A.I.M.E. Vol. 197. 1953. pp. 1378.

15. McGeary, R. and Lustman, B. Kinetics of Thermal Reorientations in Cold-Rolled Zirconium. Transactions of the A.I.M.E., Vol. 197. 1953. pp. 284.

16. McGeary, R. and Lustman, B. Preferred Orientation in Zirconium. Transactions of the A.I.M.E. Vol. 191. 1951. pp. 994.

17. Keeler, J., Hibbard, W., Jr. and Decker, B. Textures of Rolled and Annealed Iodide Zirconium. Transactions of the A.I.M.E. Vol. 197. 1953. pp. 932.

18. Rostoker, W. Observations on the Lattice Parameters of the Alpha Solid Solution in the Titanium-Aluminum System. Transactions of the A.I.M.E. Vol. 194. 1952. pp. 212.

19. Hayes, E.T., Roberson, A.H. and Paasche, O.G. Zirconium-Titanium System: Constitution Diagram and Properties. Bureau of Mines. R.I. No. 4826. 1951.

20. Smigelskas, A. and Barrett, C.S. Preferred Orientations in Rolled and Recrystallized Beryllium. Transactions of the A.I.M.E. Vol. 185. 1949. pp. 145.

21. Williams, D.N. and Eppelsheimer, D.S. A Theoretical Investigation of the Deformation Textures of Titanium. Institute of Metals, Journal. Vol. 81. September, 1953. pp. 553-562.

22. Geisler, A. Private communication. 1954.

23. Cahn, R.W. A New Theory of Recrystallization Nuclei. Proc. Phys. Soc. Vol. 63. Sec. A. 1950. pp. 323.

24. Rathenau, G. And Boas, G. Grain Growth in a Texture Studied by Means of Electron-Emission Microscopy. Physics. Vol 17. 1951. pp. 117.

25. Burgers, W.G. and Lauwerse, D.C. Relationship Between Deformation Processes and Recrystallization Texture in Al. Z. Physik. Vol. 67. 1931. pp. 605.

26. Burgers, W.G. Rekristallization vervormter Zustand und Erholung. Handbuch der Metallphysik. Leipzig. Vol. 3. 1941.

27. Kromberg, M.L. and Wilson, F.H. Secondary Recrystallization in Copper. Transactions of the A.I.M.E. Vol. 185. 1949. pp. 501.

28. Beck, P.A. and Hu, H. Annealing Textures in Rolled Face-Centered Cubic Metals. Trans. A.I.M.E. Vol. 194. 1952. pp. 83

29. Beck, P.A. Theory of Annealing Textures. Transactions of the A.I.M.E. Vol. 191. 1951. pp. 475.

30. Beck, P.A. Origin of the Cube Texture in Face-Centered Cubic Metals. Transactions of the A.I.M.E. Vol. 191. 1951. pp. 474.

31. Beck, P.A. Notes on the Theory of Annealing Textures. Acta Metallurgica. Vol. 1. 1953. pp. 230.

32. Beck, P.A., Sperry, P.R. and Hu, H. The Orientation Dependence of the Rate of Grain Boundary Migration. Journal of Applied Physics. Vol. 21. 1950. pp. 420.

33. Beck, P.A. Annealing of Colded-Worked Metals. Phil. Mag. Supplement. Vol. 3. July 1954. pp. 245.

34. Barrett, C.S. Recrystallization Texture of Aluminum After Compression. Transactions of the A.I.M.E. Vol. 137. 1940. pp. 128.

35. Beck, P.A. Recrystallization Texture and Coarsening Texture in High Purity Aluminum. Metals Transactions. Vol. 185. 1949. pp. 627.

36. Liu, Y.C. and Hibbard, W.R. Jr. Recrystallization of a Cold-Rolled Copper Single Crystal . Transactions of the A.I.M.E. Vol. 197. 1953. pp. 672.

37. Barrett, C.S. Structure of Metals. Second Edition. McGraw-Hill Book Company, Inc., New York, 1952. pp. 505.

38. Burke, J.E. and Turnbull, D. Progress in Metal Physics. First Edition. Pergamon Press Ltd., London, 1952. pp. 233.

39. Armour Research Foundation. Summary of Final Report of Phase Diagrams. United States Air Force, Air Material Command, March 1951.

40. Barrett, C.S. Structure of Metals. Second Edition. McGraw-Hill Book Company, Inc. New York, 1952. pp. 465.

41. Kurdjumow, G. and Sacks, G. Walz-und Rekristallosationstextur von Eisenblech. Z Physik. Vol. 62. 1930. pp. 592.

42. McHargue, C.J. and Hammond, J.P. Preferred Orientations in Vanadium. Transactions of the A.I.M.E. Vol. 194. 1952. pp. 745.

43. Semchyshen, M. and Timmons, G.A. Preferred Orientation of Arc-Cast Molybdenum Sheet. Transactions of the A.I.M.E. Vol. 194. 1952. pp. 279.

44. Goss, N.P. The Effect of Temperature on the Rolling Texture of Plastically Deformed Low Carbon Steel Strip. Transactions of the A.S.M. Vol. 45. 1953. pp. 333.

45. Anderson, E.A., Jillson, D.C. and Dunbar, S.R. Deformation Mechanisms in Alpha Titanium. Transaction of A.I.M.E. Vol 197. 1953. pp. 1191.

46. Liu, T.S. and Steinberg, M.A. Twinning in Single Crystals of Titanium. Journal of Metals, October 1952. pp. 1043.

47. Barrett, C.S. Structure of Metals. Second Edition. McGraw-Hill Book Company, Inc., New York, 1952. pp. 337.

48. Schmid, E.Z. Plastic Deformation of Magnesium Crystals. Ztsch Elektrochem. Vol. 31. 1931. pp. 447.

49. Bakarian, P.W. and Mathewson, C.H. Slip and Twinning in Magnesium Single Crystals at Elevated Temperatures. Transactions of the A.I.M.E. Vol. 152. 1943. pp. 226.

50.. Barrett, C.S. Structure of Metals. Second Edition. McGraw-Hill Book Company, Inc. New York, 1952. pp. 379.

51. Barrett, C.S., Ansel, G. and Mehl, R.F. Slip, Twinning, and Cleavage in Iron and Silicon Ferrite. Transactions of the A.S.M. Vol. 25. 1937. pp. 702.

52. King, R. Effect of Surface Films on Twinning of Metal Crystals. Nature (London) Vol. 169. 1952. pp. 543.

53. Brocklehurst, R.E. Private Communication. United States Air Force. Air Material Command. 1951.

54. Rosi, F.D. Mechanism of Plastic Flow in Titanium: Manifestations and Dynamics of Glide. Journal of Metals. Vol. 6. January 1954. pp. 58.

55. McHargue, C.J. Preferred Orientations in Titanium Resulting from Mechanical and Thermal Treatments. Dissertation. University of Kentucky, 1953.

56. Hibbard, W.R. Jr. and Yen, M.K. Wire Textures of Copper and Its Binary Alpha Solid Solution Alloys With Aluminum, Nickel and Zinc. Transactions of the A.I.M.E. Vol. 175. 1948. pp. 126.

57. Calnan, E.A. and Clews, C.J. Prediction of Deformation Textures of Uranium. Philosophical Magazine. Vol 43. 1952. pp. 93.

58. Burgers, W.G. Process of Transition of B.C.C. Modification into the H.C.P. Modification of Zirconium. Physica. Vol 1. 1934. pp. 561.

59. Glen, J.W. and Pugh, S.F. The Effect of Phase Transformations on the Orientations of Zirconium Crystals. Acta Metallurgica. Vol. 2. May, 1954. pp. 520.

60. Hu H., Sperry, P.R. and Beck, P.A. Rolling Textures in Face-Centered Cubic Metals. Transactions of the A.I.M.E. Vol. 194. 1952. pp. 3.

61. Anderson, E.A. and Jillson, D.C. Research and Development on Plastic Deformation and Directional Properties of Titanium. Progress Report No. 10 from New Jersey Zinc Company. Philadelphia Ordnance District. May 8, 1952.

62. Fuller, M.L. and Edmunds, G. Relation of Crystal Orientation to Bending Qualities of a Rolled Zinc Alloy. Transactions of the A.I.M.E. Vol. 99, 1932. pp. 175.

63. Staff of Metal Research Division. Rolled Zinc. New Jersey Zinc Company New York. 1929.

# SECTION XIII

# APPENDIX

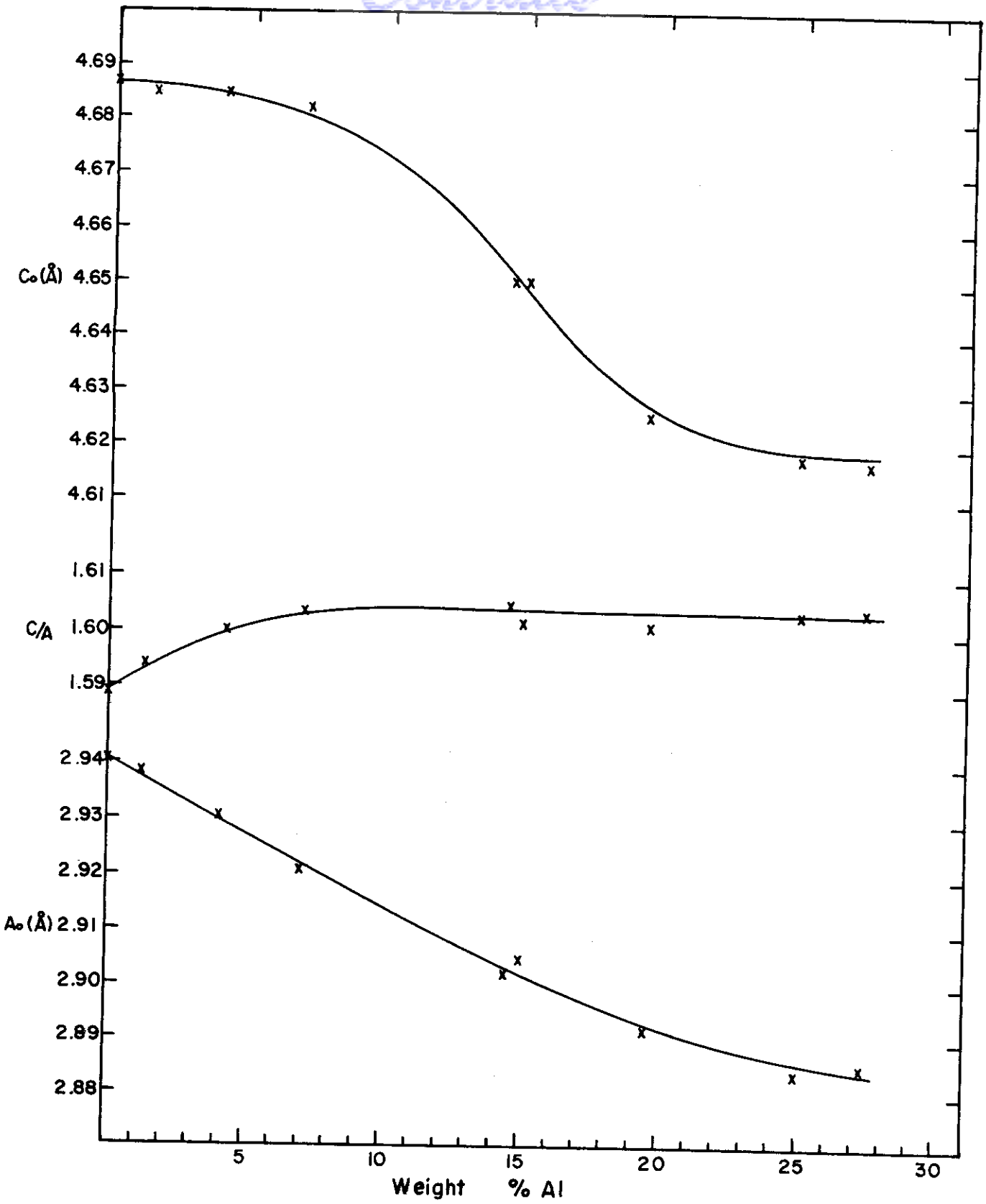


Fig. 45 Effect of Al on lattice parameters of Ti–Al system.

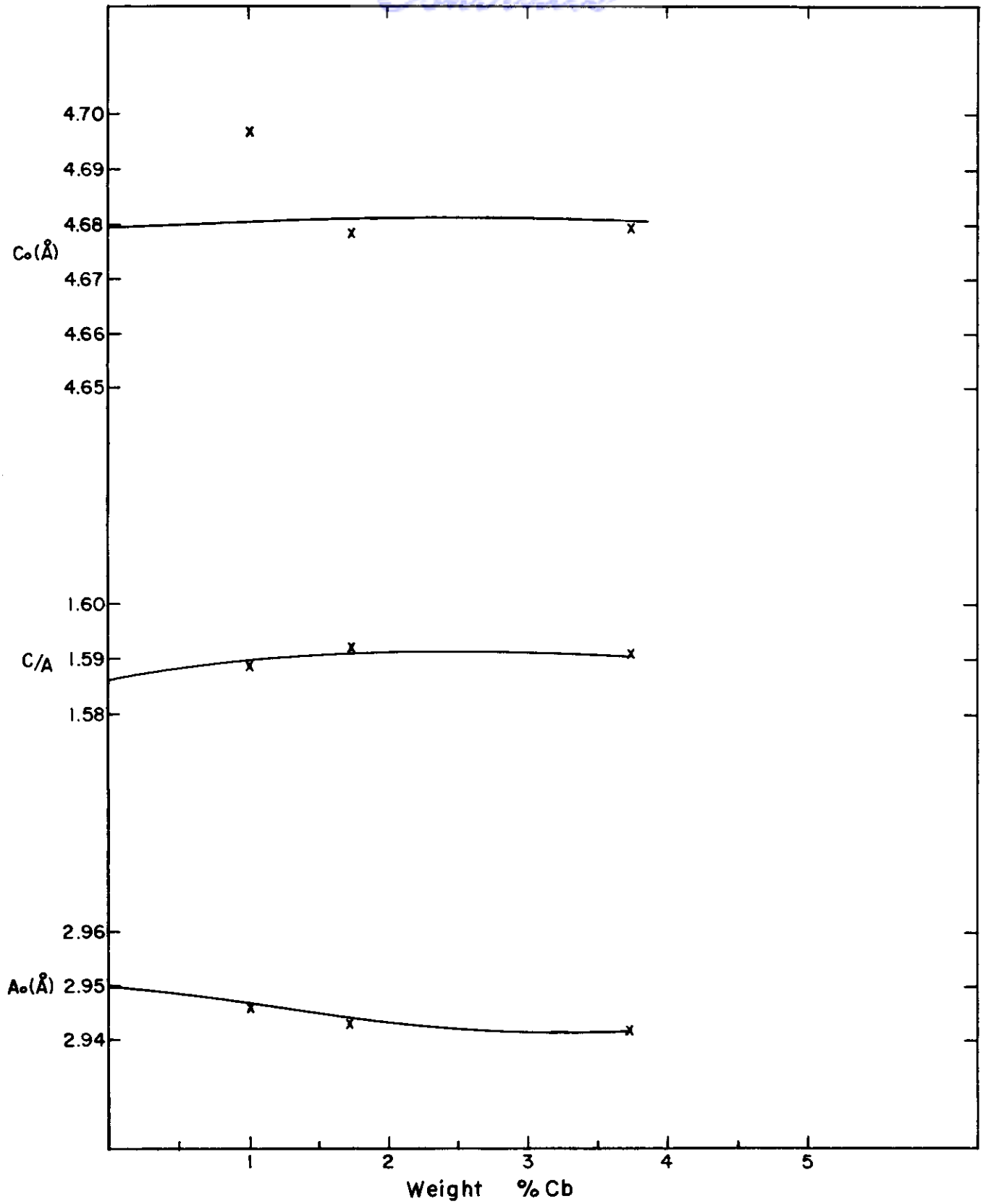


Fig. 46 Effect of Cb on lattice parameters of Ti - Cb system.

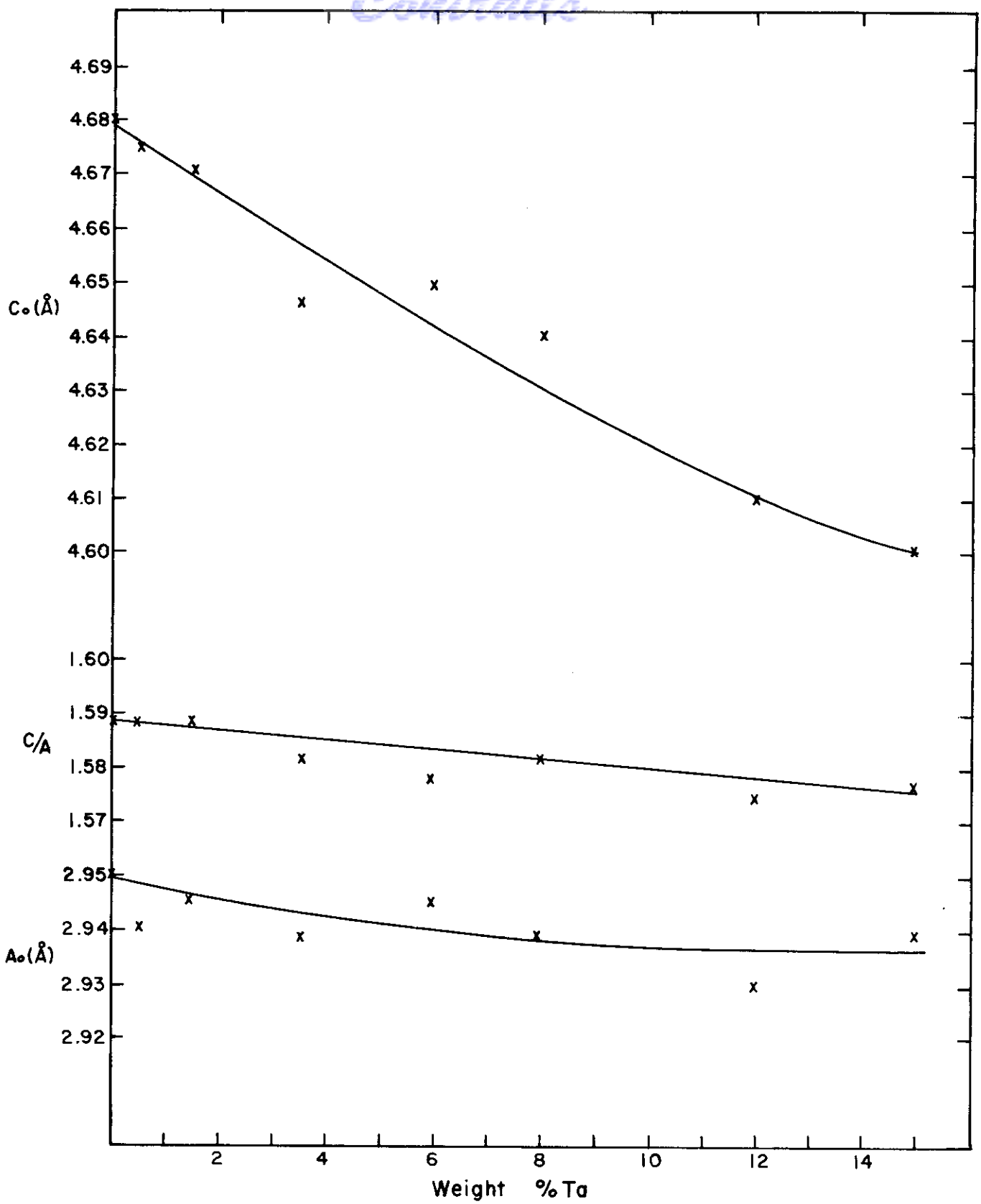


Fig.47 Effects of Ta on lattice parameters of Ti-Ta system.

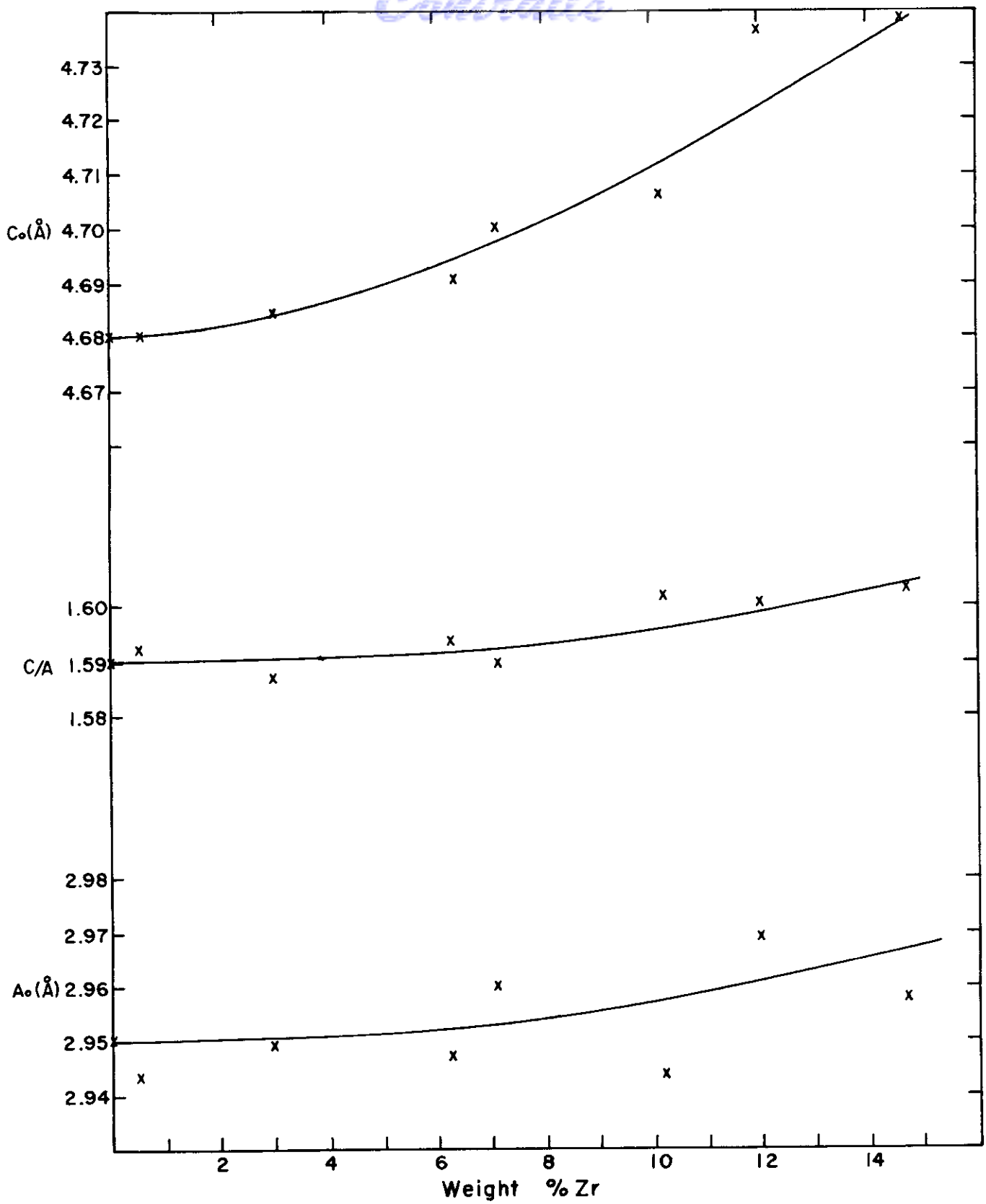


Fig. 48 Effect of Zr on lattice parameters of Ti-Zr system.

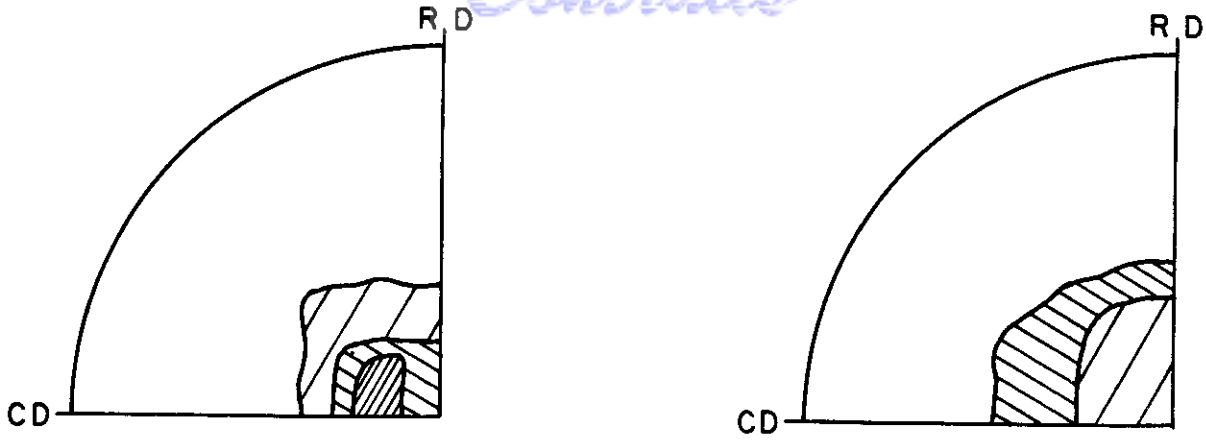


a. Surface

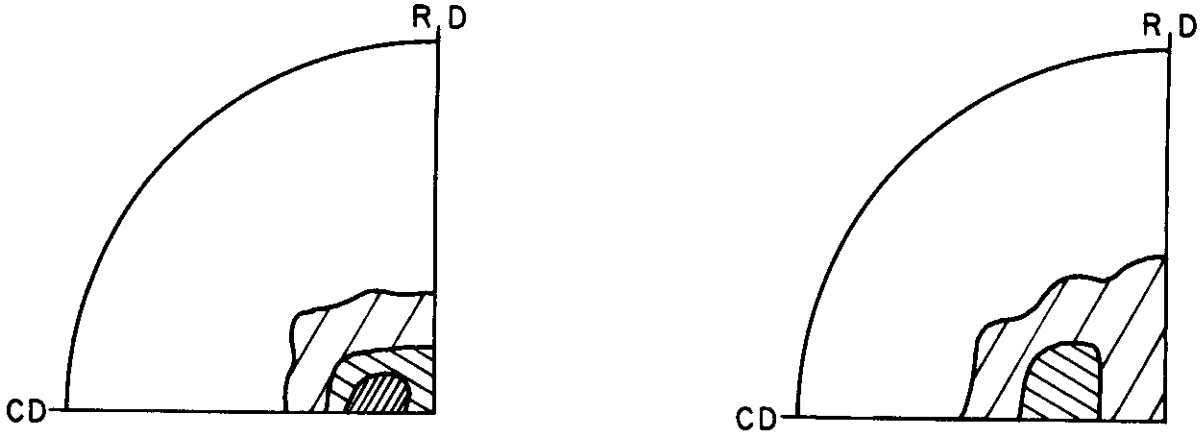


b. 0.005"

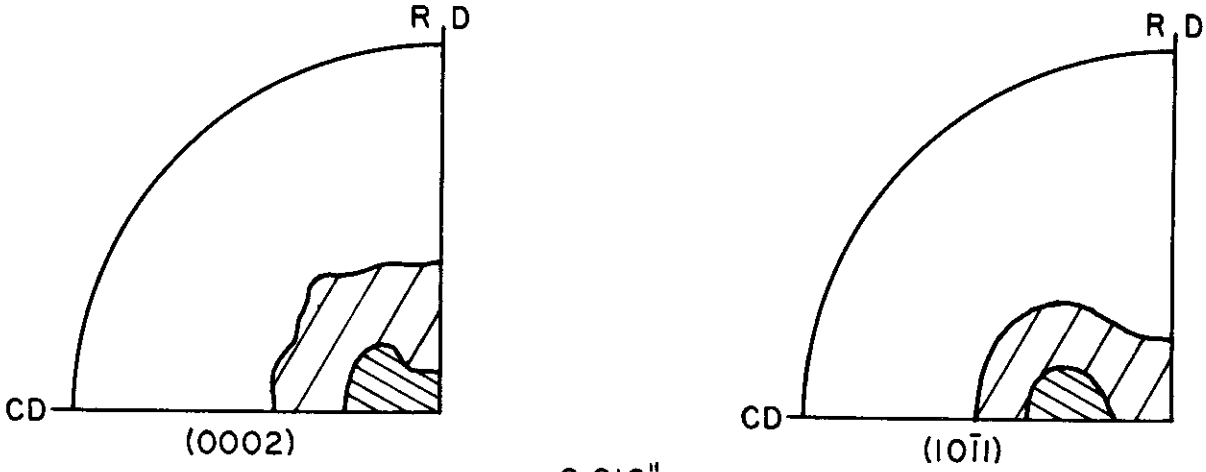


c. 0.010"

Fig.49 Orientations at various distances from the surface in sponge-type titanium cold-rolled 60%.

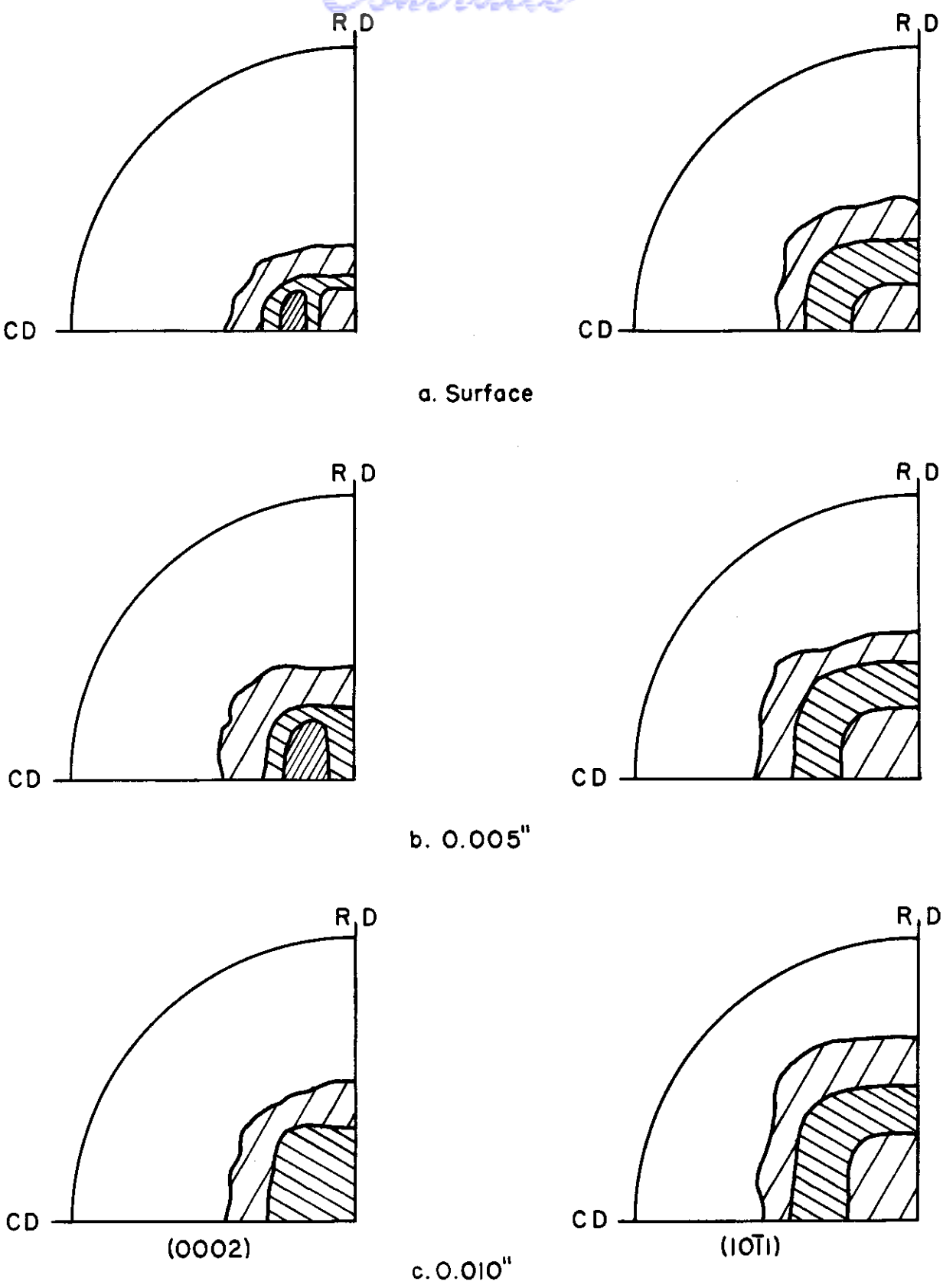


Fig. 50 Orientations at various distances from the surface in sponge-type titanium cold-rolled 70%.

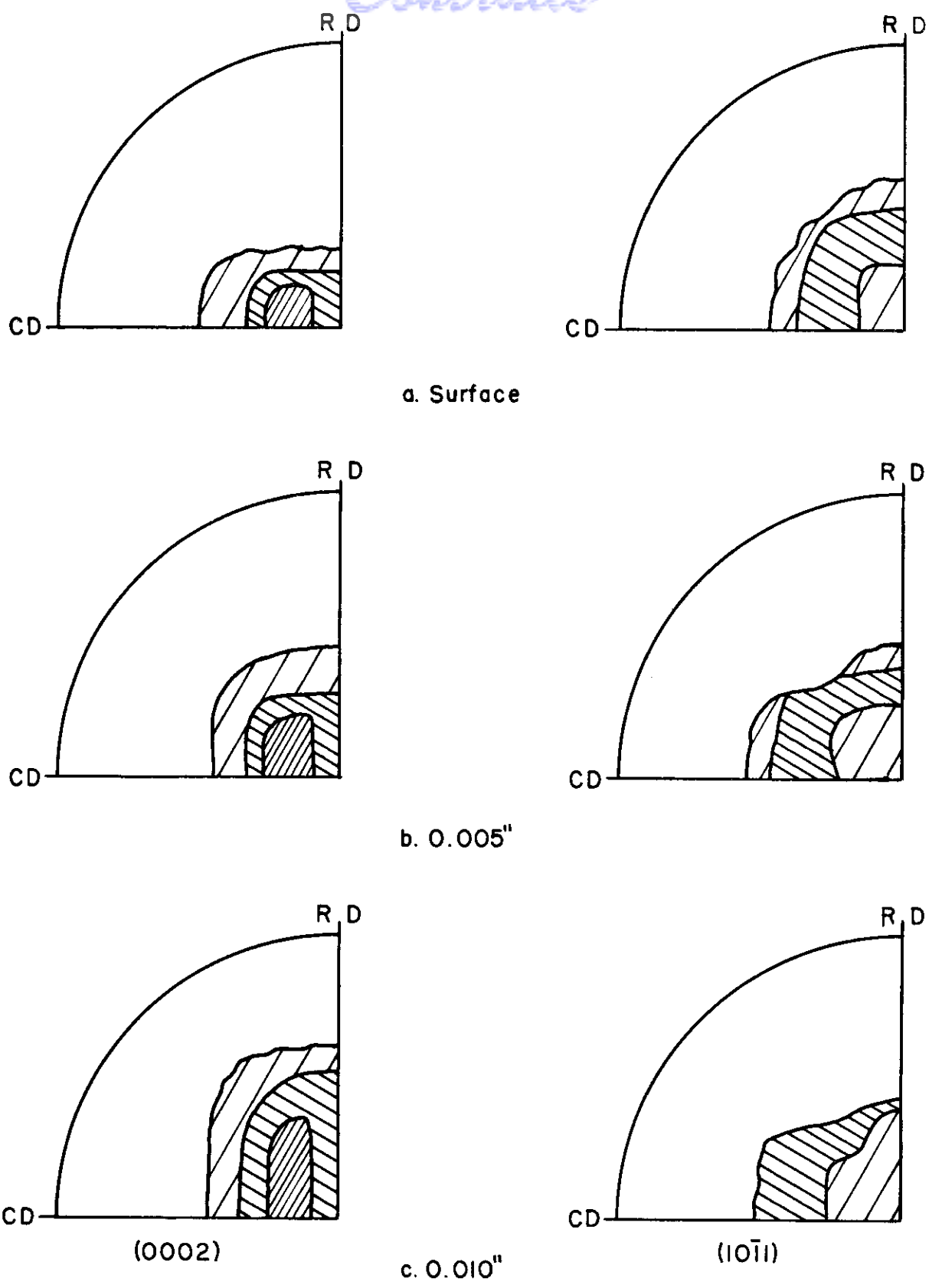


Fig. 51 Orientations at various distances from the surface in sponge-type titanium cold-rolled 80%.

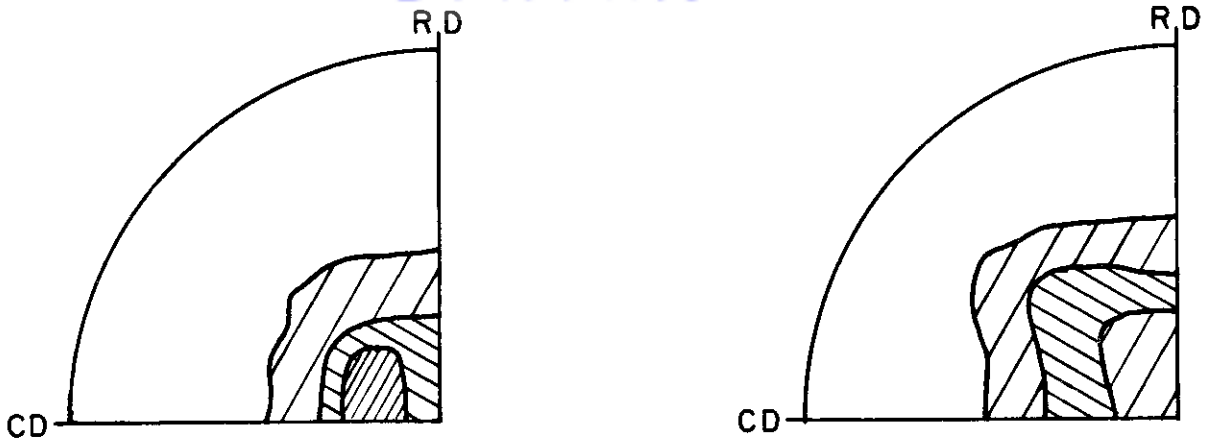


a. Surface

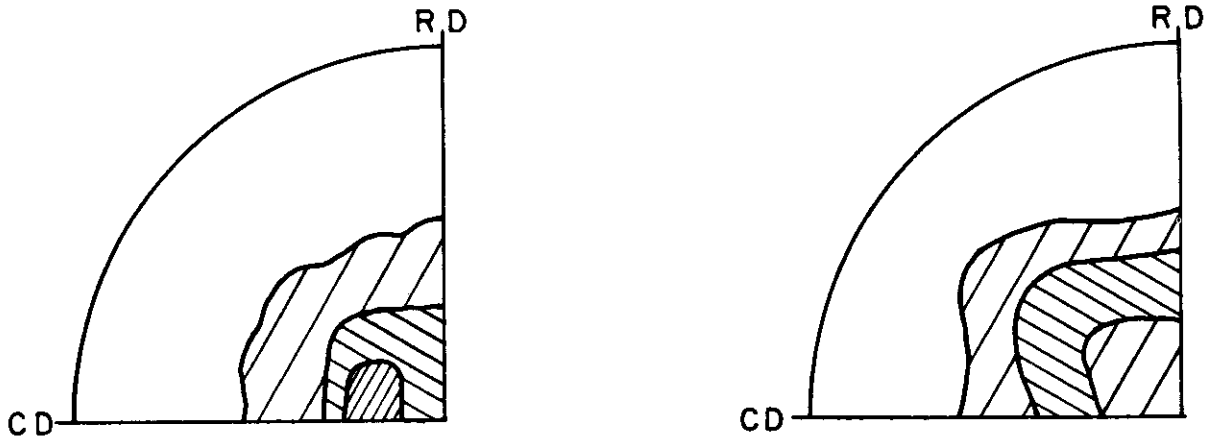


b. 0.005"

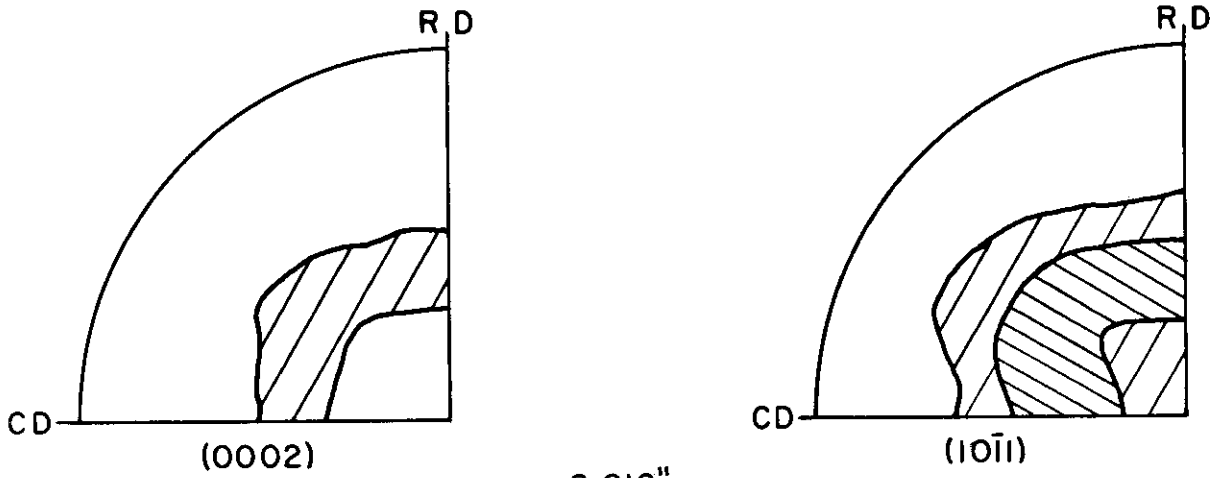


c. 0.010"

Fig.52 Orientations at various distances from the surface in sponge-type titanium cold-rolled 60%, recrystallized at 1000°F.

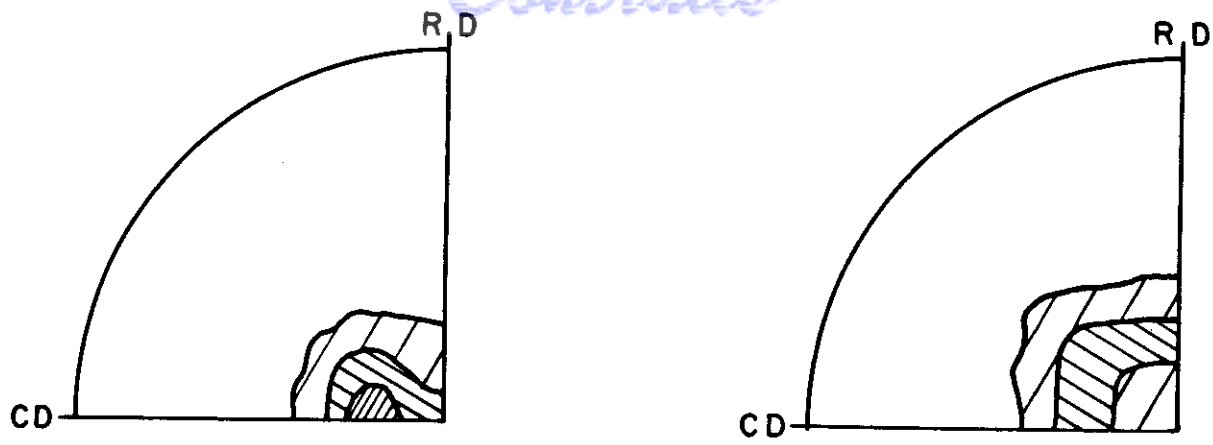


a. Surface

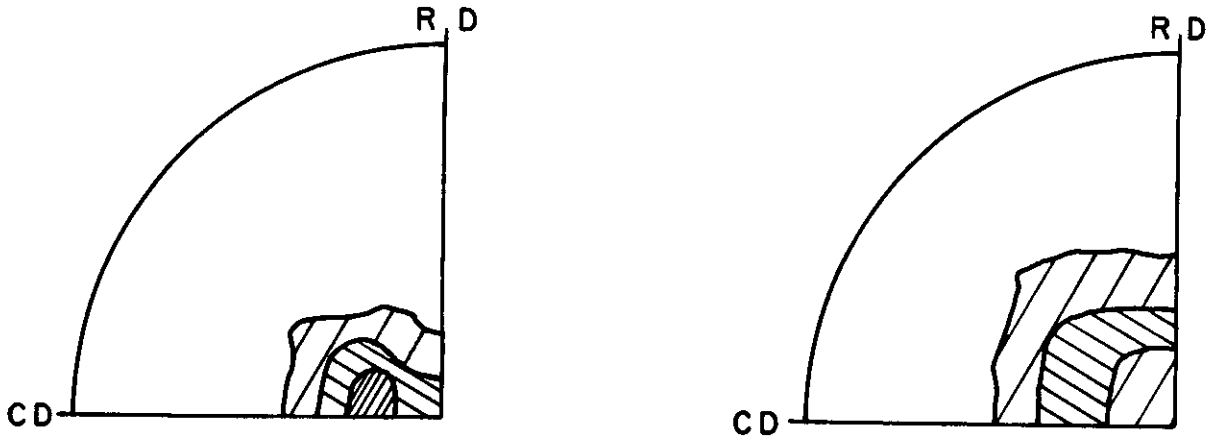


b. 0.005"

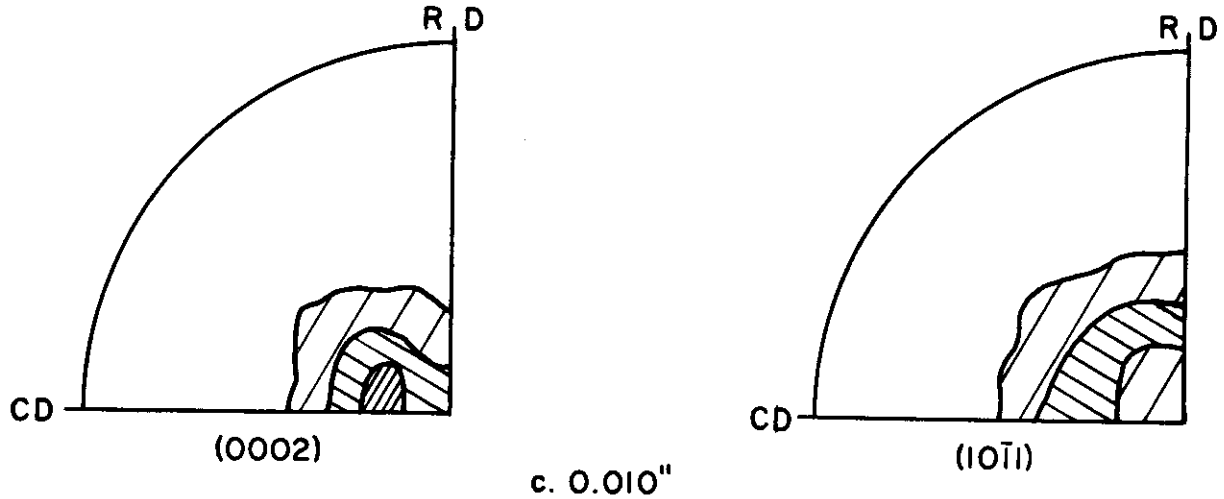


c. 0.010"

Fig. 53 Orientations at various distances from the surface in sponge-type titanium cold-rolled 70%, recrystallized at 1000°F.

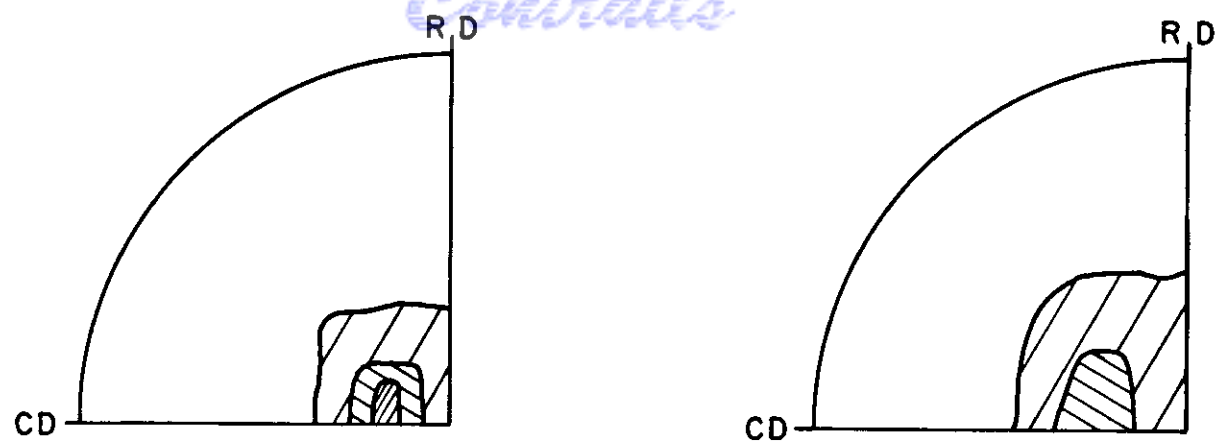


a. Surface

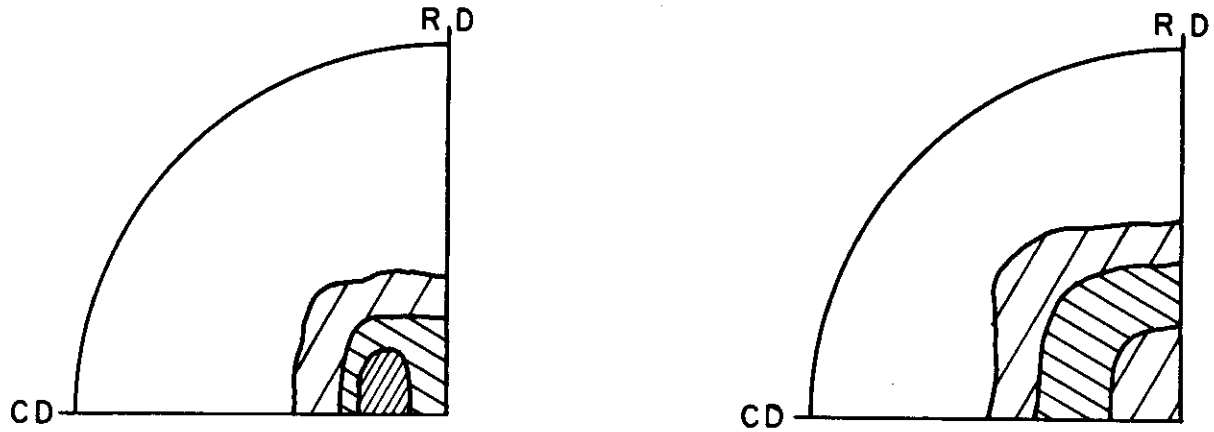


b. 0.005"

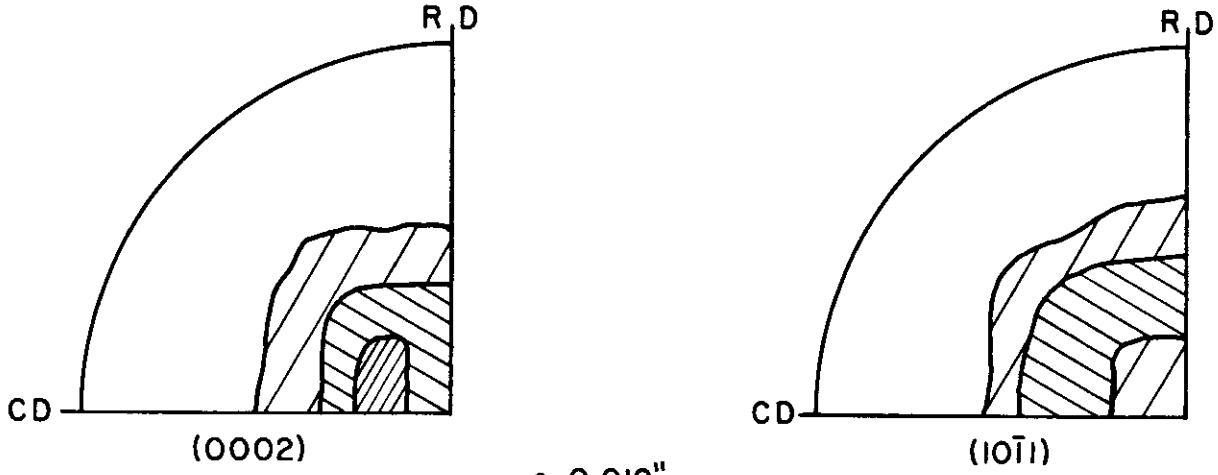


c. 0.010"

Fig. 54 Orientations at various distances from the surface in sponge-type titanium cold-rolled 80%, recrystallized at 1000°F.

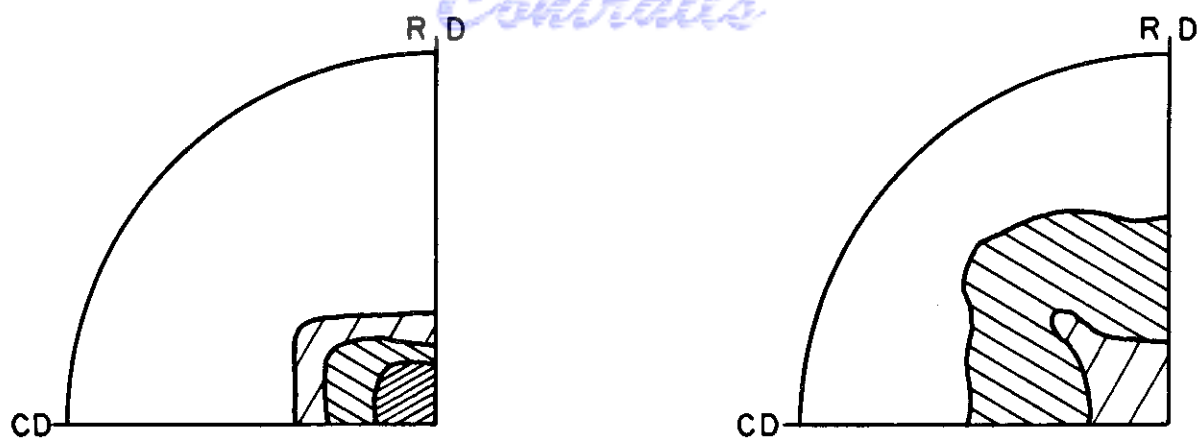


a. Surface

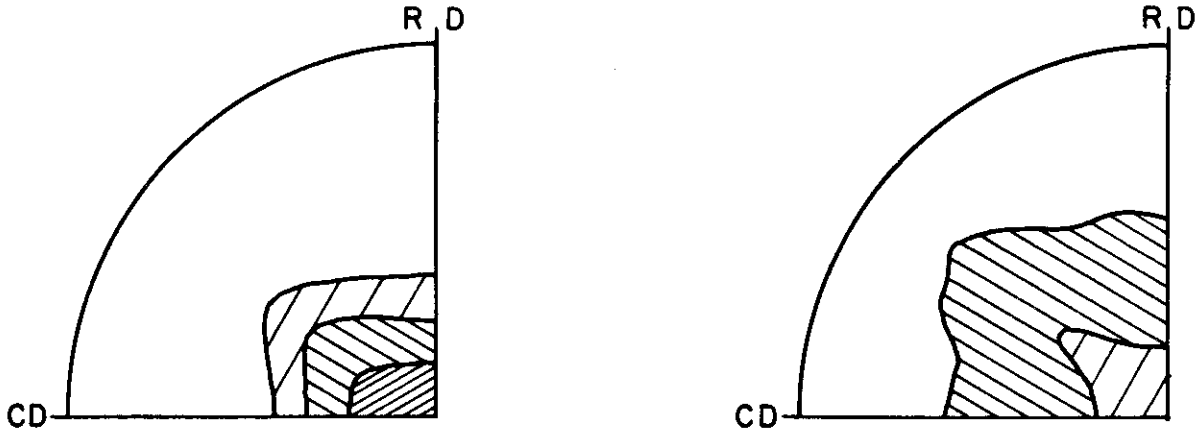


b. 0.005"

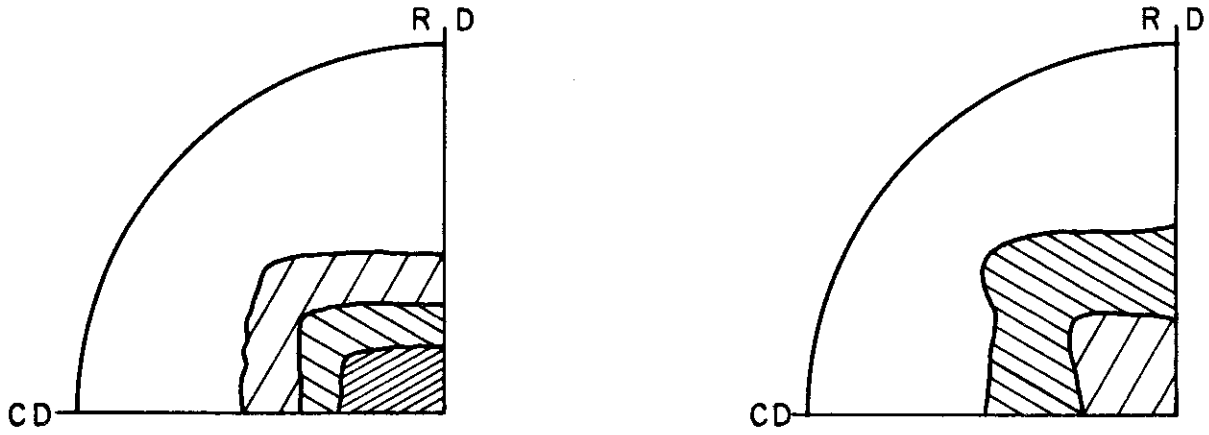


c. 0.010"

Fig.55 Orientations at various distances from the surface in sponge-type titanium hot-rolled 80% at 1050°F.

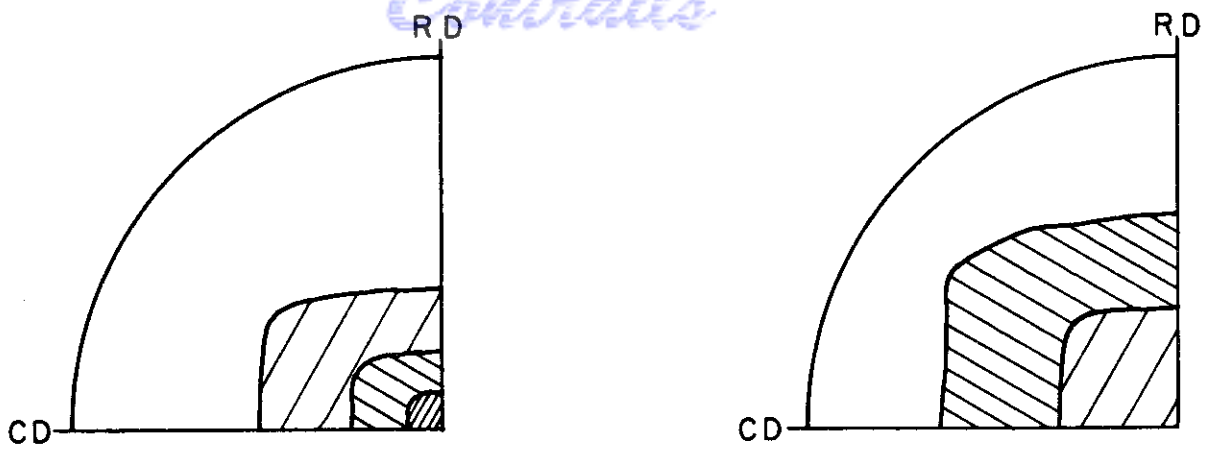


a. Surface

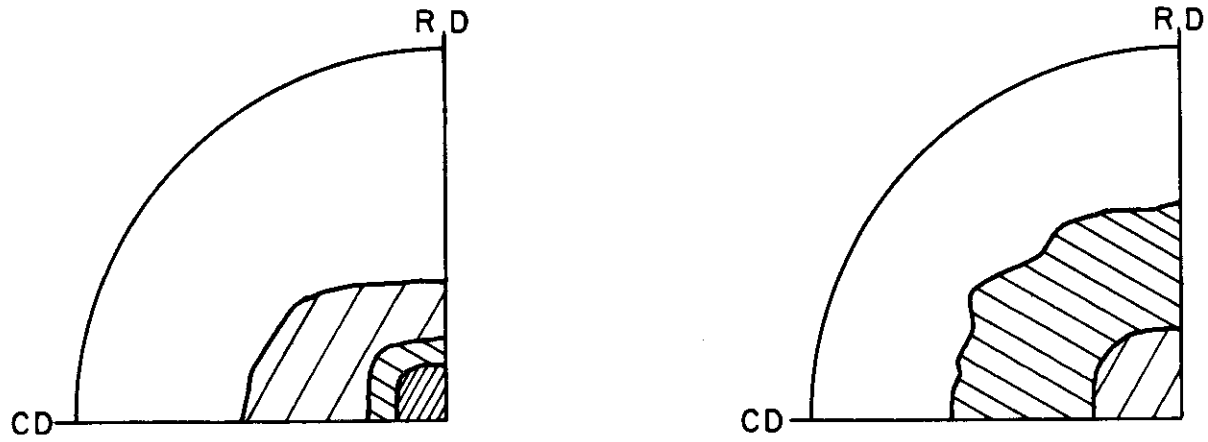


b. 0.005"

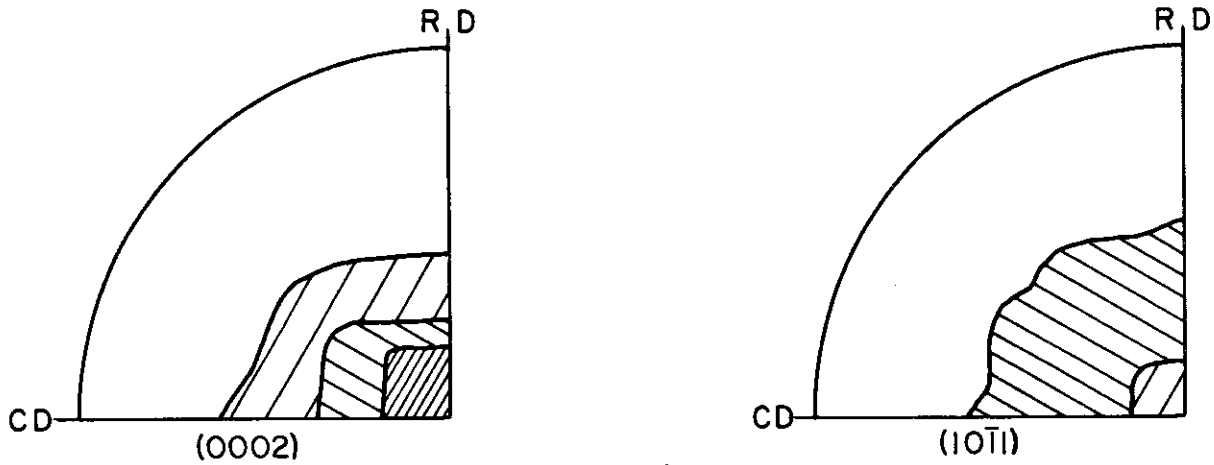


c. 0.010"

Fig. 56 Orientations at various distances from the surface in sponge-type titanium hot-rolled 80% at 1450°F.